CHEMICAL PROBES FOR LYMPHOID TYROSINE PHOSPHATASE

by

Rhushikesh Arun Kulkarni

A dissertation submitted to the faculty of
The University of Utah
in partial fulfillment of the requirements for the degree of

Doctor of Philosophy

Department of Medicinal Chemistry

The University of Utah

December 2013

Copyright © Rhushikesh Arun Kulkarni 2013

All Rights Reserved

The University of Utah Graduate School

STATEMENT OF DISSERTATION APPROVAL

The dissertation of **Rhushikesh Arun Kulkarni**

has been approved by the following supervisory committee members:

Amy M. Barrios	, Chair	**06/10/2013** Date Approved
Chris M. Ireland	, Member	**06/10/2013** Date Approved
Eric W. Schmidt	, Member	**06/10/2013** Date Approved
Grzegorz Bulaj	, Member	**06/10/2013** Date Approved
Ryan E. Looper	, Member	**06/10/2013** Date Approved

and by **Darrell R. Davis**, Chair of

the Department of **Medicinal Chemistry**

and by David B. Kieda, Dean of The Graduate School.

ABSTRACT

Lymphoid tyrosine phosphatase (LYP) is an intriguing therapeutic target for the treatment of several autoimmune disorders including anaphylaxis. Despite this, its precise biological functions in signaling cascades and cellular physiology are still poorly understood. Chemical probes can be beneficial for addressing biological questions pertaining to LYP by creating chemical knockdowns as well as for therapeutic inhibition of LYP. However, to be useful, these chemical probes need to be selective for LYP. Crucial insights about selective targeting of LYP can be gained from studying how LYP demonstrates substrate specificity *in vivo*. The substrate specificity of LYP *in vivo* can be attributed to the interactions of the substrates with the nonconserved features of LYP and to the biological regulation of LYP. Exploiting these interactions with nonconserved features of the LYP catalytic domain as well as mimicking the regulatory mechanisms can help in targeting LYP selectively over other homologous protein tyrosine phosphatases (PTPs). Peptides, being the closest mimics of biological substrates of LYP, can target both the conserved and nonconserved features of LYP. We have taken advantage of these desirable features of peptides by using a peptide substrate in screening for potent and selective LYP inhibitors. When used in inhibitor screens, the inhibitor potencies against this peptide substrate were found to correlate more strongly with the biological activity than those against a traditional small molecule substrate. From this

inhibitor screening exercise, we identified epigallocatechin-3,5-digallate as the most potent LYP inhibitor reported so far (IC_{50} = 50 nM). We have also exploited one of the regulatory mechanisms of LYP, oxidation of the catalytic cysteine residue, to identify thiuram disulfides as a new class of covalent inhibitors of LYP. The best hit from a library of thiuram disulfides screened, compound 13, was shown to inhibit LYP with K_i of 1.1 ± 0.4 μM and k_{inact} of 0.0040 ± 0.0007 s^{-1} in a pseudo-irreversible manner by forming mixed disulfide with the LYP. We have also developed peptide-based covalent inhibitors of LYP that take advantage of the selectivity offered by the peptide sequences and combine it with the utility of an electrophilic, cysteine-reactive, phosphotyrosine (pY) mimetic, warhead. We have separately optimized the electrophilic warhead and the peptide sequence to identify LDLL-(VsN)-SDDD as the best peptide-based covalent LYP inhibitor. This optimized inhibitor inhibited LYP with an IC_{50} of 20 μM and showed selective inhibition of LYP over other homologous PTPs. In summary, we have developed a toolkit of chemical probes for studying the activities of LYP.

TABLE OF CONTENTS

LIST OF TABLES

LIST OF ABBREVIATIONS

ATP	Adenosine triphosphate
PTP	Protein tyrosine phosphatase
pY	Phosphotyrosine
PTK	Protein tyrosine kinase
PTP	Protein tyrosine phosphatase
DSPs	Dual-specificity protein phosphatases
RPTPs	Receptor-like PTPs
NRPTPs	Nonreceptor PTPs
PTP1B	Protein tyrosine phosphatase 1B
TCPTP	T-cell protein tyrosine phosphatase
LYP	Lymphoid tyrosine phosphatase
MAPK	Mitogen-activated protein kinase
NT1	Nontransmembrane PTP subfamily 1
NT4	Nontransmembrane PTP subfamily 4
MKPs	MAP kinase phosphatases
pT	Phosphothreonine
LMPTP	Low molecular weight PTP
Cdks	Cyclin dependent kinases

pS	Phosphoserine
SH2	Src homology domain 2
FN	Fibronectin
TCR	T-cell receptor
MHC	Major histocompatibility complex
Lck	Lymphocyte-specific protein tyrosine kinase
ZAP-70	Zeta-chain-associated protein kinase 70
SNP	Single nucleotide polymorphism
PEP	PEST-domain enriched tyrosine phosphatase
PKC	Protein kinase C
MD	Molecular dynamics
SHP2	Src homology-2 domain-enriched tyrosine phosphatase
RNAi	RNA interference
siRNA	Small interfering RNA
kDa	Kilo Dalton
HePTP	Hematopoietic PTP
P_i	Inorganic phosphate
*p*NPP	*p*-Nitrophenyl phosphate
OMFP	3-*O*-methylfluorescein phosphate
MUP	4-Methylumbelliferone phosphate
DiFMUP	6,8-Difluoro-4-methylumbelliferone phosphate
OMF	3-*O*-methylfluorescein
MU	4-Methylumbelliferone

DiFMU	6,8-difluoro-4-methylumbelliferone
pCAP	Phosphorylated coumaryl aminopropionic acid
TZDs	Thiazolidine-2,4-diones
NHC	N-Heterocyclic carbenes
MFI	Median fluorescence intensity
DMSO	Dimethyl sulfoxide
EGCDG	Epigallocatechin-3,5-digallate
DTT	Dithiothreitol
XP	Extra precision
GST	Glutathione-S-transferase
QSAR	Quantitative-Structure-Activity-Relationship
TCEP	Tris (2-carboxyethyl)phosphine hydrochloride
RT-PCR	Reverse transcriptase polymerase chain reaction
ABPP	Activity-based protein profiling
ABPs	Activity-based probes
BrPmp	L-bromophosphonomethylphenylalanine
Mal AA	4-Maleimidophenyalanine
DIPEA	Diisopropylethylamine
DCM	Dichloromethane
TEA	Triethylamine
OBOC	One bead one compound
PhVsO	Phenyl vinyl sulfonate
2-FMPT	2-Fluoromethylphosphotyrosine

2-FMPCAP	2-Fluoromethylphosphocoumaryl aminopropionic acid
BrPmp	L-Bromophosphonomethylphenylalanine
Pra	Propargylglycine
Pra14mer	Ac-ARLIEDNE-(Pra)-TAREG-NH_2
Ala14mer	Ac-ARLIEDNE-(A)-TAREG-NH_2
Y14mer	Ac-ARLIEDNE-(Y)-TAREG-NH_2
Acr14mer	Ac-ARLIEDNE-(acrylamide)-TAREG-NH_2
PhAcBr14mer	Ac-ARLIEDNE-(phenacyl bromide)-TAREG-NH_2
VsN14mer	Ac-ARLIEDNE-(vinylsulfonamide)-TAREG-NH_2
VsO14mer	Ac-ARLIEDNE-(vinylsulfonate)-TAREG-NH_2
NMR	Nuclear magnetic resonance
TMS	Tetramethylsilane
cDNA	Complimentary DNA
IPTG	Isopropyl-β-D-1-thiogalactopyranoside
NaCl	Sodium chloride
TLC	Thin layer chromatography
EtOAc	Ethyl acetate
Na_2SO_4	Sodium sulfate
RBF	Round bottom flask
NaOH	Sodium hydroxide
HCl	Hydrogen chloride
DMF	N,N-Dimethyl formamide
$NaHCO_3$	Sodium hydrogen carbonate

RV	Reaction vessel
Fmoc	Fluorenylmethoxycarbonyl
DBU	Diazabicyclo[5.4.0]undec-7-ene
HOBT	Hydroxybenzotriazole
DICI	N, N'-Diisopropylcarbodiimide
HCTU	(2-(6-chloro-1H-benzotriazole-1-yl)-1,1,3,3-tetramethylaminium hexafluorophosphate)
TIS	Triisopropylsilane
HPLC	High-performance liquid chromatography
MALDI	Matrix assisted laser desorption ionization
TOF	Time of flight

ACKNOWLEDGEMENTS

First of all, I would like to thank my advisor, Dr. Amy M. Barrios, for giving me the opportunity to work in her lab, her tireless support, constant encouragement and unending patience. Over the last few years, the stimulating discussions with her have helped me learn a lot. She always encouraged me to think independently, which has allowed me to mature as a researcher. She has been a wonderful teacher and a great mentor. I would also like to express my sincere gratitude to my supervisory committee members- Dr. Chris M. Ireland, Dr. Eric W. Schmidt, Dr. Grzegorz Bulaj, and Dr. Ryan E. Looper- for their guidance, constructive criticism, insights, encouragement and interest in my success.

I would like to thank present and past members of the Barrios Lab, Megan Thorson, Dr. Vanessa Ahmed, Dr. Divya Krishnamurthy, Dr. Ryan Mathews, Dr. Mark Karver, Dr. Caitlin Karver, and Sara Sanders for their help with various aspects of my project, for sharing knowledge, for their support, encouragement and friendships. I would like to express my gratitude to all our collaborators- Dr. Riccardo Baron and Dr. Nadeem Vellore for excellent computational support; Dr. Nunzio Bottini and Dr. Stephanie Stanford for the cell studies; Dr. Andrew Cato and his lab for their work in mast cells. I would also like to thank the University of Utah screening resources for providing chemical libraries for screening.

I would like to express my gratitude to everyone in the medicinal chemistry department for their help from time to time, stimulating discussions, and friendships. I would especially like to thank members of the Ireland and Schmidt Lab for allowing me to use their chemicals and facilities. I would also like to thank the biochemistry department and the core facilities, especially Dr. Jim Muller, for allowing me to take advantage of their excellent facilities. I would also like to thank Vish Chandrasekaran and Dr. Mark Ji for their help on some of my projects that did not materialize. Despite that, their help was invaluable. I would also like to extend my gratitude to the administrative staff of the Medicinal Chemistry Department and the Biological Chemistry Program for excellent administrative support.

I would like to express my most sincere gratitude to my family and friends for their encouragements, support and for keeping me sane. Special thanks to my best friend, CST, and my uncle, Dr. Prabhu Kulkarni, for their never ending support. I extend my heartfelt thanks to my wife, Priya, for her constant encouragement, dedication and love. No words can express my gratitude to my parents who have made innumerable sacrifices for my success. I would not be the person I am without them. Therefore, I dedicate this dissertation and all my achievements so far to them.

CHAPTER 1

INTRODUCTION

1.1 Protein tyrosine phosphatases

1.1.1 Phosphotyrosine-dependent cellular signaling

Protein phosphorylation is the most common posttranslational modification, playing a key role in signal transduction (*1*). Besides its role in signal transduction, protein phosphorylation can also determine the rate of protein degradation, the ability of proteins to translocate from one subcellular compartment to another, and the interaction of a protein with other proteins and bivalent cations. It has been estimated that 30% of all cellular proteins are phosphorylated on at least one residue (*2, 3*). Analysis of acid-stable phospho-amino acids reveals that of the residues that are phosphorylated in cellular proteins, 90% are serine (S), 10% are threonine (T) and 0.05% are tyrosine (Y) (*4*). There are two broad classes of enzymes that regulate the levels of protein phosphorylation in cells. Protein kinases catalyze the transfer of the γ-phosphate from adenosine triphosphate (ATP) to a specific residue on a protein. Protein phosphatases dephosphorylate the phosphorylated amino acid residue. Abnormalities in levels of protein phosphorylation play a role in pathogenesis of human diseases and many naturally occurring toxins exert their effects by altering the phosphorylation of proteins. For example, a virulence factor for *Yersinia pestis*, the bacteria that causes bubonic plague, is a protein tyrosine phosphatase (PTP) called YopH, which causes uncontrolled dephosphorylation of many phosphotyrosine (pY) residues helping the bacteria evade host defense mechanisms resulting in fatality (*5, 6*).

Although tyrosine phosphorylation is rare compared to serine and threonine phosphorylation, it plays numerous important roles in eukaryotic physiology. Tyrosine phosphorylation is used for controlling many aspects of cell growth, decision making

related to proliferation and differentiation, shape, motility, metabolism, migration and survival of the cell, communication between and within cells and cellular processes like regulation of gene transcription, mRNA processing and transport of molecules in or out cells (*7, 8*). Abnormal levels of tyrosine phosphorylation result in several human diseases including cancers, diabetes, hypertension and autoimmune disorders such as rheumatoid arthritis (*9*). Therefore, restoring the normal levels of tyrosine phosphorylation is crucial for treatment of these disorders.

Tyrosine phosphorylation levels in the cells are regulated by the balancing actions of two classes of enzymes, protein tyrosine kinases (PTKs) and protein tyrosine phosphatases (PTPs). However, until the late 1990s, PTKs were thought to be the main regulators of the tyrosine phosphorylation in cells while PTPs were considered primarily housekeeping enzymes because development of our knowledge about actions, targets, regulation and roles in normal human physiology and human diseases of PTKs had outpaced that of PTPs (*10*). This can be partially attributed to the fact that PTPs were discovered about a decade later than the PTKs. Therefore, until recently, barring protein tyrosine phosphatase 1B (PTP1B), the majority of drug discovery efforts were focused on developing compounds targeting PTKs. However, it is now clear that PTPs are actually highly specific and tightly regulated enzymes that play crucial roles in several biological processes (*11*).

The human genome contains a total of 107 genes that encode for the amino acid sequence (H/V)**C**$(X)_5$**R**(S/T), also called the PTP signature motif, in the catalytic domain (*12*). Eighty one out of these 107 genes are predicted to encode a catalytically active PTP domain that dephosphorylates pY residue. This number is comparable to a total of 90

genes encoding for PTKs resulting in 85 catalytically active PTKs (*13*). The approximately equal numbers of active PTPs and PTKs in humans, coupled with recent experimental evidence that both the PTPs and PTKs have similar specificities for their substrates, both are tightly regulated and are critical in cellular signaling, indicate that both PTKs and PTPs are interesting therapeutic targets (*14*).

Although the developments over the last decade or so have helped us understand PTPs a little better, there is still a dearth in knowledge about pathological and physiological roles of individual PTPs and the mechanisms of regulations of PTPs (*15*). The major barrier towards developing this understanding is a lack of tools suitable for studying activities and regulations of the PTPs *in vivo*. Complimentary use of genomic and chemical approaches can help in improving our understanding of this class of enzymes.

1.1.2 The protein tyrosine phosphatase enzyme family

Unlike kinases where PTKs share sequence identity with serine/threonine kinases, PTPs do not show sequence similarity with serine/threonine phosphatases or alkaline phosphatases (*16*). The PTP superfamily of enzymes is defined by the amino acid sequence (H/V)**C**$(X)_5$**R**(S/T), also called the PTP signature motif, in the catalytic domain (*17*). This signature motif includes the catalytic cysteine residue and an arginine residue that play a key role in recognizing the pY moiety of the substrate. The presence of a conserved histidine residue and the **α**-helix following the phosphate binding loop (P-loop) in PTPs generates a dipole that contributes to the extremely low pK_a (4.5-5.5) of the catalytic cysteine residue, leaving it unprotonated and therefore, highly nucleophilic at

physiological pH (*18*). Owing to the highly conserved active site, all PTPs use a common catalytic mechanism for hydrolysis of their phosphorylated substrate as shown in Figure 1.1 (*19, 20*). Upon binding of the pY substrate to the active site of the PTPs, the phosphate undergoes nucleophilic attack from the catalytic cysteine residue. The phosphate group is cleaved off of the substrate and is transferred to the catalytic cysteine residue to form a phospho-cysteinyl intermediate (*21, 22*). A conserved aspartic acid residue then acts as a general acid, transferring a proton to the leaving group (tyrosine-containing substrate) and facilitating the expulsion of the product (*23*). The same aspartic acid residue then acts as a general base by abstracting a proton from a water molecule, which in turn nucleophilically attacks and hydrolyzes the phospho-cysteinyl intermediate to regenerate the active enzyme.

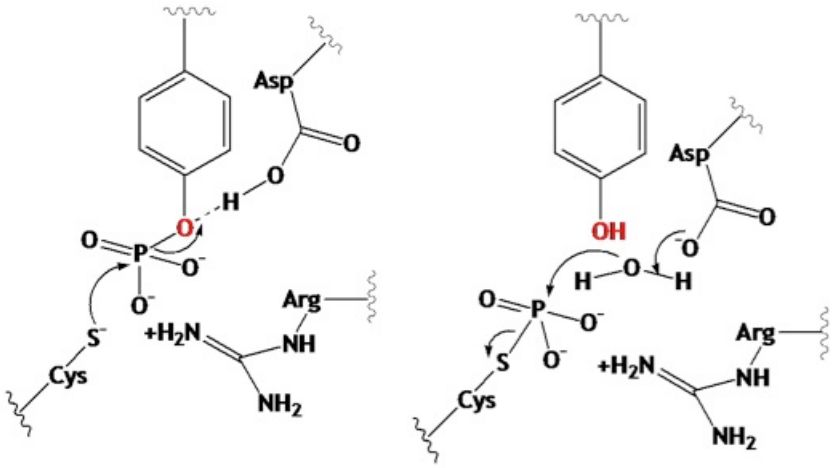

Figure 1.1. Catalytic mechanism of PTPs.

Owing to the conserved active site, the catalytic domains of all the PTPs show high similarity. All 107 PTPs contain at least one ~280 amino acid residue PTP catalytic domain. Based on the amino acid sequences in this catalytic domain, PTPs can be classified into four families (Figure 1.2) (*12*). Another key structural feature of PTPs is their multiple modular domains. These additional domains may include SH2 domains, extracellular fibronectin type (FN) and immunoglobulin repeats. The additional non-catalytic domains of PTPs help in their regulation, interaction with other proteins, and subcellular localization. The arrangement and homology between these additional non-catalytic domains help in further subclassification of PTPs.

Class I cysteine-based PTPs constitute the largest family of PTPs with a total of 99 members. This class of PTPs can be broadly divided based on their substrate preferences into two subclasses comprising of 38 classical PTPs and 61 "dual-specific" protein phosphatases (DSPs). Each of these subclasses can be further divided into several subfamilies based on arrangement and homology between the domains. The 38 classical PTPs contain homologous PTP domains that strictly dephosphorylate only the pY residues. Classical PTPs contain a tyrosine residue in the pY recognition loop present adjacent to the P-loop, which forms one side of the phosphate binding cleft to determine the depth of the active site (typically ~ 9Å) (*11*). This in turn renders classical PTPs selective for pY over phosphoserine (pS) and phosphothreonine (pT) as the phosphate group of only pY can be accessible to the catalytic cysteine residue located at the bottom of the P-loop. Classical PTPs can be further divided into 21 receptor-like PTPs (RPTPs) and 17 intracellular nonreceptor PTPs (NRPTPs) (*24*). Members of the individual subfamilies of NRPTPs especially show high sequence identities in the catalytic domain.

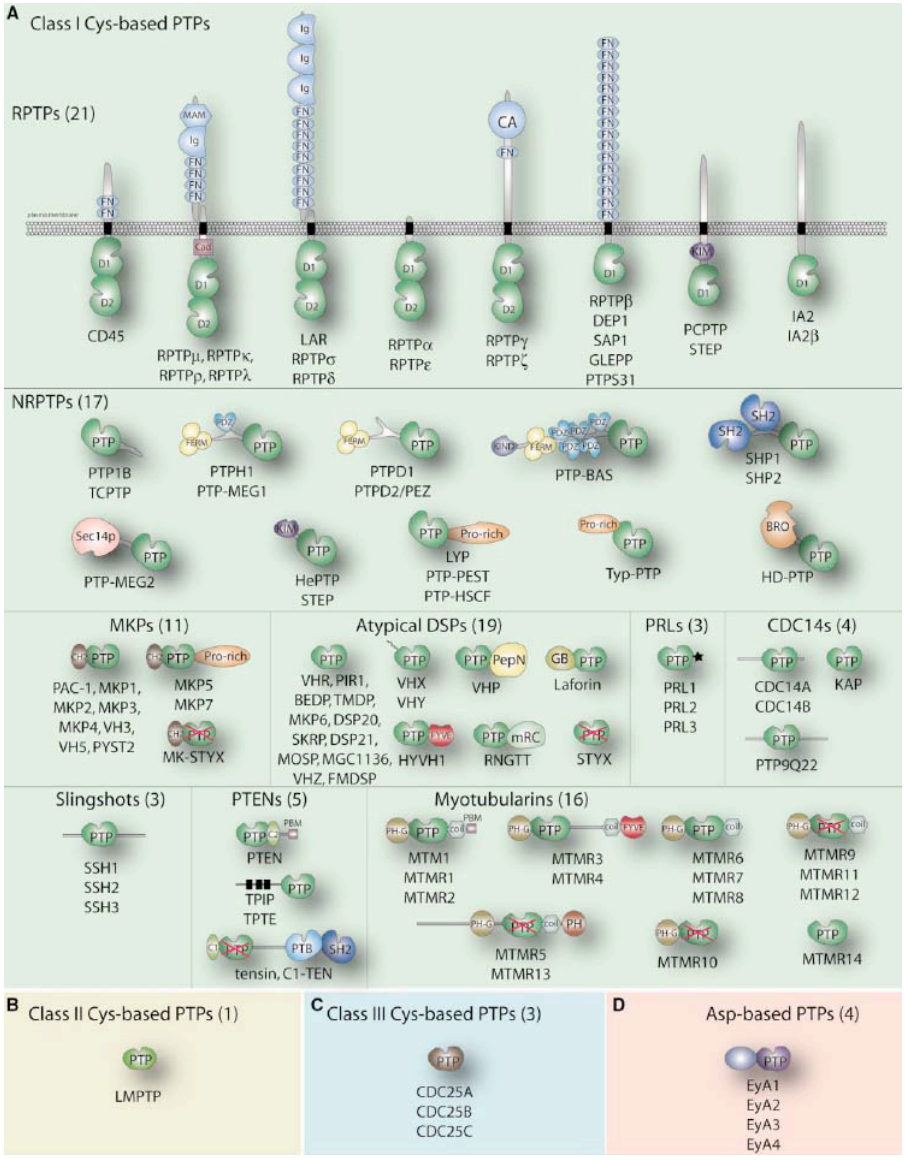

Figure 1.2. Classification and domain structures of all 107 genetically encoded PTPs. This figure is reproduced with permission (*12*).

For example, PTP1B and T-cell protein tyrosine phosphatase (TCPTP), the members of NT1 subfamily of classical PTPs, show 74% sequence identity in the catalytic domain while the members of NT4 subfamily of classical PTPs, lymphoid tyrosine phosphatase (LYP) and PTP-PEST, show 70% sequence identity in the catalytic domain (*25, 26*).

The 61 DSPs are much less conserved and can be subdivided into several subfamilies. The subfamily of DSPs that specifically dephosphorylate proteins from the mitogen-activated protein (MAP) kinase family, namely Erk, Jnk and p38, contain 11 PTPs (*27, 28*). These MAP kinase phosphatases (MKPs) contain a MAP kinase targeting motif and show dual specificity for pY and phosphothreonine (pT) residues. The subfamily of atypical DSPs consists of 19 poorly characterized PTPs that contain fewer than 250 amino acid residues each and lack specific MAP kinase targeting motif (*27*). Members of the PRL subfamily are found in regenerative liver while slingshot phosphatases are thought to dephosphorylate proteins involved in actin reorganization (*29, 30*). CDC14 subfamily is involved in dephosphorylation of pT of the Cdk-activation loop and inactivation of cyclin-dependent kinases (*31*). Members of the PTEN subfamily of PTPs dephosphorylate phosphatidylinositol-3,4,5-triphosphate at the plasma membrane while the members of the myotubularins dephosphorylate phosphatidylinositol-3-phosphate on internal cell membranes (*32*).

The class II cysteine-based PTPs family is represented in the human genome by a single gene encoding for an 18 kDa low molecular weight PTP (LMPTP). Human LMPTP can dephosphorylate a number of tyrosine kinases and their substrates but the physiological role of human LMPTP is still unclear (*12*). The class III cysteine-dependent

PTPs consists of 3 cell cycle regulators that dephosphorylate cyclin dependent kinases (Cdks) at their dually phosphorylated N-terminal threonine-tyrosine motif (*33*). Dephosphorylation of pY and pT of Cdks by the class III PTPs in turn drives progression of cells through the cell cycle. The class IV aspartate-based PTPs use a nucleophilic aspartate residue for the dephosphorylation of pY and possibly phosphoserine (pS) residue (*34*). However, a clear, structurally based definition of this subfamily of PTPs is not available.

1.2 Chemical probes for protein tyrosine phosphatases

1.2.1 Need for chemical probes for protein tyrosine phosphatases

Despite sharing a conserved active site and a common mechanism for substrate dephosphorylation, PTPs have distinct physiological functions *in vivo*. Establishing the crucial roles of PTPs has led to the identification of several therapeutic targets. For example, PTP1B is a key negative regulator of insulin receptor and leptin receptor-mediated signaling pathways and plays important roles in regulating body weight, glucose homeostasis and energy expenditure (*35, 36*). Therefore, PTP1B is an interesting therapeutic target for treatment of diabetes and obesity. Another well-studied PTP, Src homology-2 domain-enriched tyrosine phosphatase (SHP2) is associated with development of Noonan syndrome and acute myeloid leukemia, and therefore it is an important target for anticancer therapeutics (*37*). Despite some improvements in our knowledge of the mechanisms and functions of PTPs in last two decades, there are still gaps in our understanding of how they drive particular biological processes. PTP catalyzed dephosphorylation can function as both ‘on’ and ‘off’ switches for signal

transduction. For example, CD45 catalyzed dephosphorylation of its substrate turns on TCR signaling while LYP catalyzed dephosphorylation of its substrates turns off TCR signaling (*38*). Therefore a detailed understanding of how malfunction of a particular PTP causes a human disease is extremely critical. Also, isolating and establishing activities of individual PTPs is essential for PTP target identification and validation.

Our current appreciation of the PTPs has been developed primarily through the use of genomic techniques such as gene knockout and protein overexpression. However, these genomic approaches have several limitations (*37*). Overexpression of a protein in cells enhances its effects on its targets, which helps in their identification. However, at high expression levels, proteins can show several nonspecific effects that would not be observed at physiological or pathological concentrations. Gene knockout is a powerful technique because of its specificity for the target of interest but it is quite tedious and can lead to lethality. In addition, the loss of activity of one PTP can sometimes be compensated for through other mechanisms during embryonic development, making it difficult to attribute all of the biological effects of the knockout solely to loss of PTP activity. RNA interference (RNAi) typically uses a small interfering RNA (siRNA) that causes ablation of expression of the target protein by destroying mRNA encoding for it. However, RNAs are highly polar and charged and therefore, sufficient cellular delivery is challenging. Besides, RNAi can cause general translational attenuation as well as non-specific destruction of mRNAs leading to the off-target effects (*39*). Measurement of enzyme abundance by determining mRNA levels suffers from the disadvantage that it does not reflect the activities of the PTPs. PTP activity is highly regulated through several mechanisms such as posttranslational modifications and therefore the abundance

of the protein often does not correlate with the activity (*11*). The limitations of genomic approaches warrant the complimentary use of chemical approaches for studying PTPs (*37*). Chemical probes are effective in profiling the functional states of various enzymes in complex environments by providing temporal control of their activities, which in turn can lead to target identification and the discovery of previously uncharacterized enzyme activity by creating chemical knockdowns of the proteins of interest (*40-42*). In addition, the chemical probes used for the chemical knockdown can provide a direct validation of novel therapeutic targets and offer insights that can help in subsequent development of new therapeutic agents.

1.2.2 Challenges for chemical probes for protein tyrosine phosphatases

There are two major challenges in development of chemical probes for PTPs, namely, selectivity and bioavailability (*43*). Both of these challenges arise from features inherent in the active site of the PTPs. As described earlier, all PTPs share a conserved active site and a common catalytic mechanism for substrate dephosphorylation. Therefore, achieving selectivity for one PTP over the others by using inhibitors binding only to the active site of PTPs is extremely challenging. In addition, the conserved active site of PTPs is highly positively charged. Therefore it is no surprise that most of the inhibitors targeting the PTP active site are negatively charged and suffer from low cell permeability and bioavailability. However, similar challenges have been resolved in the design of therapeutically relevant PTK inhibitors, and it is likely that the right approaches can lead to PTP-targeted therapeutics as well. The key to overcoming these challenges

lies in carefully designing chemical probes, taking hints from how PTPs achieve their remarkable substrate selectivity *in vivo*.

1.3 The lymphoid tyrosine phosphatase: an intriguing therapeutic target

1.3.1 The lymphoid tyrosine phosphatase in autoimmunity

Recently, LYP has been recognized as an intriguing therapeutic target because of its association with human autoimmunity (*44-48*). LYP is a classical NRPTP belonging to the NT4 subfamily. Encoded by PTPN22 gene, LYP is expressed exclusively in hematopoietic cells (*44, 49*). It is a 105 kDa protein that contains two distinct domains; an approximately 300 amino acid N-terminal PTP domain and an approximately 200 amino acid C-terminal domain that contains four proline-rich motifs. The N-terminal catalytic domain and the C-terminal domain are separated by approximately 300 amino acids, frequently called the 'interdomain' (*50*). LYP is a potent negative regulator of T-cell receptor (TCR) signaling (*51*). When an antigenic peptide bound to the major histocompatibility complex (MHC) class II molecule binds to the TCR and the coreceptor CD4, it initiates a signaling cascade (Figure 1.3). LYP elicits its potent inhibitory effect on TCR signaling by dephosphorylating several key proteins in this signaling cascade including the Src family kinases lymphocyte-specific protein tyrosine kinase (Lck) and Fyn, zeta-chain-associated protein kinase 70 (ZAP-70) and TCRzeta (*52*). A single nucleotide polymorphism (SNP), C1858T, in the *PTPN22* gene results in a variant of LYP carrying W620 instead of R620 in the C-terminal domain (*53*). This LYP-W620 is a gain of function variant of LYP that shows increased phosphatase activity and therefore more potent inhibition of TCR signaling (*54*). Reduced TCR signaling is a risk factor for

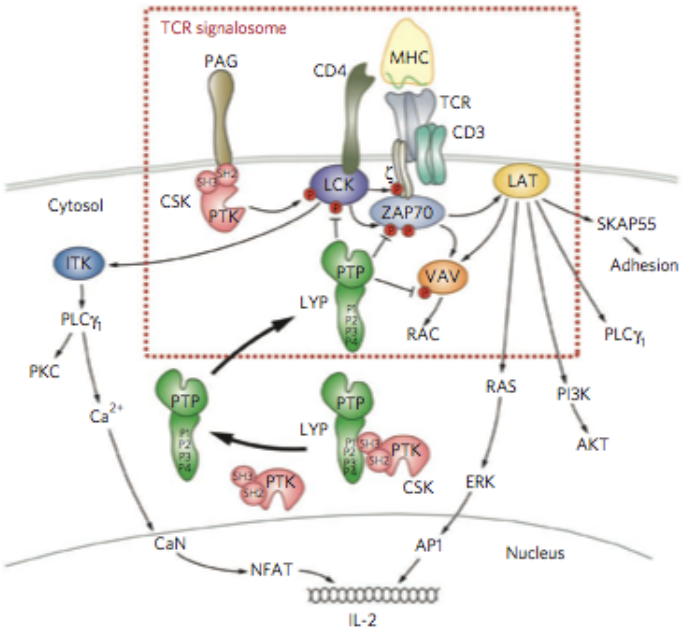

Figure 1.3. Proposed model for negative regulatory role of LYP in TCR signaling (*55*). Reprinted by permission from Macmillan Publishers Ltd, *Nat. Chem. Biol. 8*, 437-446, 2012.

autoimmunity causing disease predisposition through a variety of mechanisms including altered thymic selection, reduced T-helper activity and decreased function of regulatory T-cells (*56*). LYP-W620 has been found to predispose humans to a range of autoimmune disorders including type 1 diabetes, rheumatoid arthritis, systemic lupus erythematosus, myasthenia gravis, Graves' and Addison's disease and others (*57*). Correspondingly, the G788A SNP in the *PTPN22* gene leads to a LYP variant containing Q263 instead of R263 in the catalytic domain (*58*). This LYP-Q263 is a loss of function variant with reduced phosphatase activity and it is found to be protective against systemic lupus erythematosus. Taken together, these findings reinforce the importance of LYP in the

immune response and potential for development of LYP inhibitors for treatment of autoimmune disorders.

1.3.2 Chemical probes for lymphoid tyrosine phosphatase: need and utility

While inhibition of LYP activity could be therapeutically beneficial, nonspecific inhibition of other T-cell derived PTPs is likely to be detrimental. For example, the ubiquitously expressed PTP-PEST is an enzyme that shares 70% sequence identity with LYP in the catalytic domain (*26*). PTP-PEST is essential in development, and cannot be removed without embryotoxicity in mice (*59*). Another PTP, CD45, catalyzes dephosphorylation of its substrate (Lck pY505) that turns on TCR signaling (*38*). Therefore, inhibition of CD45 activity would counteract any benefit obtained from inhibition of LYP. In addition to LYP, PTP-PEST and CD45, about 50 PTPs including HePTP, TCPTP, SHP1, SHP2, PTPH1, PTP36, PTP-MEG1, LMPTP, PTEN are expressed in T cells (*60*). These PTPs, just like LYP, play specific roles in T cells and therefore, nonselective inhibition of LYP can lead unwanted side effects. Therefore if therapeutic LYP inhibitors are to be developed, the issue of PTP selectivity must be addressed.

Considerable effort has been devoted to the development of potent, selective inhibitors of LYP and other PTPs for use as chemical probes and potential therapeutic leads, but there are still several challenges in the field (*16, 37, 61-64*). Our efforts of screening compound libraries in the quest for identifying potent and selective LYP inhibitors has lead us to the gold(I)-based drugs, aurothioglucose and auranofin, as potent LYP inhibitors (*46, 65*). Further SAR on auranofin analogs has resulted in identifying

C28 (Figure 1.4*A*) as the most selective LYP inhibitor reported so far (*45, 66*). The papers describing this work are published in *J. Med. Chem.* and *J. Inorg. Biochem.* Recently, our collaborators have used C28 to create a chemical knockdown of LYP in mast cells and this work is published in *Allergy* (*67*). The chemical knockdown accurately mimicked effects of gene knockout and was instrumental in establishing the positive regulatory role of LYP in mast cell degranulation and anaphylaxis. Furthermore, chemical knockdown of the mouse ortholog of LYP, PEST-domain enriched tyrosine phosphatase (PEP), has been shown to alleviate anaphylaxis in mice (Figure 1.4*B*). It was also shown that inhibition of PEP is synergistic with dexamethasone in the treatment of anaphylaxis. This study underlines the importance of chemical knockdowns in studying the physiological and pathological roles of PTPs.

Despite this significant finding, very little information is available about the substrates, abundance, localization and regulation of LYP in mast cells. Also, details of regulation of LYP in TCR signaling are still missing especially those pertaining to the abundance and subcellular localization of active versus inactive LYP in presence and absence of TCR stimulation. Although C28 has been instrumental in establishing the role of LYP in anaphylaxis, it cannot help in addressing other problems pertinent to LYP. Other potent and selective inhibitors, which can be covalently attached to LYP, can help in addressing these issues. For developing potent and selective inhibitors, key insights can be obtained by taking a closer look at how LYP achieves substrate selectivity *in vivo*.

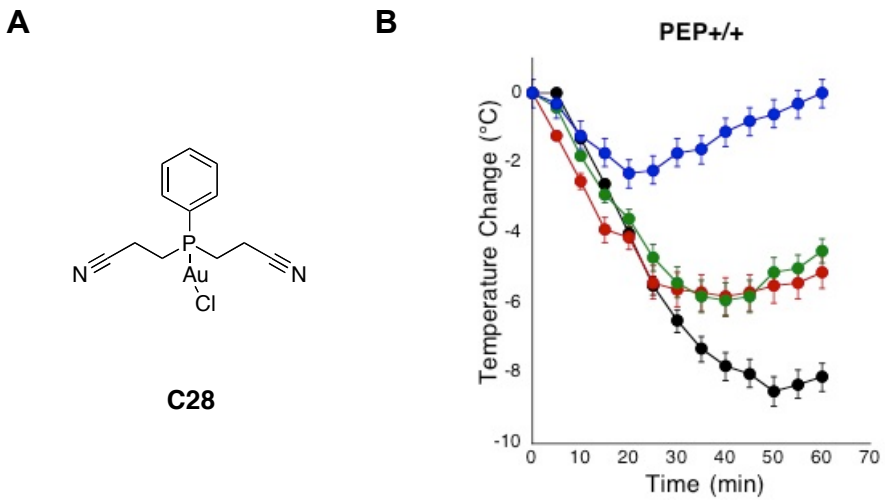

Fig. 1.4. Utility of a LYP inhibitor in the treatment of anaphylaxis. (A) C28, the best LYP inhibitor from the library of gold (I) phosphines, (B) change in body temperature of mice induced with anaphylaxis upon treatment with PBS (control, black), dexamethasone 1 mg/kg (green), C28 5 μM (red) and a combination of dexamethasone and C28 (blue).

1.4 Substrate selectivity in lymphoid tyrosine phosphatase

Like several other PTPs, LYP exhibits high substrate specificity *in vivo*, which can be attributed both to the nonconserved features in the catalytic domain as well as the regulatory mechanisms (*68, 69*). Exploiting these nonconserved features of LYP as well as mimicking the regulatory mechanisms can help in targeting LYP selectively over other homologous PTPs. Therefore a detailed understanding biological regulation, structural features and interaction between the substrates and LYP is essential for developing potent and selective chemical probes for LYP.

1.4.1 Biological regulation of lymphoid tyrosine phosphatase activity

The activity of LYP is regulated through several different mechanisms including posttranslational modifications, regulatory domains, restricted subcellular localization and reversible oxidation (*48, 50, 55, 70*). LYP may be regulated by phosphorylation of a serine residue in the catalytic domain (*48*). Serine35 in the catalytic domain of LYP is phosphorylated by protein kinase C (PKC) and the resulting phospho-LYP shows impaired dephosphorylation of endogenous LYP substrate, Lck. The catalytic domain of LYP interacts with the proximal interdomain and this intramolecular interaction has been shown to inhibit the catalytic domain (*50*). Another proposed mechanism of regulation of LYP is spatial control of its activity through interaction with the kinase CSK (*55*). It has been proposed that under the resting conditions in T cells, LYP forms a complex with CSK, thereby physically separating LYP from its substrates present in the lipid rafts (Figure 1.3). When TCR signaling is initiated, the resulting signaling cascade eventually leads to formation of TCR signalosome, a multimeric signaling complex in the plasma

membrane. The substrates of LYP including Lck and ZAP-70 are a part of this TCR signalosome. TCR stimulation also leads to dissociation of LYP from CSK and recruits LYP to TCR signalosome in the lipid rafts. Once in TCR signalosome, LYP can dephosphorylate its substrates turning off TCR signaling. It has also been proposed that the gain of function variant, LYP-W620, cannot bind to CSK and therefore has unregulated access to its substrates even under resting conditions (*55*). However, concrete evidence showing that LYP does not have access to its substrate when in the cytoplasm is lacking. Another mechanism of LYP regulation is through oxidation of the catalytic cysteine residue with oxidizing agents such as H_2O_2 and NO, rendering it non-nucleophilic and therefore, inactive (*71-74*). A crystal structure of the catalytic domain of LYP reveals that this enzyme contains two additional cysteine residues within disulfide bonding distance from the catalytic C227: C129 and C231. Cysteine231 is a part of the P-loop while C129 is a backdoor cysteine residue (*75*). These additional cysteine residues are not present in other PTPs, barring other members of NT4 subfamily: PTP-PEST and BDP1. *In vitro*, the presence of excess of H_2O_2 causes the C227 residue to form a disulfide bond with C129 that reversibly inactivates the enzyme. The presence of these additional cysteine residues presents a unique opportunity for targeting LYP selectively over other homologous PTPs.

1.4.2 Structural features of the lymphoid tyrosine phosphatase

Apart from the regulatory mechanisms, interaction of substrates with conserved and nonconserved features of the catalytic domain play a crucial role in determining substrate selectivity of LYP and other PTPs. A detailed structural understanding is

necessary in order to appreciate this. A ribbon diagram of LYP highlighting the key structural features is shown in Figure 1.5. The pY binding site or P-loop (residues 226-233) forms a deep pocket on the surface of LYP and has a strong positive charge. The pY recognition loop (residues 54-60) contributes to the selective recognition of pY over pS and pT. The other conserved features in the catalytic domain include the Q-loop (residues 274-301) and β3-β4 loop (residues 131-139), which are important in interactions with the pY residue of the substrate. One of the key substrate recognition features of PTPs is the dynamic opening and closing of the WPD loop (residues 193-204 in LYP). The closing of WPD loop over the active site is essential for the phosphatase activity, and, therefore, the closed state of WPD loop leads to the active form while the open state of WPD loop leads to the inactive form of PTPs. In LYP crystal structure 2P6X shown in Figure 1.5, the WPD loop is in an inactive, atypically open state. A highly nonconserved hydrophobic pocket adjacent to the WPD loop is exposed only in the open state of the WPD loop of LYP (*55*). Locking the WPD loop in the open state through interactions with this hydrophobic pocket adjacent to the WPD loop provides an attractive approach for selective inactivation of LYP. Besides the fairly conserved features, highly non-conserved features like secondary substrate binding pockets are also found in some of the PTPs including PTP1B and LYP. The secondary substrate binding pocket in PTP1B has been exploited previously for the development of selective inhibitors of PTP1B and TCPTP (*76-78*). The second-site-loop in LYP, the LYP insert, is highly nonconserved and is present only in the other members of NT4 subfamily of classical PTPs, PTP-PEST and BDP1. Therefore, the interactions with the LYP insert are also likely to provide selectivity for LYP targeting.

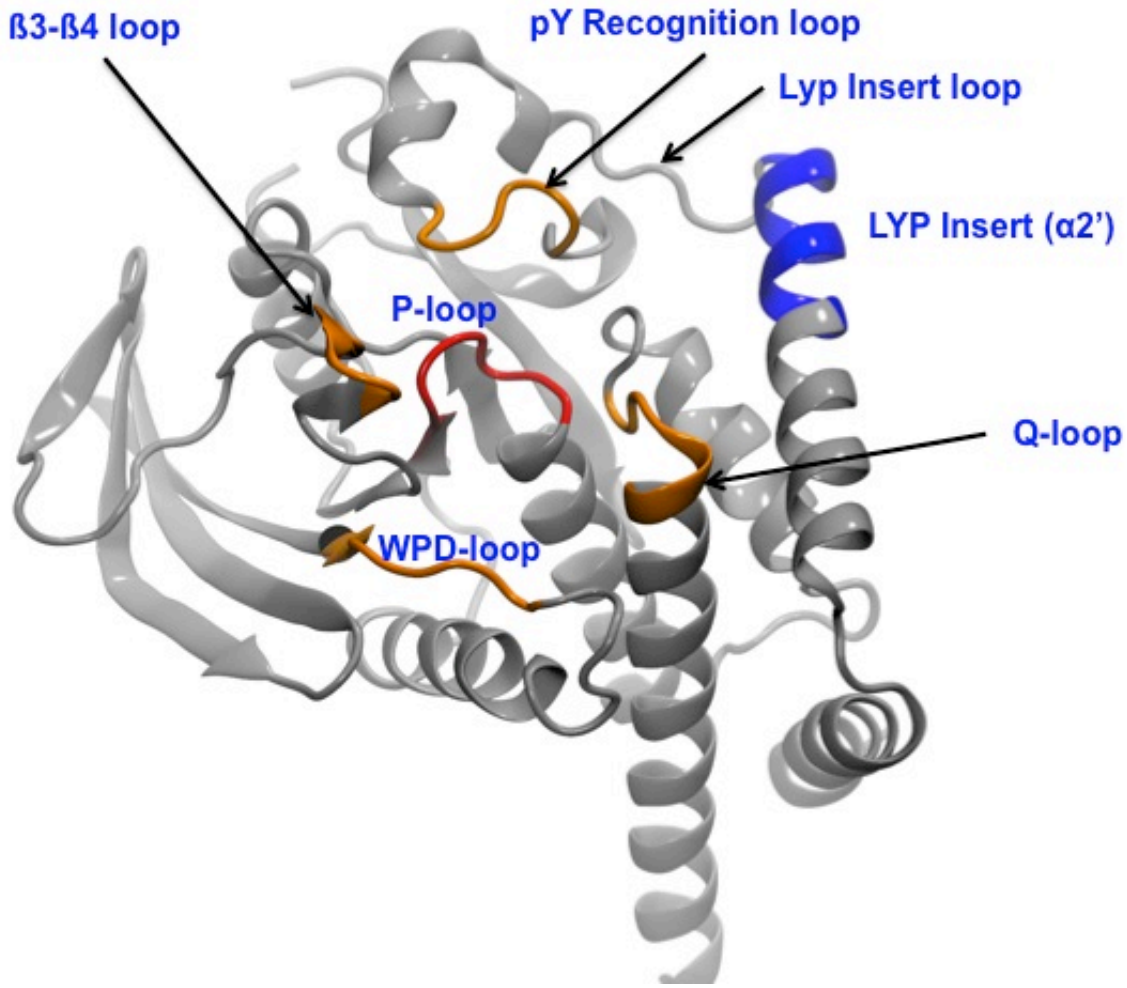

Figure 1.5. Crystal structure of LYP (PDB entry 2P6X). The regions surrounding the P-loop (red) are highlighted in gold (pY recognition loop, Q-loop, WPD loop and β3-β4 loop); the LYP insert is highlighted in blue.

1.4.3 Using peptides to achieve selectivity

Although LYP has been identified as an intriguing therapeutic target for autoimmune disorders, its precise biological functions in signaling cascades and cellular physiology are still poorly understood (*79*). It is quite likely that LYP may act on one or more unidentified substrates apart from Lck and ZAP-70 in TCR signaling, while its substrates and precise role in mast cell signaling is completely unknown. Therefore, it is essential to develop a full repertoire of LYP substrates and the signaling cascades modulated by LYP (*80*).

Peptides containing pY are the most accurate mimics of the biological substrates of the PTPs. For example, ARLIEDNE-pY-TAREG-NH_2 (**peptide 1**) is a peptide sequence based on the amino acid residues flanking Lck pY394, a known physiological substrate of LYP, and it is the most accurate mimic of the biological substrate of LYP (*38, 52*). Substrate library screening approaches have been employed for screening combinatorial peptide libraries with the aim of identifying unknown substrates of LYP as well as peptide sequences that will target LYP potently and selectively (*80, 81*). These studies have established that LYP shows distinct amino acid preferences for each position flanking pY in its substrate establishing the importance of the interaction between LYP surface with these amino acids flaking pY in the substrate. A couple of the best peptide substrates of LYP identified from this study, YGEE-pY-DDLY and DGEE-pY-DDPF, have been cocrystallized with catalytic domain of LYP (*80*). These cocrystal structures have established that these peptide substrates interact with the active site as well as the other secondary sites on LYP surface including the LYP insert.

However, crystallography can provide only a snapshot of the enzyme-peptide interaction and cannot provide the fluxional details of this dynamic interaction. Therefore, we decided to investigate the dynamic and transient interactions between LYP and its peptide substrate. To understand how the selectivity is derived through interactions with nonconserved features of catalytic domain, Dr. Nadeem Vellore from Dr. Riccardo Baron's laboratory simulated the interaction between LYP and **peptide 1**, the accurate mimic of the biological substrate of LYP, using computer modeling and molecular dynamics (MD) simulations (Figure 1.5). Dr. Vellore found that **peptide 1** shows high conformational diversity, and samples transient binding modes throughout the simulation, as summarized in Figure 1.6. As expected, the pY residue was found to hydrogen bond with S228, A229 and R233 of the P-loop, K138 of the β3-β4 loop and Q274 residue of the Q-loop. A detailed list of all hydrogen bonding interactions between **peptide 1** and LYP are documented in Table 1.1. Overall, pY forms at least one hydrogen bond throughout the 150 ns ensemble (98% of time). The first five residues of the N-terminus (ARLIE) and the two residues from the C-terminus region (RE) of **peptide 1** showed b-turn propensity (~10% and ~20% time occurrences). The N-terminal 'AR' residues of the peptide were found to be solvated during most of the simulation time with no dominant and/or specific interactions with the protein. The C-terminus of the peptide was involved in interacting with the Q-loop and partially with WPD loop, as displayed in Figure 1.6. During the course of the simulation, **peptide 1** made favorable contacts with the P-loop and pY recognition loop and showed little interaction with the LYP-specific insert. Taken together, MD simulation data confirmed that the peptide interacts with the active site and multiple additional sites on the LYP surface. It can also be suggested

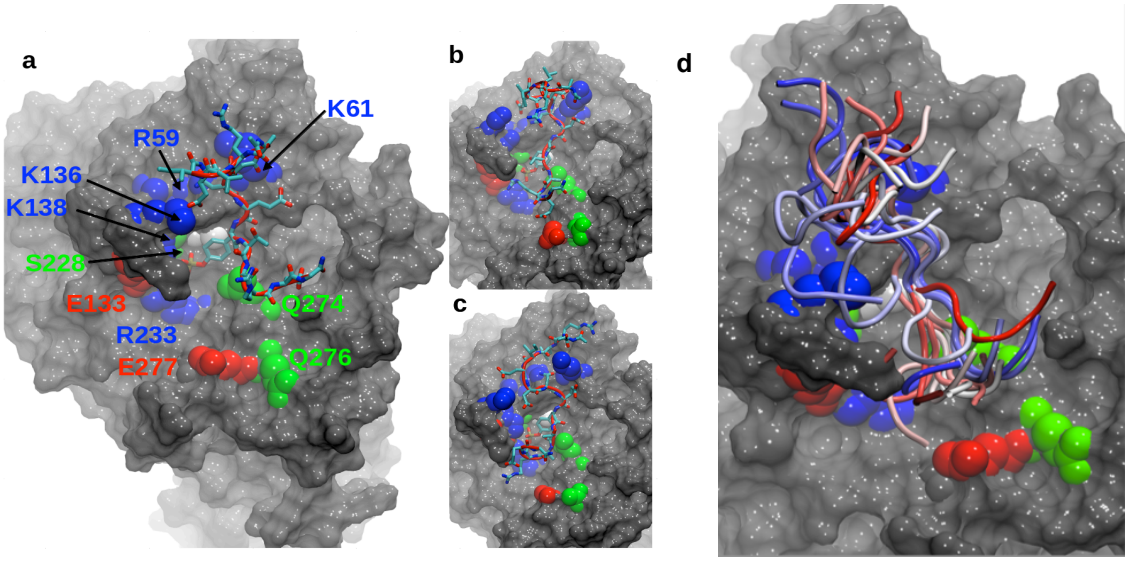

Figure 1.6. Dynamics of the LYP-**peptide 1** bound ensemble as revealed by 150 ns of molecular dynamics simulation. The Lyp surface is shown (gray) together with **peptide 1** (licorice model; red tube: backbone). Key residues making hydrogen bonds with the peptide at least 5% of the time during the simulation are highlighted using van der Waals spheres and color-coding depending on residue type. Key LYP-**peptide 1** snapshots correspond to simulation periods of (a) 0 ns (b) 70 ns and (c) 150 ns. (d) Ensemble of binding poses of **peptide 1** with LYP in MD simulation over 150 ns.

Table 1.1. List of residues involved in the intermolecular hydrogen bonding between the **peptide 1** and LYP from the 150 ns MD simulation. Only the residues involved in hydrogen bonding at least 5% of time are reported.

Peptide 1	LYP (Percentage)
E5	K136 (64%)
D6	K61 (7%)
	K136 (6%)
N7	K61 (24%)
	R59 (18%)
pY9	K138 (32%)
	S228 (93%)
	A229 (12%)
	R233 (98%)
	Q274 (10%)
T10	Q274 (7%)
R12	E133 (14%)
	E277 (9%)
E13	Q276 (6%)

based on this discussion that peptides can target LYP potently and selectively through their interactions with both conserved and nonconserved features on the LYP surface.

1.5 Summary

PTPs are highly specific and tightly regulated enzymes that play crucial roles in several biological processes and are important therapeutic targets. LYP is an interesting therapeutic target for treatment of several autoimmune disorders including anaphylaxis. However, precise biological functions of LYP in signaling cascades and cellular physiology are still poorly understood. Chemical probes can be beneficial for addressing biological questions pertaining to LYP by creating chemical knockdowns as well as for

therapeutic inhibition of LYP. For their optimum utility, these chemical probes need to be selective for LYP. Crucial insights about selective targeting of LYP can be gained from studying how LYP demonstrates substrate specificity *in vivo*. The substrate specificity of LYP *in vivo* can be attributed to the interactions of the substrates with the nonconserved features of LYP and to the biological regulation of LYP. Exploiting these interactions with nonconserved features of LYP catalytic domain as well as mimicking the regulatory mechanisms can help in targeting LYP selectively over other homologous PTPs. Peptides are arguably the most accurate mimics of biological substrates of LYP, which can target both the conserved and nonconserved features of LYP. Therefore, we suggest that peptides can play a huge role in developing chemical probes for LYP and other PTPs.

1.6 Perspective

The broad aim for this dissertation is to develop potent and selective inhibitors of LYP, which can find utility as chemical probes. As I have discussed earlier, LYP exhibits high substrate specificity *in vivo* that can be attributed both to the nonconserved features in the catalytic domain as well as the regulatory mechanisms. Therefore, we have hypothesized that exploiting these nonconserved features of LYP as well as mimicking the regulatory mechanisms can help improve LYP selectively over other homologous PTPs. Towards this end, we have taken several approaches for identifying potent and selective inhibitors of LYP that involve use of either peptides for exploiting non-conserved features of LYP or mimicry of a regulatory mechanism of LYP. Each of these approaches is discussed below in brief with the aim of introducing the following chapters of the dissertation.

Assay design is an important variable that influences the identification of biologically relevant inhibitors in a screen. The choice of substrate in the PTP inhibitor screen is crucial in guiding the outcome of the screen. Small molecule pY mimics bind only to the active site of LYP and, therefore, cannot accurately mimic biological substrates of LYP. Peptides are the accurate mimics of biological substrates of LYP, and they can target both the conserved and nonconserved features of LYP. Therefore, we hypothesized that using a peptide substrate can help in identifying more biologically relevant hits. With the aim of comparing the utility of a peptide substrate and a small molecule substrate as well as finding potent and selective LYP inhibitors, we have screened several compound libraries against LYP using both substrates. The results of this exercise are discussed in detail in Chapter 2.

We believe that potent inhibitors of LYP can be developed by mimicking the mechanisms of biological regulation. LYP is regulated by oxidation of the low pK_a catalytic cysteine residue in the active site. We decided to take advantage of oxidation of the catalytic cysteine residue of LYP to identify thiuram disulfides as pseudo-irreversible, covalent inhibitors of LYP that inhibit LYP by the formation of mixed disulfides. The results of this study are discussed in detail in Chapter 3.

Activity-based probes (ABPs) can serve as effective tools for addressing important biological questions pertaining to LYP. When developing ABPs for LYP, potent and selective covalent inhibitors of LYP must first be developed. Nonselective covalent inhibitors of PTPs usually contain pY-mimicking, cysteine-reactive electrophilic moiety. Peptide sequences can target LYP potently and selectively. We have combined selectivity offered by the peptide sequence with the utility of the covalent inhibitors to

develop peptide-based covalent inhibitors of LYP. The detailed results of this study are discussed in Chapter 4.

1.7 Experimental section

1.7.1. Computational modeling

An initial model of the human LYP protein was prepared with the Schrödinger Protein-Preparation wizard (*82*) based on PDB entry 2P6X (resolution 1.90 Å) assuming an apparent neutral pH (*68*). An initial model for **peptide 1** (ARLIEDNEpYTAREG) was prepared in which the pY moiety was created with tLEaP program (*83*), all the backbone dihedrals were set in *trans* configuration, and the N-and C-termini were capped with acetyl and methylamine groups, respectively. The initial model was generated by placing the P atom of the phosphotyrosine residue at a distance of 5 Å from the C227 C^{α} atom. The configuration of **peptide 1** was selectively minimized using the 'relax' procedure in xLEaP by constraining the position of the protein atoms in the system.

1.7.2 Molecular dynamics simulations

The AMBER12 simulation package was used for preparation of the system. The GPU version of PMEMD was used for trajectory production (*84, 85*). The Amber ff99SB force field (*86*) was employed for standard protein and peptide parameters. Parameters for the nonstandard phosphotyrosine residue were taken from the literature (*87*). The initial model was solvated using a pre-equilibrated box of TIP3P water molecules (*88*) maintaining a minimum distance of 15 Å between any protein atom and the box edges. The final truncated-octahedron box (56,762 atoms) contained a conservative number of

17,716 water molecules and 5 Cl^- ions added at random positions to neutralize the overall system.

The LYP-peptide system was minimized using the steepest descent algorithm (500 steps) and the conjugate gradient algorithm (500 steps). During the minimization protocol, the protein heavy atoms were kept close to their position in the X-ray model by an atom-positional harmonic restraining potential (total force constant of 250 kcal/mol/$Å^2$) in order to eliminate any strain between protein and solvent interactions. During the next standard stages of heating, equilibration, and production simulation run, Langevin dynamics (*89*) was used as the integrator with a collision frequency (γ) of 2 ps^{-1}. All the bonds involving hydrogen atoms were constrained using the SHAKE algorithm (*90*). The Particle Mesh Ewald approximation (*91*) was used for full electrostatic treatment (real space interactions truncated at 10 Å). In the initial stage of heating, 50 ps of the restrained MD simulation was performed with the protein heavy atoms restrained (total force constant of 10 kcal/mol/$Å^2$; 1 fs time step up to 200 K). Further, 100 ps of heating was performed with no restrains using canonical (NVT) ensemble to a final temperature of 300 K. The equilibration simulation was performed for 5 ns using a 2 fs time step and the pressure was maintained at 1 atm using an isotropic weak-coupling algorithm (*92*). The system was simulated for 150 ns at 300 K, saving MD snapshots every 10 ps for analysis.

1.8 References

1. Cohen, P. (2000) The regulation of protein function by multisite phosphorylation--a 25 year update, *Trends Biochem. Sci. 25*, 596-601.

2. Pinna, L. A., and Ruzzene, M. (1996) How do protein kinases recognize their substrates?, *Biochim. Biophys. Acta 1314*, 191-225.

3. Ubersax, J. A., and Ferrell, J. E., Jr. (2007) Mechanisms of specificity in protein phosphorylation, *Nat. Rev. Mol. Cell Biol. 8*, 530-541.

4. Hunter, T., and Sefton, B. M. (1980) Transforming gene product of Rous sarcoma virus phosphorylates tyrosine, *Proc. Natl. Acad. Sci. U.S.A. 77*, 1311-1315.

5. Cohen, P. (2001) The role of protein phosphorylation in human health and disease. The Sir Hans Krebs Medal Lecture, *Eur. J. Biochem. 268*, 5001-5010.

6. Guan, K. L., and Dixon, J. E. (1990) Protein tyrosine phosphatase activity of an essential virulence determinant in Yersinia, *Science 249*, 553-556.

7. Hunter, T. (1995) Protein kinases and phosphatases: The yin and yang of protein phosphorylation and signaling, *Cell 80*, 225-236.

8. Stoker, A. W. (2005) Protein tyrosine phosphatases and signalling, *J. Endocrinol. 185*, 19-33.

9. Zhang, Z.-Y. (2002) Protein tyrosine phosphatases: Structure and function, substrate specificity, and inhibitor development, *Annu. Rev. Pharmacol. Toxicol. 42*, 209-234.

10. Neel, B. G., and Tonks, N. K. (1997) Protein tyrosine phosphatases in signal transduction, *Curr. Opin. Cell Biol. 9*, 193-204.

11. Tonks, N. K., and Neel, B. G. (2001) Combinatorial control of the specificity of protein tyrosine phosphatases, *Curr. Opin. Cell Biol. 13*, 182-195.

12. Alonso, A., Sasin, J., Bottini, N., Friedberg, I., Friedberg, I., Osterman, A., Godzik, A., Hunter, T., Dixon, J., and Mustelin, T. (2004) Protein tyrosine phosphatases in the human genome, *Cell 117*, 699-711.

13. Manning, G., Whyte, D. B., Martinez, R., Hunter, T., and Sudarsanam, S. (2002) The protein kinase complement of the human genome, *Science 298*, 1912-1934.

14. Bialy, L., and Waldmann, H. (2005) Inhibitors of protein tyrosine phosphatases: Next-generation drugs?, *Angew. Chem. Int. Ed. 44*, 2-27.

15. Krishnamurthy, D., and Barrios, A. M. (2009) Profiling protein tyrosine phosphatase activity with mechanistic probes, *Curr. Opin. Chem. Biol. 13*, 375-381.

16. Zhang, Z.-Y. (2001) Protein tyrosine phosphatases: Prospects for therapeutics, *Curr. Opin. Chem. Biol. 5*, 416-423.

17. Zhang, Z.-Y. (2003) Chemical and mechanistic approaches to the study of protein tyrosine phosphatases, *Acc. Chem. Res. 36*, 385-392.

18. Buist, A., Zhang, Y. L., Keng, Y. F., Wu, L., Zhang, Z. Y., and den Hertog, J. (1999) Restoration of potent protein-tyrosine phosphatase activity into the membrane-distal domain of receptor protein-tyrosine phosphatase alpha, *Biochemistry 38*, 914-922.

19. Denu, J. M., Stuckey, J. A., Saper, M. A., and Dixon, J. E. (1996) Form and function in protein dephosphorylation, *Cell 87*, 361-364.

20. Zhang, Z. Y., Wang, Y., and Dixon, J. E. (1994) Dissecting the catalytic mechanism of protein-tyrosine phosphatases, *Proc. Natl. Acad. Sci. U.S.A. 91*, 1624-1627.

21. Denu, J. M., Lohse, D. L., Vijayalakshmi, J., Saper, M. A., and Dixon, J. E. (1996) Visualization of intermediate and transition-state structures in protein-tyrosine phosphatase catalysis, *Proc. Natl. Acad. Sci. U.S.A. 93*, 2493-2498.

22. Zhang, Z.-Y., Wang, Y., and Dixon, J. E. (1994) Dissecting the catalytic mechanism of protein tyrosine phosphatases, *Proc. Natl. Acad. Sci. U.S.A. 91*, 1624-1627.

23. Lohse, D. L., Denu, J. M., Santoro, N., and Dixon, J. E. (1997) Roles of aspartic acid-181 and serine-222 in intermediate formation and hydrolysis of the mammalian protein-tyrosine-phosphatase PTP1, *Biochemistry 36*, 4568-4575.

24. Andersen, J. N., Jansen, P. G., Echwald, S. M., Mortensen, O. H., Fukada, T., Del Vecchio, R., Tonks, N. K., and Moller, N. P. (2004) A genomic perspective on protein tyrosine phosphatases: Gene structure, pseudogenes, and genetic disease linkage, *FASEB J. 18*, 8-30.

25. Iversen, L. F., Moller, K. B., Pedersen, A. K., Peters, G. H., Petersen, A. S., Andersen, H. S., Branner, S., Mortensen, S. B., and Moller, N. P. (2002) Structure determination of T cell protein-tyrosine phosphatase, *J. Biol. Chem. 277*, 19982-19990.

26. Mustelin, T., Vang, T., and Bottini, N. (2005) Protein tyrosine phosphatases and the immune response, *Nat. Rev. Immunol. 5*, 43-57.

27. Alonso, A., Rahmouni, S., Williams, S., van Stipdonk, M., Jaroszewski, L., Godzik, A., Abraham, R. T., Schoenberger, S. P., and Mustelin, T. (2003) Tyrosine phosphorylation of VHR phosphatase by ZAP-70, *Nat. Immunol. 4*, 44-48.

28. Saxena, M., and Mustelin, T. (2000) Extracellular signals and scores of phosphatases: All roads lead to MAP kinase, *Semin. Immunol. 12*, 387-396.

29. Jung, S. K., Jeong, D. G., Yoon, T. S., Kim, J. H., Ryu, S. E., and Kim, S. J. (2007) Crystal structure of human slingshot phosphatase 2, *Proteins 68*, 408-412.

30. Diamond, R. H., Cressman, D. E., Laz, T. M., Abrams, C. S., and Taub, R. (1994) PRL-1, a unique nuclear protein tyrosine phosphatase, affects cell growth, *Mol. Cell Biol. 14*, 3752-3762.

31. Visintin, R., Craig, K., Hwang, E. S., Prinz, S., Tyers, M., and Amon, A. (1998) The phosphatase Cdc14 triggers mitotic exit by reversal of Cdk-dependent phosphorylation, *Mol. Cell 2*, 709-718.

32. Wishart, M. J., and Dixon, J. E. (2002) PTEN and myotubularin phosphatases: From 3-phosphoinositide dephosphorylation to disease, *Trends Cell Biol. 12*, 579-585.

33. Honda, R., Ohba, Y., Nagata, A., Okayama, H., and Yasuda, H. (1993) Dephosphorylation of human p34cdc2 kinase on both Thr-14 and Tyr-15 by human cdc25B phosphatase, *FEBS Lett. 318*, 331-334.

34. Rayapureddi, J. P., Kattamuri, C., Steinmetz, B. D., Frankfort, B. J., Ostrin, E. J., Mardon, G., and Hegde, R. S. (2003) Eyes absent represents a class of protein tyrosine phosphatases, *Nature 426*, 295-298.

35. Elchebly, M., Payette, P., Michaliszyn, E., Cromlish, W., Collins, S., Loy, A. L., Normandin, D., Cheng, A., Himms-Hagen, J., Chan, C. C., Ramachandran, C., Gresser, M. J., Tremblay, M. L., and Kennedy, B. P. (1999) Increased insulin sensitivity and obesity resistance in mice lacking the protein tyrosine phosphatase-1B gene, *Science 283*, 1544-1548.

36. Klaman, L. D., Boss, O., Peroni, O. D., Kim, J. K., Martino, J. L., Zabolotny, J. M., Moghal, N., Lubkin, M., Kim, Y. B., Sharpe, A. H., Stricker-Krongrad, A., Shulman, G. I., Neel, B. G., and Kahn, B. B. (2000) Increased energy expenditure, decreased adiposity, and tissue-specific insulin sensitivity in protein-tyrosine phosphatase 1B-deficient mice, *Mol. Cell Biol. 20*, 5479-5489.

37. He, R., Zeng, L. F., He, Y., Zhang, S., and Zhang, Z. Y. (2013) Small molecule tools for functional interrogation of protein tyrosine phosphatases, *FEBS J. 280*, 731-750.

38. Vang, T., Miletic, A. V., Arimura, Y., Tautz, L., Rickert, R. C., and Mustelin, T. (2008) Protein tyrosine phosphatases in autoimmunity, *Annu. Rev. Immunol. 26*, 29-55.

39. Swaminathan, S. (2003) Whither RNAi?, *Nat. Cell Biol. 5*, 489-490.

40. Cravatt, B. F., Wright, A. T., and Kozarich, J. W. (2008) Activity-based protein profiling: From enzyme chemistry to proteomic chemistry, *Annu. Rev. Biochem. 77*, 383-414.

41. Evans, M. J., and Cravatt, B. F. (2006) Mechanism-based profiling of enzyme families, *Chem. Rev. 106*, 3279-3301.

42. Fonovic, M., and Bogyo, M. (2007) Activity based probes for proteases: Applications to biomarker discovery, molecular imaging and drug screening, *Curr. Pharm. Des. 13*, 253-261.

43. Zhang, Z. Y. (2005) Functional studies of protein tyrosine phosphatases with chemical approaches, *Biochim. Biophys. Acta 1754*, 100-107.

44. Cohen, S., Dadi, H., Shaoul, E., Sharfe, N., and Roifman, C. M. (1999) Cloning and characterization of a lymphoid-specific, inducible human protein tyrosine phosphatase, Lyp, *Blood 93*, 2013-2024.

45. Karver, M. R., Krishnamurthy, D., Kulkarni, R. A., Bottini, N., and Barrios, A. M. (2009) Identifying potent, selective protein tyrosine phosphatase inhibitors from a library of Au(I) complexes, *J. Med. Chem. 52*, 6912-6918.

46. Krishnamurthy, D., Karver, M. R., Fiorillo, E., Orru, V., Stanford, S. M., Bottini, N., and Barrios, A. M. (2008) Gold(I)-mediated inhibition of protein tyrosine phosphatases: A detailed in vitro and cellular study, *J. Med. Chem. 51*, 4790-4795.

47. Xie, Y., Liu, Y., Gong, G., Rinderspacher, A., Deng, S.-X., Smith, D. H., Toebben, U., Tzilianos, E., Branden, L., Vidovic, D., Chung, C., Schurer, S., Tautz, L., and Landry, D. W. (2008) Discovery of a novel submicromolar inhibitor of the lymphoid tyrosine phosphatase, *Bioorg. Med. Chem. Lett. 18*, 2840-2844.

48. Yu, X., Sun, J.-P., He, Y., Guo, X., Liu, S., Zhou, B., Hudmon, A., and Zhang, Z.-Y. (2007) Structure, inhibitor and regulatory mechanism of LYP, a lymphoid-specific tyrosine phosphatase implicated in autoimmune diseases, *Proc. Natl. Acad. Sci. U.S.A. 104*, 19767-19772.

49. Gjorloff-Wingren, A., Saxena, M., Williams, S., Hammi, D., and Mustelin, T. (1999) Characterization of TCR-induced receptor-proximal signaling events negatively regulated by the protein tyrosine phosphatase PEP, *Eur. J. Immunol. 29*, 3845-3854.

50. Liu, Y., Stanford, S. M., Jog, S. P., Fiorillo, E., Orru, V., Comai, L., and Bottini, N. (2009) Regulation of lymphoid tyrosine phosphatase activity: Inhibition of the catalytic domain by the proximal interdomain, *Biochemistry 48*, 7525-7532.

51. Veillette, A., Rhee, I., Souza, C. M., and Davidson, D. (2009) PEST family phosphatases in immunity, autoimmunity, and autoinflammatory disorders, *Immunol. Rev. 228*, 312-324.

52. Wu, J., Katrekar, A., Honigberg, L. A., Smith, A. M., Conn, M. T., Tang, J., Jeffery, D., Mortara, K., Sampang, J., Williams, S. R., Buggy, J., and Clark, J. M. (2006) Identification of substrates of human protein-tyrosine phosphatase PTPN22, *J. Biol. Chem. 281*, 11002-11010.

53. Bottini, N., Musumeci, L., Alonso, A., Rahmouni, S., Nika, K., Rostamkhani, M., MacMurray, J., Pellecchia, M., Eisenbarth, G. S., Comings, D., and Mustelin, T. A. (2004) A functional polymorphism in lymphoid tyrosine phosphatase is associated with type I diabetes, *Nat. Genet. 36*, 337-338.

54. Vang, T., Congia, M., Macis, M. D., Musumeci, L., Orru, V., Zavattari, P., Nika, K., Tautz, L., Tasken, K., Cucca, F., Mustelin, T., and Bottini, N. (2005) Autoimmune-associated lymphoid tyrosine phosphatase is a gain-of-function variant, *Nat. Genet. 37*, 1317-1319.

55. Vang, T., Liu, W. H., Delacroix, L., Wu, S., Vasile, S., Dahl, R., Yang, L., Musumeci, L., Francis, D., Landscron, J., Tasken, K., Tremblay, M. L., Lie, B. A., Page, R., Mustelin, T., Rahmouni, S., Rickert, R. C., and Tautz, L. (2012) LYP inhibits T-cell activation when dissociated from CSK, *Nat. Chem. Biol. 8*, 437-446.

56. Siggs, O. M., Miosge, L. A., Yates, A. L., Kucharska, E. M., Sheahan, D., Brdicka, T., Weiss, A., Liston, A., and Goodnow, C. C. (2007) Opposing functions of the T cell receptor kinase ZAP-70 in immunity and tolerance differentially titrate in response to nucleotide substitutions, *Immunity 27*, 912-926.

57. Bottini, N., Vang, T., Cucca, F., and Mustelin, T. (2006) Role of PTPN22 in type 1 diabetes and other autoimmune diseases, *Semin. Immunol. 18*, 207-213.

58. Orru, V., Tsai, S., Rueda, B., Fiorillo, E., Stanford, S. M., Dasgupta, J., Hartiala, J., Zhao, L., Ortego-Centeno, N., D'Alfonso, S., Group, I. C., Arnett, F., Wu, H., Gonzalez-Gay, M., Tsao, B., Pons-Estel, B., Alarcon-Riquelme, M., He, Y., Zhang, Z.-Y., Allayee, H., Chen, X., Martin, J., and Bottini, N. (2009) A loss-of-function variant of PTPN22 is associated with reduced risk of systemic lupus erythematosus, *Hum. Mol. Genet. 18*, 569-579.

59. Cote, J. F., Charest, A., Wagner, J., and Tremblay, M. L. (1998) Combination of gene targeting and substrate trapping to identify substrates of protein tyrosine phosphatases using PTP-PEST as a model, *Biochemistry 37*, 13128-13137.

60. Gjorloff-Wingren, A., Saxena, M., Han, S., Wang, X., Alonso, A., Renedo, M., Oh, P., Williams, S., Schnitzer, J., and Mustelin, T. (2000) Subcellular localization of intracellular protein tyrosine phosphatases in T cells, *Eur. J. Immunol. 30*, 2412-2421.

61. Barr, A. J. (2010) Protein tyrosine phosphatases as drug targets: Strategies and challenges of inhibitor development, *Future Med. Chem. 2*, 1563-1576.

62. Heneberg, P. (2009) Use of protein tyrosine phosphatase inhibitors as promising targeted therapeutic drugs, *Curr. Med. Chem. 16*, 706-733.

63. Zhang, S., and Zhang, Z.-Y. (2007) PTP1B as a drug target: Recent developments in PTP1B inhibitor discovery, *Drug Discov. Today 12*, 373-381.

64. Zhang, Z.-Y., and Lee, S. Y. (2003) PTP1B inhibitors as potential therapeutics in the treatment of type 2 diabetes and obesity, *Exp. Opin. Investig. Drugs 12*, 223-233.

65. Kulkarni, R. A., Vellore, N. A., Bliss, M. R., Stanford, S. M., Falk, M. D., Bottini, N., Baron, R., and Barrios, A. M. (2013) Substrate selection influences molecular recognition in a screen for lymphoid tyrosine phosphatase inhibitors, *Submitted*.

66. Karver, M. R., Krishnamurthy, D., Bottini, N., and Barrios, A. M. (2010) Gold(I) phosphine mediated selective inhibition of lymphoid tyrosine phosphatase, *J. Inorg. Biochem. 104*, 268-273.

67. Obiri, D., Flink, N., Maier, J., Neeb, A., Maddalo, D., Thiele, W., Menon, A., Stassen, M., Kulkarni, R. A., Garabedian, M., Barrios, A. M., and Cato, A. (2012) PEST-domain-enriched tyrosine phosphatase and glucocorticoids as regulators of anaphylaxis in mice, *Allergy 67*, 175-182.

68. Barr, A. J., Ugochukwu, E., Lee, W. H., King, O. N., Filippakopoulos, P., Alfano, I., Savitsky, P., Burgess-Brown, N. A., Muller, S., and Knapp, S. (2009) Large-scale structural analysis of the classical human protein tyrosine phosphatome, *Cell 136*, 352-363.

69. Tiganis, T., and Bennett, A. M. (2007) Protein tyrosine phosphatase function: The substrate perspective, *Biochem. J. 402*, 1-15.

70. Karver, C. E., Ahmed, V. F., and Barrios, A. M. (2011) Oxidative inactivation of the lymphoid tyrosine phosphatase mediated by both general and active site directed NO donors, *Bioorg. Med. Chem. Lett. 21*, 285-287.

71. Biswas, S., Chida, A. S., and Rahman, I. (2006) Redox modifications of protein-thiols: Emerging roles in cell signaling, *Biochem. Pharmacol. 71*, 551-564.

72. den Hertog, J., Groen, A., and van der Wijk, T. (2005) Redox regulation of protein-tyrosine phosphatases, *Arch. Biochem. Biophys. 434*, 11-15.

73. Verweij, C. L., and Gringhuis, S. I. (2002) Oxidants and tyrosine phosphorylation: Role of acute and chronic oxidative stress in T-and B-lymphocyte signaling, *Antioxid. Redox Signal. 4*, 543-551.

74. Mahadev, K., Zilbering, A., Zhu, L., and Goldstein, B. J. (2001) Insulin-stimulated hydrogen peroxide reversibly inhibits protein-tyrosine phosphatase 1b in vivo and enhances the early insulin action cascade, *J. Biol. Chem. 276*, 21938-21942.

75. Tsai, S. J., Sen, U., Zhao, L., Greenleaf, W. B., Dasgupta, J., Fiorillo, E., Orru, V., Bottini, N., and Chen, X. S. (2009) Crystal structure of the human lymphoid

tyrosine phosphatase catalytic domain: Insights into redox regulation, *Biochemistry 48*, 4838-4845.

76. Asante-Appiah, E., Ball, K., Bateman, K., Skorey, K. I., Friesen, R., Desponts, C., Payette, P., Bayly, C., Zamboni, R., Scapin, G., Ramachandran, C., and Kennedy, B. P. (2001) The YRD motif is a major determinant of substrate and inhibitor specificity in T-cell protein tyrosine phosphatase, *J. Biol. Chem. 276*, 26036-26043.

77. Shen, K., Keng, Y. F., Wu, L., Guo, X. L., Lawrence, D. S., and Zhang, Z.-Y. (2001) Acquisition of a specific and potent PTP1B inhibitor from a novel combinatorial library and screening procedure, *J. Biol. Chem. 276*, 47311-47319.

78. Zhang, S., Chen, L., Luo, Y., Gunawan, A., Lawrence, D. S., and Zhang, Z.-Y. (2009) Acquisition of a potent and selective TC-PTP inhibitor via a stepwise fluorophore-tagged combinatorial synthesis and screening strategy, *J. Am. Chem. Soc. 131*, 13072-13079.

79. Siminovitch, K. A. (2004) PTPN22 and autoimmune disease, *Nat. Genet. 36*, 1248-1249.

80. Yu, X., Chen, M., Zhang, S., Yu, Z. H., Sun, J. P., Wang, L., Liu, S., Imasaki, T., Takagi, Y., and Zhang, Z. Y. (2011) Substrate specificity of lymphoid-specific tyrosine phosphatase (Lyp) and identification of Src kinase-associated protein of 55 kDa homolog (SKAP-HOM) as a Lyp substrate, *J. Biol. Chem. 286*, 30526-30534.

81. Mathews, R. A., and Barrios, A. M. (2013) Unpublished data.

82. Suite 2011: Epik, version 2.2, Schrödinger, LLC, New York, NY, 2011.

83. Case, D. A., Cheatham, T. E., Darden, T., Gohlke, H., Luo, R., Merz, K. M., Onufriev, A., Simmerling, C., Wang, B., and Woods, R. J. (2005) The Amber biomolecular simulation programs, *J. Comput. Chem. 26*, 1668-1688.

84. Case, D., Darden, T., Cheatham, T. E., 3rd, Simmerling, C. L., Wang, J., Duke, R., Luo, R., Walker, R., Zhang, W., Merz, K., Roberts, S., Hayik, S., Roitberg, A., Seabra, G., Swails, J., Götz, A., Klossvary, I., Wong, K., Paesani, F., Vanicek, J., Wolf, R., Liu, J., Wu, X., Brozell, S., Steinbrecher, T., Gohlke, H., Cai, Q., Ye, X., Wang, J., Hsieh, M.-J., Cui, G., Roe, D., Mathews, D., Seetin, M., Salomon-Ferrer, R., Sagui, C., Babin, V., Luchko, T., Gusarov, S., Kovalenko, A., and Kollman, P. (2012) AMBER 12, University of California, San Francisco.

85. Gotz, A. W., Williamson, M. J., Xu, D., Poole, D., Le Grand, S., and Walker, R. C. (2012) Routine microsecond molecular dynamics simulations with AMBER on GPUs. 1. Generalized Born, *J. Chem. Theory Comput. 8*, 1542-1555.

86. Hornak, V., Abel, R., Okur, A., Strockbine, B., Roitberg, A., and Simmerling, C. (2006) Comparison of multiple amber force fields and development of improved protein backbone parameters, *Proteins 65*, 712-725.

87. Homeyer, N., Horn, A. H., Lanig, H., and Sticht, H. (2006) AMBER force-field parameters for phosphorylated amino acids in different protonation states: Phosphoserine, phosphothreonine, phosphotyrosine, and phosphohistidine, *J. Mol. Model. 12*, 281-289.

88. Jorgensen W L, C. J., Madura J D, Impey R W, Klein M L. (1983) Comparison of simple potential functions for simulating liquid water, *J. Chem. Phys. 79*, 926.

89. Pastor, R., Brooks, B., and Szabo, A. (1988) An analysis of the accuracy of Langevin and molecular dynamics algorithms, *Mol. Phys. 65*, 1409-1419.

90. Miyamoto, S., and Kollman, P. (1992) Settle: An analytical version of the SHAKE and RATTLE algorithm for rigid water models, *J. Comput. Chem. 13*, 952-962.

91. Darden, T., York, D., and Pedersen, L. (1993) Particle mesh Ewald: An N·log(N) method for Ewald sums in large systems, *J. Chem. Phys. 98*, 10089-10092.

92. Martyna, G., Tobias, D., Klein, M., and Glenn J Martyna, D. J. T., and Michael L Klein. (1994) Constant pressure molecular dynamics algorithms, *J. Chem. Phys. 101*, 4177-4189.

CHAPTER 2

SUBSTRATE SELECTION INFLUENCES HIT IDENTIFICATION IN A SCREEN FOR LYMPHOID TYROSINE PHOSPHATASE INHIBITORS

2.1 Introduction and preliminary studies

Tyrosine phosphorylation is one of the most important cellular posttranslational modifications, generating recognition motifs for protein-protein interactions, modulating enzyme activity and controlling many aspects of cell growth, differentiation, metabolism, migration and survival (*1, 2*). The enzymes responsible for modulating tyrosine phosphorylation, PTPs and PTKs, have been recognized as relevant therapeutic targets for the treatment of diabetes, cancer and autoimmunity, but only PTK inhibitors have made it to the clinic thus far (*3, 4*). Considerable effort has been devoted to the development of potent, selective PTP inhibitors for use as chemical probes and potential therapeutic leads, but there are still several challenges in the field (*5-10*). Specifically, many of the PTP inhibitors identified to date are phosphotyrosine mimetic compounds with poor bioavailability. In addition, due to the highly conserved nature of the PTP active site, inhibitors that target the pY binding pocket tend to inhibit many members of the PTP family of enzymes and selectivity has been difficult to obtain. However, similar challenges have been resolved in the design of therapeutically relevant PTK inhibitors, and it is likely that with the right set of tools for inhibitor screening, PTP-targeted therapeutics can be developed as well.

The human genome contains a total of 107 genes encoding a PTP domain; 81 of these genes are predicted to encode an active PTP domain (*11*). The PTP catalytic domain is highly conserved and contains the PTP signature motif, (H/V)**C**$(X)_5$**R**(S/T), which includes the catalytic cysteine residue and the arginine residue which plays a key role in recognizing the pY moiety of the substrate (*12*). However, PTPs exhibit diverse surface features outside the pY binding pocket that remain largely unexplored in inhibitor

development (*4, 13*). An exception is the secondary substrate-binding pocket, which has been exploited for the development of selective inhibitors of PTP1B and TCPTP (*14-16*).

Recently, the lymphoid tyrosine phosphatase (LYP or PTPN22) has been recognized as an intriguing therapeutic target because of its association with human autoimmunity (*17-21*). LYP is a negative regulator of T-cell receptor signaling (*22*). A single nucleotide polymorphism (SNP) (C1858T) in the *PTPN22* gene results in a gain of function variant of LYP that is associated with an increased risk of autoimmune disorders including type 1 diabetes, rheumatoid arthritis, systemic lupus erythematosus, Grave's disease and myasthenia gravis (*23-25*). Correspondingly, the G788A SNP in the *PTPN22* gene leads to a loss of function variant that is protective against systematic lupus erythematosus (*26*). Furthermore, the mouse ortholog of LYP (PEP) is a positive regulator of anaphylaxis in mice and both genetic and chemical knockdown of LYP (PEP) activity has been shown to alleviate anaphylaxis in mice (*27*). Taken together, these findings reinforce the importance of LYP in the immune response. While inhibition of LYP activity could be therapeutically beneficial, inhibition of other T-cell derived PTPs is likely to be detrimental. Therefore, if therapeutic LYP inhibitors are to be developed, the issue of PTP selectivity must be addressed.

Assay design is an important variable that influences the identification of biologically relevant inhibitors in a screen. We (*18, 28*) and others (*29*) have hypothesized that the choice of substrate in the PTP inhibitor screen is crucial in guiding the outcome of the screen. PTPs catalyze conversion of pY (Figure 2.1) to tyrosine (Y) and inorganic phosphate (P_i). Therefore, PTP activity can be monitored by measuring the

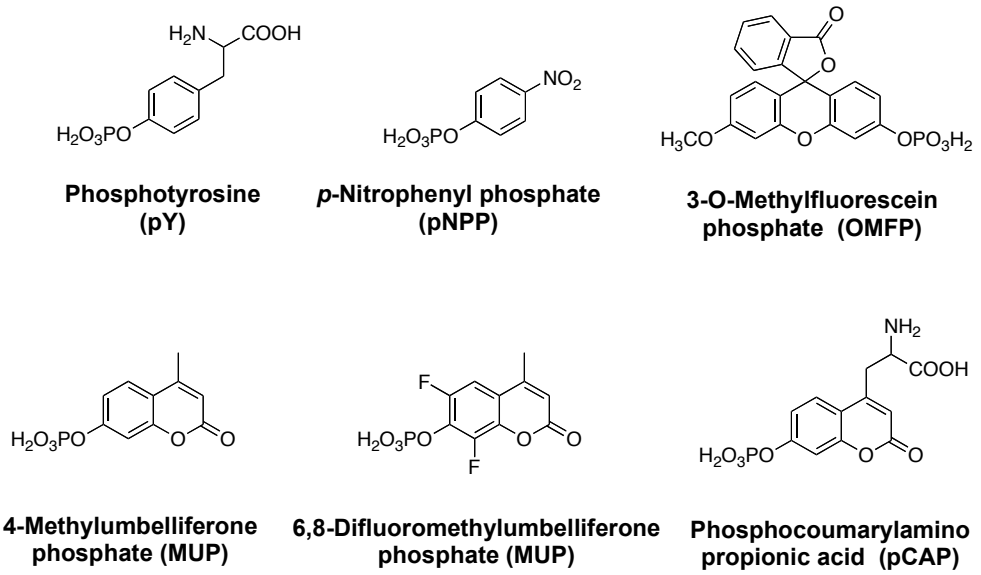

Figure 2.1. Colorimetric and fluorogenic PTP substrates.

formation of either of the product of this reaction P_i or tyrosine. The released P_i can react readily with molybdenum(VI) to form phosphomolybdate. Malachite green can form a green colored complex with phosphomolybdate at low pH. Therefore, by measuring the absorption at 620-660 nm, amount of P_i can be determined which is a direct indicator of the PTP activity (*30*). However, malachite green assay is a discontinuous assay and therefore, measuring kinetics with this assay is laborious. Peptides containing pY are the most accurate mimics of the biological substrates of the PTPs and therefore, monitoring the dephosphorylation of pY peptides gives most optimum measure of PTP activity. Products of dephosphorylation of pY peptides, the corresponding Y peptides show increased absorption at 280 nm and increase in fluorescence at 305 nm and therefore, PTP activity can be monitored by measuring the increase in absorption or fluorescence. The biggest downfall to this method is that increase in absorbance and fluorescence is

very small and in this region of spectrum the background, due to interference caused even by buffer components, is usually very high. Therefore, this assay has a low sensitivity.

To overcome these problems, traditional assays for PTP inhibitor screening use nonpeptidic pY mimetic substrate such as *p*-nitrophenyl phosphate (*p*NPP), 3-*O*-methylfluorescein phosphate (OMFP), 4-methylumbelliferone phosphate (MUP), and 6,8-difluoro-4-methylumbelliferone phosphate (DiFMUP) (Figure 2.1) (*31*). One of the most commonly used substrates of PTPs, *p*NPP itself is colorless. However, upon hydrolysis it forms *p*-nitrophenol, which at alkaline pH ionizes to bright yellow phenolate ion that can be detected by measuring absorbance at 405 nm. OMFP is a fluoregenic substrate of phosphatases that upon hydrolysis forms 3-*O*-methylfluorescein (OMF). The formation of OMF can be monitored at emission wavelength of 528 nm upon excitation at 485 nm. Other fluoregenic substrates for PTPs include MUP and DiFMUP. These substrates are slightly fluorescent themselves but upon dephosphorylation produce highly fluorescent 4-methylumbelliferone (MU) and 6,8-difluoro-4-methylumbelliferone (DiFMU), respectively. The formation of MU and DiFMU can be monitored at emission wavelength of 455 nm upon excitation at 360 nm. However, *p*NPP and DiFMUP are highly activated substrates due to the presence of strong electron withdrawing groups and therefore, both these substrates are susceptible to autohydrolysis resulting in high background. MUP is not an activated substrate and therefore it mimics pY more accurately than *p*NPP and DiFMUP. However, all these nonpeptidic pY mimetic substrates, owing to their size, predominantly only interact with the active site of the PTPs. These small molecule substrates, therefore, cannot accurately mimic biological substrates of PTPs like pY peptides. It has also been suggested that a substrate capable of

interacting with sites on the enzyme outside of the pY binding site would be superior to a simple small molecule pY mimetic substrate in identifying hits with biological activity and selectivity for the enzyme of interest (*18, 29*). Our collaborators have shown in Chapter 1 through molecular dynamics (MD) simulation that peptide substrates interact with both conserved and nonconserved features of LYP. Together with the known problems associated with the spectroscopic properties of pY peptides, it is clear that an ideal substrate should combine the utility of the fluoregenic pY mimics with the bio-mimetic properties of the peptides.

With this in mind, our group has developed a phosphorylated coumaryl aminopropionic acid (pCAP, Figure 2.1). This phosphotyrosine mimetic amino acid can be readily incorporated into a peptide chain and, upon PTP-mediated dephosphorylation, undergoes a large increase in fluorescence, providing a facile, high-throughput assay for PTP activity (*18, 32*). For example, by incorporating pCAP in the place of pY in a peptide sequence based on the amino acid residues flanking Y394 of Lck, a known physiological substrate of LYP (*25, 33*), **peptide 1** (Figure 2.2), an excellent substrate for LYP was obtained (*18*). In order to establish the similarity of **peptide 1** with the biological substrate of the LYP, we decided to compare the kinetic properties of **peptide 1** with the most accurate mimic of biological substrate of LYP, **peptide 1A** (Figure 2.2). LYP showed similar Michaelis binding constant (K_m) and turnover number (k_{cat}) within errors for **peptide 1** and **peptide 1A** (Table 2.1). Therefore, we think that **peptide 1** can be used as a surrogate for **peptide 1A** in a screen for LYP inhibitors.

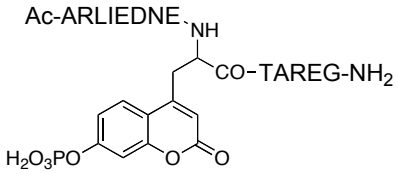

Peptide 1

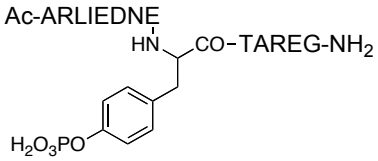

Peptide 1A

Figure 2.2. Peptides based on sequence of amino acid residues flanking Lck Y394, a biological substrate of LYP.

Table 2.1. Kinetics of LYP mediated dephosphorylation of peptides based on sequence of amino acid residues flanking Lck Y394, a biological substrate of LYP.

Peptide	k_{cat}, x10^3 (s^{-1})	K_m, x10^{-4} (M)	k_{cat}/K_m, x10^7 ($M^{-1}s^{-1}$)
Peptide 1	5.4 ± 1.0	2.0 ± 0.6	2.7
Peptide 1A	6.7 ± 0.4	1.3 ± 0.2	5.2

With the aim of qualitatively comparing the different PTP assays, we calculated the signal to background ratio (S/B) and the signal to noise ratio (S/N) for these assays (Table 2.2). The working concentration of the substrate used was selected to get the S/B roughly around 10, with maximum substrate concentration used fixed at 500 μM. A high concentration of **peptide 1A** was required to get reasonable S/B in malachite green assay. However despite low S/B, this assay was still found to be very sensitive owing to the very little variability in the background. Next, monitoring increase in fluorescence upon dephosphorylation of **peptide 1A** was found to be a low sensitivity assay, primarily owing to the high background values in this region of the spectrum. Requirement of high concentrations of **peptide 1A** for these assays along with the low sensitivity of the flurescence assay and tedious nature of the malachite green assay warrant development of a better approach towards assaying LYP activity.

Among the fluoregenic substrates of PTPs, MUP showed fairly low S/B and but reasonable sensitivity at 500 μM concentration. This finding indicates that a much higher concentration of MUP is required to render the assay sensitive. On the other hand, DiFMUP was found to be an excellent substrate that showed very high values for S/B and S/N even at low to submicromolar concentration. Next, we tested the sensitivity of the LYP assay using **Peptide 1** as a substrate. **Peptide 1** is a fluoregenic substrate that combines the desirable properties of **peptide 1A** and MUP. Assay using low micromolar concentration of **peptide 1** as a substrate showed much better S/B and S/N than assays for both **peptide 1A** and MUP. Therefore, we hypothesized that owing to its resemblance to the biological substrate of LYP and fluoregenic property, **peptide 1** will be more useful in a screen for LYP inhibitors in identifying more biologically relevant hits.

Table 2.2. Qualitative comparison of some of the important PTP assays. All assays were carried out using final concentration of 5 nM LYP, preactivated with 1 mM DTT in the same activity buffer described in the experimental section.

Substrate	Method and readout	[Substrate]	S/B	S/N
Peptide 1A	Malachite Green Assay Absorption 620 nm	250 μM 500 μM	6 6	394 1748
Peptide 1A	Fluorescence Excitation 280 nm Emission 305 nm	500 μM	2	12
MUP	Fluorescence Excitation 360 nm Emission 455 nm	500 μM	6.5	94
DiFMUP	Fluorescence Excitation 360 nm Emission 455 nm	0.5 μM 1.5 μM	25 235	188 1325
Peptide 1	Fluorescence Excitation 360 nm Emission 455 nm	10 μM 25 μM	10 55	235 730

In the past 6 years, several LYP inhibitors with high nanomolar to low micromolar potencies were reported in the literature (Figure 2.3). A benzofuran salicylic acid derivative (I-C11) was identified from a library of 80 compounds synthesized using click chemistry (*21*). A cocrystal structure of I-C11 and LYP revealed that benzofuran salicylic acid core occupied the LYP active sight while the naphthalene ring occupied the neighboring hydrophobic pocket. This bidentate salicyclic acid derivative showed some selectivity for LYP over other T-cell derived PTPs, but only a little selectivity was observed over PTP1B and no information about PTP-PEST inhibition was reported. Thiazolidine-2,4-diones (TZDs) and 2-thiaoxothiazolidin-4-ones were identified as LYP inhibitors from a screen of the NIH molecular libraries using DiFMUP (*20*). Further SAR studies on the hits led to identification of TZD 8P as a submicromolar inhibitor of LYP (Figure 2.3). Compounds in this series also owed their potent inhibitory activity to the presence of salicylate moiety. However, no information was provided about the selectivity or the cellular activity of these inhibitors. WPD loop of LYP is known to be highly mobile and it keeps switching between an active closed conformation and an inactive open conformation. With the aim of identifying inhibitors that bind to and stabilize the inactive open conformation of LYP, a virtual ligand screen was performed with this open conformation of LYP (*34*). Further experimental evaluation of the hits from this virtual screening exercise, helped in identifying a series of 2-benzamidobenzoic acid derivatives as submicromolar inhibitors of LYP but no selectivity or cellular activity data was reported for these inhibitors either.

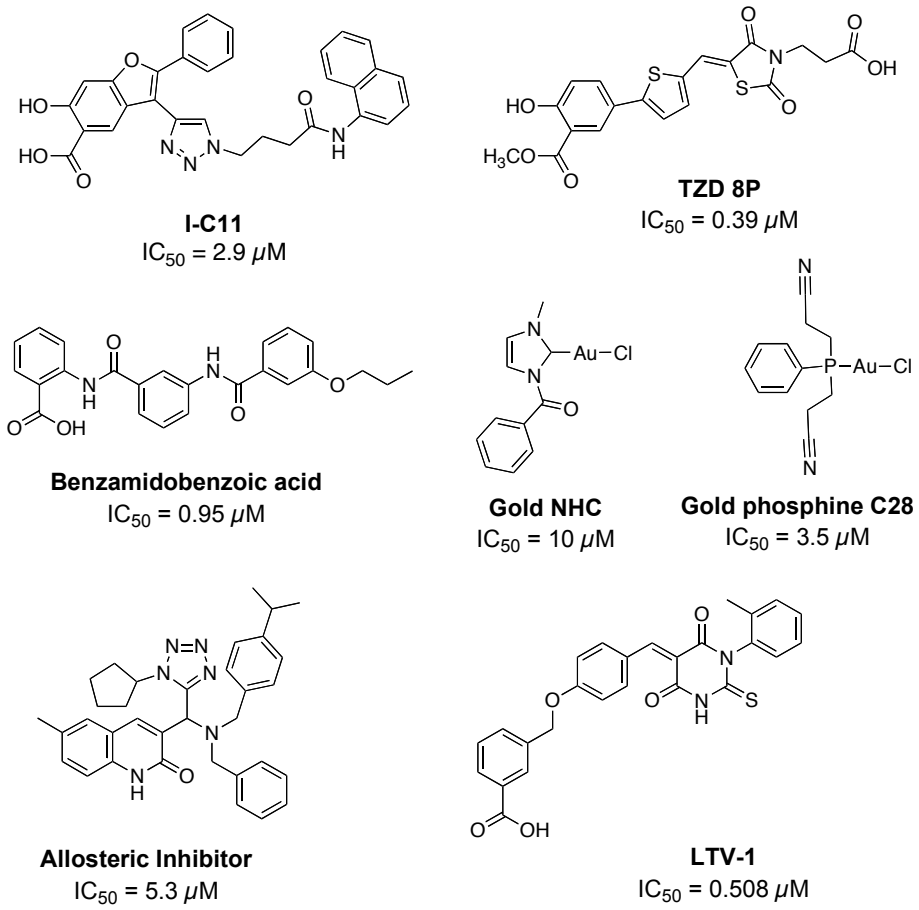

Figure 2.3. LYP inhibitors reported in the literature.

Auranofin and other gold(I) compounds have been used in the treatment of autoimmune disorders for decades but their biological targets are not completely known. Owing to the thiophilicity of gold, these compounds have been shown to inhibit cysteine proteases such as cathepsins and thioredoxin reductase (*35-38*). Our laboratory has demostrated that the gold-based antiarthitic drug auranofin inhibits PTP-PEST activity 20-fold better than LYP activity and several gold(I) *N*-heterocyclic carbenes (gold NHC, Figure 2.3) inhibit LYP (*19*). Although these compounds show excellent cellular

inhibition of LYP, they do not show selectivity for LYP inhibition over PTP-PEST, HePTP and PTP1B. Our lab also identified a related gold(I) phosphine complex with up to 25-fold selectivity for LYP over PTP-PEST from a library of 40 different gold(I) phosphines, providing perhaps the best evidence inhibitors that show selectivity for LYP over PTP-PEST can be developed (*18*).

An allosteric inhibitor of LYP was identified from a screen of a 4000 compound library. The mode of inhibition for this inhibitor was found to be noncompetitive. This inhibitor was shown to bind to a hydrophobic patch located outside the active site of LYP. It showed excellent cellular activity and it was shown to increase T-cell signaling in primary T-cells. Although this inhibitor showed some selectivity for LYP over the homologous PTPs, selectivity over PTP-PEST was not obtained. LTV-1 was identified through high-throughput screening effort. Impressively, this compound showed >200-fold selectivity for inhibition of LYP over PTP-PEST but showed only about 3-fold selectivity for LYP over TCPTP and PTP1B.

Although these LYP inhibitors have proven useful as chemical probes of the biological activity of LYP, greater potency and selectivity must be achieved in order to obtain a widely applicable probe. With this in mind and with the aim of establishing the utility of **peptide 1**, we screened compound libraries for LYP inhibition using **peptide 1** and a small molecule pY mimic, DiFMUP, as substrates.

2.2 Results and discussion

The screening conditions were first optimized for each substrate to achieve acceptable assay performance, sensitivity and robustness. The Z′ value of 0.68 for

peptide 1 and 0.81 for DiFMUP indicated excellent performance in the screening assays. The signal to background ratio (S/B) of ~10 and ~128, and the signal to noise ratio (S/N) of ~235 and ~1325, for **peptide 1** and DiFMUP assays, respectively, indicate sensitive and robust assay conditions. To test the hypothesis that substrate selection can influence screening results, two, parallel, medium-throughput experimental screens of the Spectrum collection, a commercially available collection of 2000 compounds, were carried out, one using **peptide 1** as the substrate and the second using DiFMUP. The spectrum collection consists of FDA approved drugs (50%), other bioactive compounds that have either not reached the developmental stages or been dropped for toxicological or other reasons (20%) and natural products with known and unknown biological activity isolated from variety of natural sources (30%). The compounds in this library are selected to provide a wide range of biological activities and structural diversities. Extensive studies have already been carried out with the known FDA approved drugs as well as several other bioactive compounds and natural products in this library to ensure their viability as therapeutics in humans. The availability of adequate information about the SAR of these compounds also means that the optimization of the hits from the library screening is relatively easy. Libraries of this kind have been used to obtain hits for many different applications including cancer, malaria and amebiasis (*35, 39-41*). Taken together, screening of small, focused libraries of chemically diverse, drug-like compounds can accelerate the drug discovery process by finding new applications of known compounds (*35, 39, 41*). The chemical and biological diversity of this library, together with the knowledge that several drugs and natural products are already known to inhibit different PTPs (*7*), warrant the possibility of finding new classes of compounds that are previously

unknown to inhibit PTPs. Besides this, identifying PTP inhibitors from a library of drug-like compounds also validates the utility of peptidic substrates in PTP inhibitor screenings.

The results of the initial screen using **peptide 1** as the substrate are shown in Figure 2.4. The most potent hits, along with hits that showed significantly different inhibition of LYP activity depending on whether **peptide 1** or DiFMUP was used as the substrate were selected for follow-up. The initial cut-off for the hits was set to inhibition of at least 30% of LYP activity at 10 μM. Although about 10% of the compounds fulfilled this criterion, the hit rate was then brought down to 4% (a total of 80 compounds) by cherry-picking the hits for the follow-up studies. The most potent hits, along with hits that inhibited LYP activity significantly better or worse with DiFMUP as a substrate than with **peptide 1** as a substrate, were selected in the cherry picking. These top 80 compounds (Table 2.3) were rescreened against LYP and counter-screened against PTP-PEST at 5 μM and 50 μM concentrations. Results are shown in Figure 2.5 (rescreening with LYP), Figure 2.6 (counter-screening with PTP-PEST) and Figure 2.7 (selected results from rescreening with LYP). A few previously known PTP inhibitors including suramin (compound 1), purpurin (compound 5) and aurothioglucose (compound 9) came up as top hits in both of our screens, validating our screening protocol (*7, 19, 42-44*). However, most of the top hits were compounds that had not been identified as phosphatase inhibitors previously. While some of the hits were equally potent inhibitors of LYP activity regardless of substrate used, others inhibited LYP activity on **peptide 1** significantly better than on DiFMUP or vice versa (Figure 2.7, Table 2.4). Finally, a more detailed investigation was carried out on several top hits by

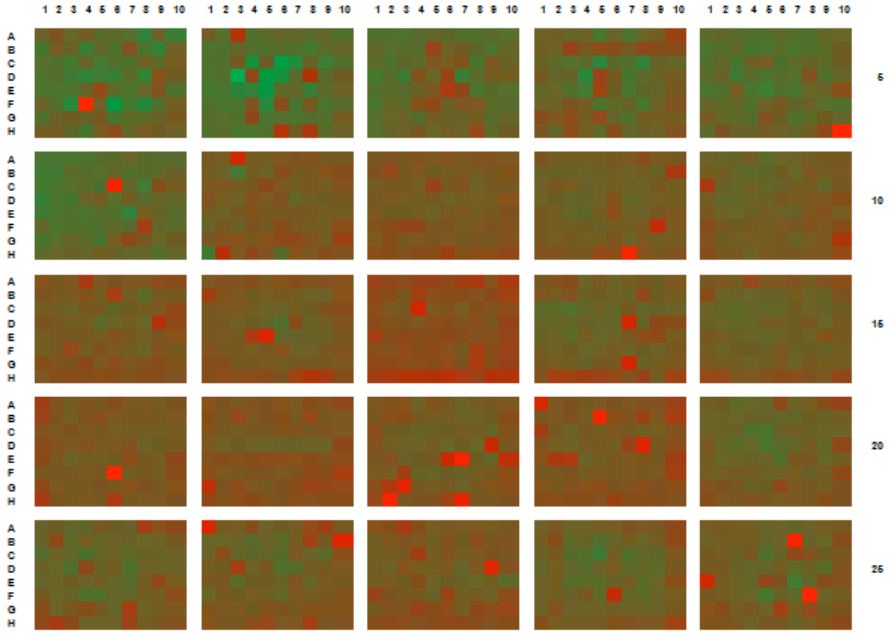

Figure 2.4. Results from the Spectrum collection screen for LYP inhibitors using **peptide 1** as the substrate. Each compound is represented by its position in one of the 25 96-well plates in the collection. Compounds showing significant inhibition at 10 μM are indicated as red squares, compounds showing no inhibition are indicated as green squares, compounds with intermediate inhibitory properties are shown in the intermediate colors (gradient from red to green).

Table 2.3. List of top 80 hits from Spectrum library screen (numbering as in Figures 2.5 and 2.6).

1	COUMARIN	41	CLOFAZIMINE
2	AMPHOTERICIN B	42	CAPERATIC ACID
3	CEFOTAXIME SODIUM	43	XANTHONE
4	CYCLIZINE	44	IRIGENOL
5	PYRITHIONE ZINC	45	GINKGOLIC ACID
6	ESTRADIOL CYPIONATE	46	LARIXOL ACETATE
7	GUANETHIDINE SULFATE	47	2',2'-BISEPIGALLOCATECHIN DIGALLATE
8	HALOPERIDOL	48	OSAJIN
9	HEXACHLOROPHENE	49	3β-HYDROXY-DEOXODIHYDRODEOXYGEDUNIN
10	HYDROCORTISONE ACETATE	50	PURPURIN
11	INOSITOL	51	HEMATEIN
12	MERBROMIN	52	ELLAGIC ACID
13	FLUFENAMIC ACID	53	PRIMULETIN
14	FENSPIRIDE HYDROCHLORIDE	54	7,4'-DIHYDROXYFLAVONE
15	RONIDAZOLE	55	3',4'-DIMETHOXYFLAVONE
16	TRANEXAMIC ACID	56	JUGLONE
17	CEPHALEXIN	57	CAMPTOTHECIN
18	CEFSULODIN SODIUM	58	EMBELIN
19	SURAMIN	59	EPIGALLOCATECHIN 3,5-DIGALLATE
20	VIGABATRIN	60	3,4'-DIHYDROXYFLAVONE
21	THIRAM	61	HARMALOL HYDROCHLORIDE
22	IOPANIC ACID	62	OXONITINE
23	CEFTIBUTEN	63	AESCULIN
24	SERTRALINE HYDROCHLORIDE	64	5,7-DIHYDROXYISOFLAVONE
25	CHLOROPHYLLIDE Cu COMPLEX Na SALT	65	THEAFLAVIN
26	METHYLDOPATE HYDROCHLORIDE	66	4-NONYLPHENOL
27	BENZOXYQUINE	67	5beta-12-METHOXY-4,4-BISNOR-8,11,13-PODOCARPATRIEN-3-ONE
28	GEMIFLOXACIN MESYLATE	68	L-BUTHIONINE SULFOXIMINE
29	PRAVASTATIN SODIUM	69	METHYLPREDNISOLONE SODIUM SUCCINATE
30	DESOXYMETASONE	70	2,4-DINITROPHENOL
31	BENZBROMARONE	71	EFAROXAN HYDROCHLORIDE
32	DIMERCAPROL	72	NEORUSCOGENIN
33	METHYLBENZETHONIUM CHLORIDE	73	PROTOPORPHYRIN IX
34	CHLOROGUANIDE HYDROCHLORIDE	74	PRIDINOL METHANESULFONATE
35	MOXIDECTIN	75	BENZANTHRONE
36	PHYTONADIONE	76	NIPECOTIC ACID
37	BETAMETHASONE ACETATE	77	AZOBENZENE
38	BROMPERIDOL	78	HYDROXYTACRINE MALEATE
39	OXANTEL PAMOATE	79	ANTHRACENE-9-CARBOXYLIC ACID
40	ORNIDAZOLE	80	5,7-DIHYDROXY-4-METHYLCOUMARIN

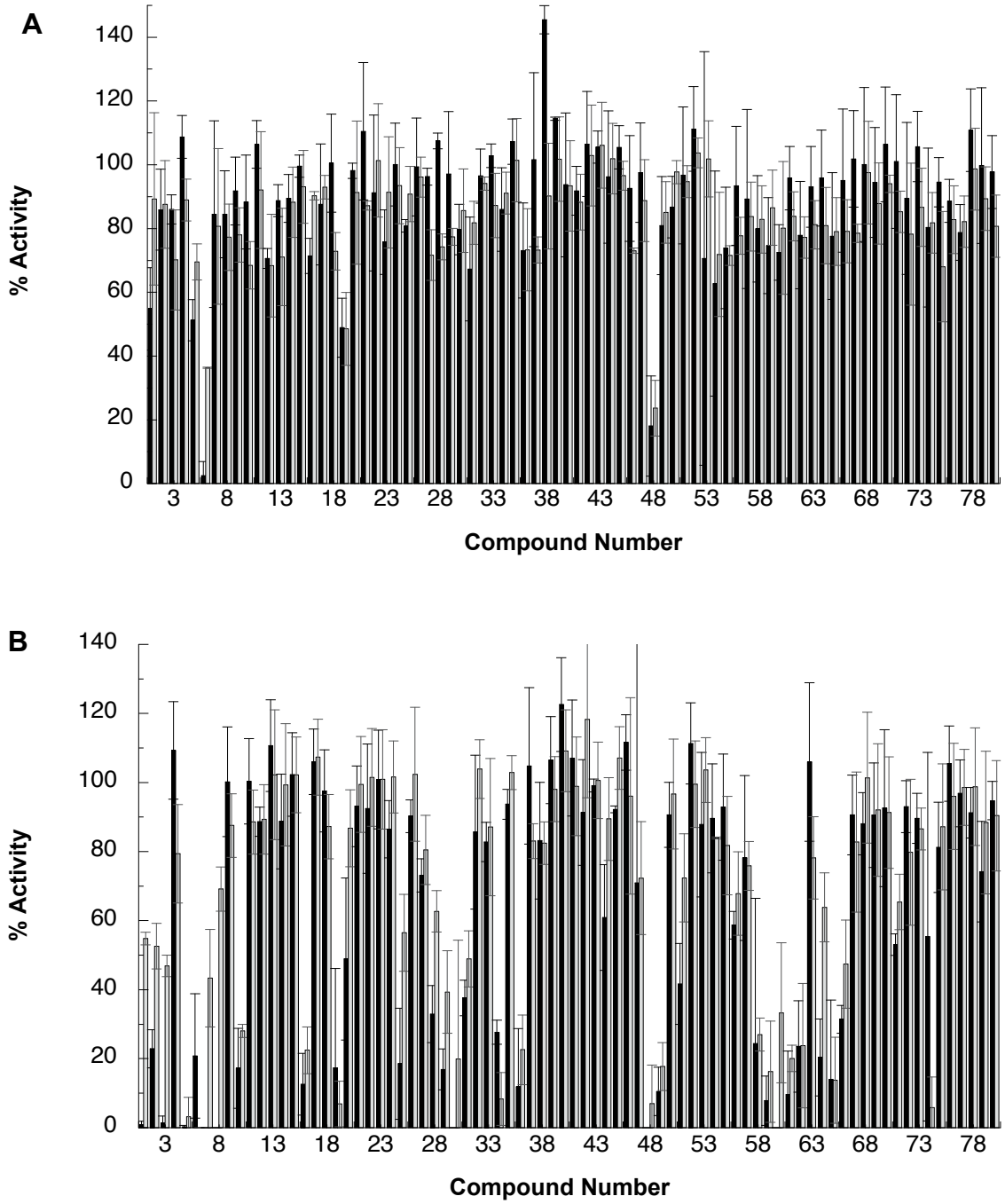

Figure 2.5. Secondary screen showing the ability of the top 80 hits from the Spectrum library screen to inhibit LYP activity at (A) 5 μM and (B) 50 μM using **peptide 1** (black bars) or DiFMUP (grey bars) as the substrate.

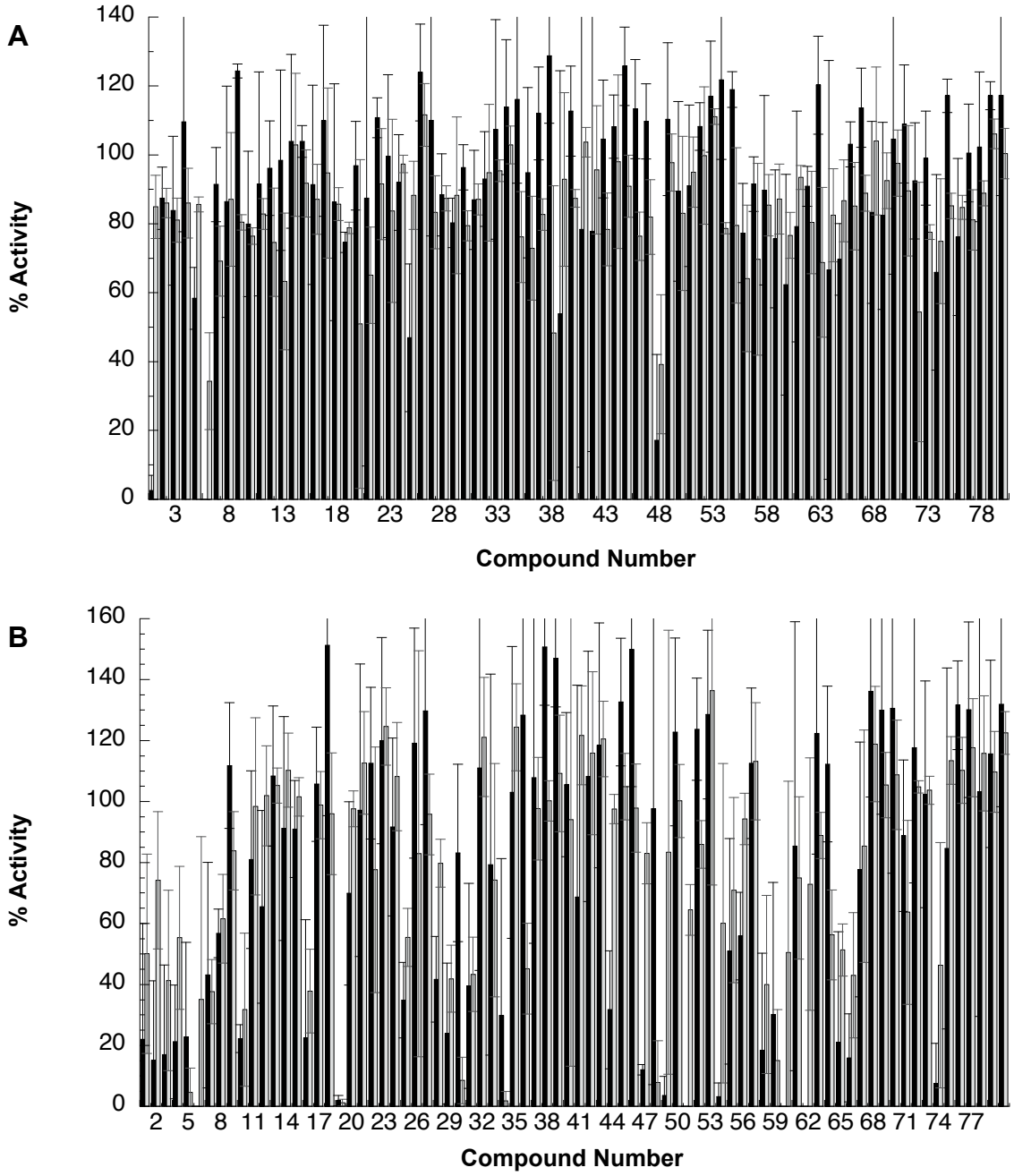

Figure 2.6. Secondary screen showing the ability of the top 80 hits from the Spectrum library screen to inhibit PTP-PEST activity at (A) 5 μM and (B) 50 μM using **peptide 1** (black bars) or DiFMUP (grey bars) as the substrate.

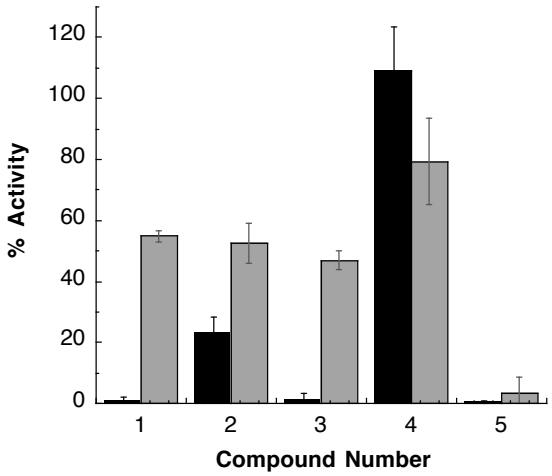

Figure 2.7. Select hits from the rescreening of top 80 compounds from the Spectrum collection at 50 μM using peptide 1 (black bars) or DiFMUP (grey bars) as the substrate.

Table 2.4. Hit validation and counter screening of selected hits from the Spectrum library screen. IC_{50} values are shown in μM.

Compound number	Compound name	LYP (DiFMUP)	LYP (peptide 1)	PTP-PEST (DiFMUP)	PTP-PEST (peptide 1)	HePTP (DiFMUP)	CD45 (DiFMUP)
1	Suramin	25.0 ± 0.3	3.0 ± 0.1	27 ± 3	11 ± 1	30 ± 3	42 ± 5
2	Caperatic acid	12 ± 1	6.5 ± 0.7	NA	NA	NA	NA
3	Cefotaxime	40 ± 2	17 ± 2	70.0 ± 0.8	NA	NA	NA
4	Sertraline	44 ± 3	150 ± 10	55 ± 5	NA	110 ± 5	80 ± 4
5	Purpurin	4.0 ± 0.2	2.0 ± 0.1	7.0 ± 0.6	5.0 ± 0.6	NA	6 (ref 43)
6	Epigallocatechin 3,5-digallate	0.050 ± 0.002	0.050 ± 0.003	0.020 ± 0.001	0.020 ± 0.001	NA	0.50 ± 0.03
7	Harmalol HCl	15 ± 2	7.0 ± 0.8	35 ± 2	35 ± 2	NA	14 ± 1
8	Benzanthrone	28 ± 1	13 ± 1	> 150	> 150	35 ± 5	> 150
9	Aurothioglucose	4.0 ± 0.1	1.5 ± 0.1	8 ± 1	5 ± 0.8	NA	NA
10	Sennoside A	5.0 ± 0.3	5.0 ± 0.1	0.40 ± 0.03	0.20 ± 0.01	1.0 ± 0.1	2.0 ± 0.1

determining their IC_{50} values against LYP using both DiFMUP and **peptide 1** in secondary dose-response screens. The selectivity of these top hits was profiled by determining their IC_{50} values against PTP-PEST, HePTP and CD45 (Figure 2.8, Table 2.4).

Several of the top hits were flat, rigid, aromatic compounds with negative charge, mimicking the pY moiety. Quite a few of the hits contained a coumarin, flavone or polyphenolic moiety, features that are also known to mimic the pY residue. Metal containing compounds including aurothioglucose and merbromin were also found among the most potent LYP inhibitors, which may be attributed to the thiophilicity of gold and mercury, respectively. More unexpected, however, was the result that several cephalosporin derivatives inhibit LYP activity. This may be attributed to the carboxylate functionality present in many of the cephalosporins, including cefotaxime. While some of the top hits bear a resemblance to compounds known to frequent hitting false positives showing promiscuous activity in many assays by virtue of aggregate formation (*45*), it has been shown that nonspecific inhibition by aggregates can be eliminated by the addition of a detergent to the assay buffer (*46, 47*). Our assay buffer contained 0.01% of a nonionic detergent to ensure that nonspecific aggregates were not formed. As evidence that our screens were designed to avoid false positives due to aggregation, known aggregate forming compounds in our library (such as quercetin) were not hits with either substrate (*45*). On the contrary, suramin, once falsely thought to be a nonspecific aggregate forming inhibitor, was found to inhibit LYP (*45*). Although suramin is known to inhibit several targets, it does not form aggregates with proteins but instead inhibited

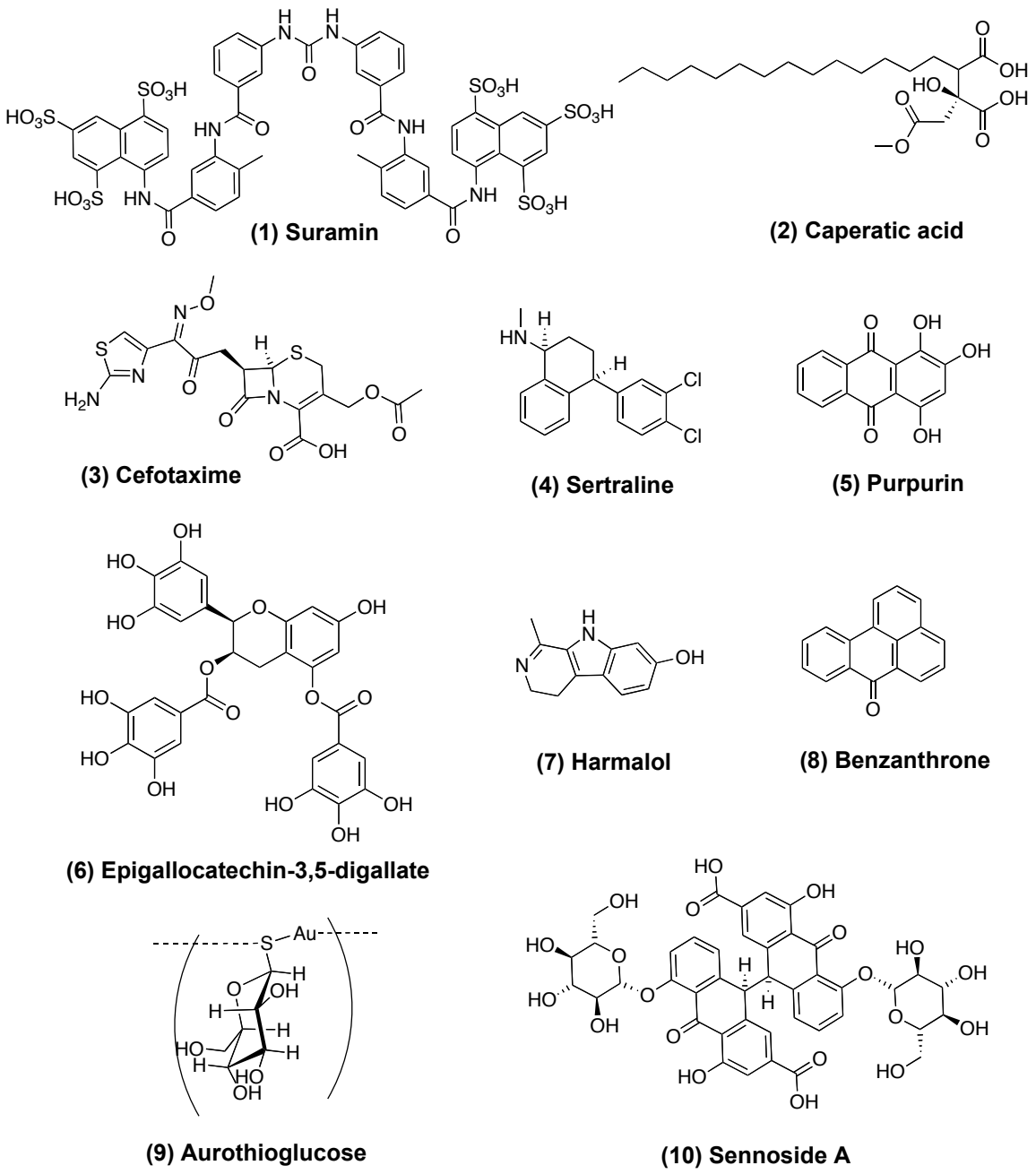

Figure 2.8. Selected hits from the Spectrum collection screen for LYP inhibitors.

its targets through key interactions with the proteins. For example, it has also been shown to be an active site directed, reversible, tight binding and competitive inhibitor of PTPs (*43*). Together, these results underline the validity of our results.

It is interesting to note that greater activity against one substrate or the other in the initial screen (Figure 2.7) often translated into differing potencies with the two substrates. For example, suramin appeared slightly more potent against the **peptide 1** as a substrate than DiFMUP in the initial screen and has an IC_{50} that is 8-fold lower against the peptide *in vitro*. Conversely, sertraline (compound 4) appeared more potent against DiFMUP in the initial screen and has an IC_{50} that is 3.4-fold lower with DiFMUP. While the IC_{50} values for these two compounds are less than 2-fold different against the substrate DiFMUP, they are 50-fold different against **peptide 1**. Most importantly, these *in vitro* differences in inhibitory potency seem to translate into differential biological activity. We tested the ability of suramin and sertraline to inhibit LYP activity in Jurkat T cells by monitoring the phosphorylation of LckY394, a known biological substrate of LYP. While suramin showed marked LYP inhibitory activity, manifested as an increase in phosphorylation at LckY394 (Figure 2.9), sertraline had no activity. It would appear that the ability of a compound to inhibit LYP-mediated hydrolysis of the more biologically relevant substrate, **peptide 1**, is a better predictor of biological activity than ability to inhibit LYP-mediated hydrolysis of a small molecule substrate. Inhibition of a peptide substrate has been used as a secondary screen to narrow down a panel of LYP inhibitors previously, but has not been explicitly demonstrated to improve prediction of biological activity.

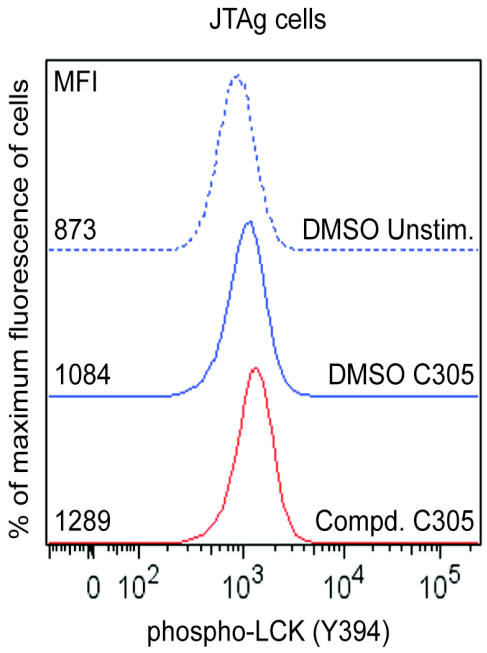

Figure 2.9. Suramin increases phosphorylation of Lck Y394 in human T cells. JTAg cells were preincubated with 25 μM compound (red graph) or DMSO alone (blue graphs) for 30 min at 37°C followed by stimulation with C305 supernatent (solid graphs) or left unstimulated (dashed graphs) for 2 min at 37°C. Graphs show cell fluorescence after staining with an AlexaFluor-488-conjugated antiphospho-Lck(Y394) antibody. Median fluorescence intensity (MFI) of each sample is shown. The % positive cells in the compound-treated, TCR-stimulated sample compared to the DMSO-treated, TCR-stimulated control was 16.7%

The most potent hit from our screen, epigallocatechin-3,5-digallate (EGCDG, compound 6), a pigment from green tea, is the most potent inhibitor of LYP and PTP-PEST reported so far with IC_{50} of 50 nM against LYP and 20 nM against PTP-PEST. Notably, EGCDG is significantly less potent against CD45 (IC_{50} = 500 nM). In order to validate the biological relevance of this hit, we investigated the ability of EGCDG to inhibit LYP activity in T cells. In this case, we monitored the phosphorylation levels of Zap-70 Y319, a direct substrate of Lck and an extremely sensitive read-out of Lck activity. Gratifyingly, we found that treatment of Jurkat T cells with 500 nM EGCDG resulted in a significant increase in phosphorylation of Y319 in ZAP-70 as measured by phosphoflow cytometry (Figure 2.10), indicating inhibition of intracellular LYP activity resulting in an increase in intracellular Lck activity and restored T cell signaling.

Molecular docking of EGCDG in LYP active site was performed to obtain a model for this binding and to gain further insight into this interaction (Figure 2.11). A binding score of -9.4 kcal/mol for EGCDG indicated high propensity of binding considering that the average docking score from 160 compounds selected randomly was -4.7, and that the top 80 hits displayed an average docking score of -5.2 kcal/mol. The gallate moiety at 5-position of the EGCDG compound docked into the active site and was stabilized by cation-π interactions provided by R233 in the P-loop (residues 226-233), hydrogen bonding with K138 of the β3-β4 loop (residues 131-139) and T-shaped aromatic interaction with the Y60 residue of the pY recognition loop (residues 54-60). The gallate moiety at 5-position thus mimicked the key interactions observed in pY binding to the active site. This explains our experimental observation that the gallate moiety at 5-position is essential for the LYP inhibition. The gallate ring at 3-position

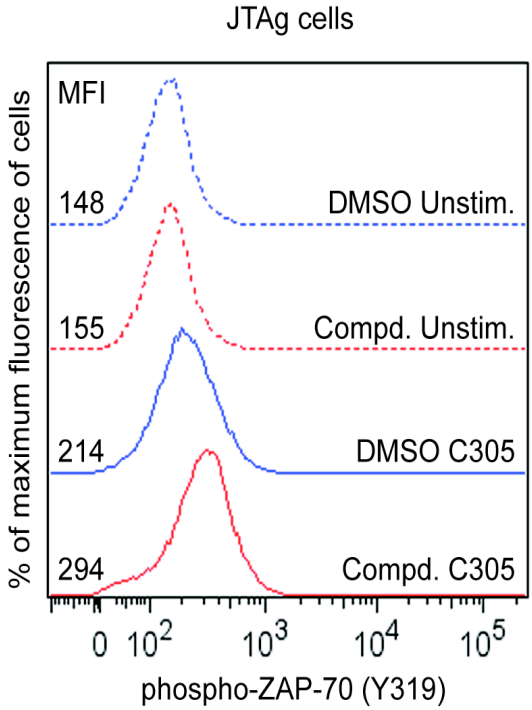

Figure 2.10. Epigallocatechin-3,5-digallate increases activation of ZAP-70 in human T cells. JTAg cells were preincubated with 500 nM compound (red graphs) or DMSO alone (blue graphs) for 30 min at 37°C, followed by stimulation with C305 supernatant (solid graphs) or left unstimulated (dashed graphs) for 2 min at 37°C. Graphs show cell fluorescence after staining with an AlexaFluor-488-conjugated antiphospho-ZAP-70 (Y319) antibody. Median fluorescence intensity (MFI) of each sample is shown. The % positive cells in the compound-treated, TCR-stimulated sample compared to the DMSO-treated, TCR-stimulated sample was 22.8%. The % positive cells in the compound-treated unstimulated sample compared to the DMSO control was 3.4%.

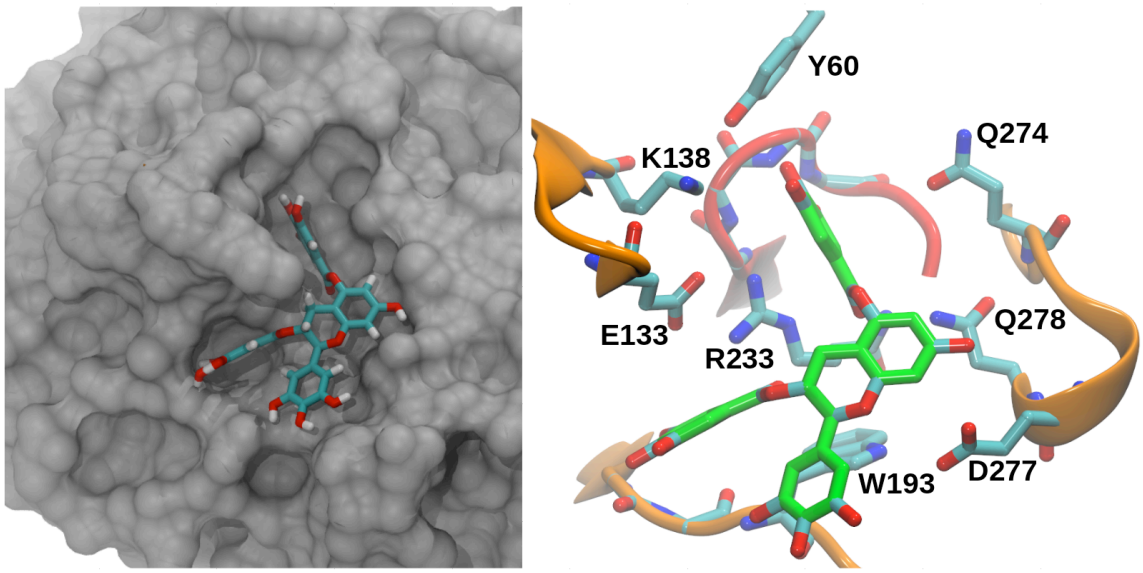

Figure 2.11. EGCDG docked pose. Most representative docked pose of Epigallocatechin-3,5-digallate from computer modeling. Left panel: LYP surface representation. Right panel: key residues interacting with the inhibitor.

docked into the hydrophobic pocket adjacent to the WPD-loop (residues 193-204) adjacent to M130 and is stabilized by hydrogen bonding provided by backbone of K191. The pyrogallol-like ring of epigallocatechin preferentially interacted with WPD-loop, making hydrogen bonds with D195 and favorable Van der Waal interaction with W193, while the 7-hydroxy group of the epigallocatechin ring was found to make hydrogen bonds with T275 and E277 in the Q-loop (274-301). Interestingly, all the interactions involved in EGCDG docking were also observed in the MD simulations of the peptide substrate over the LYP surface (discussed in detail in Chapter 1). This observation further strengthens the rationale for using **peptide 1** as a substrate in compound screening.

A closer investigation into the activity of compounds closely related to EGCDG supports some of the interactions found in the docking study, and provides insight into the structure-activity relationships of these compounds. EGCDG is a flavonoid belonging to the flavan-3-ol class. There were several closely related flavan-3-ols in our initial screen, as shown in Figure 2.12. With the exception of 2',2'-bisepigallocatechin digallate, which showed some LYP inhibition (25% at 10 μM in the initial screen), several related epigallocatechins and catechins showed little to no inhibition of LYP activity (Table 2.5). In this series of compounds, EGCDG is the only compound with a gallate moiety at 5-position of EGCDG. These data support the docking pose in which the 5-gallate moiety is involved in key interactions within the pY binding pocket. Gallic acid alone and other gallate esters did not inhibit LYP, indicating that the pY-mimicking ability of the polyphenols is not enough for potent inhibition of LYP. Furthermore, neither the interactions between LYP and the 3-gallate moiety nor the 7-hydroxy moiety are sufficient for potent inhibition, as evidenced by the fact that epigallocatechin-3-gallate had very little inhibitory activity. Finally, the presence of multiple gallate moieties is helpful but not sufficient for potent inhibition, as demonstrated by the moderate inhibitory potency of 2,2'-bisepigallocatechin digallate. Other closely related compounds from other classes of flavonoids such as, quercetin (3-hydroxyflavone) and naringenin (flavonone), did not inhibit LYP. However, several dihydroxyflavones and dihydroxyisoflavones showed varying degrees of LYP inhibition without a clear structure-activity relationship. Theaflavin, another polyphenolic compound from tea was found to inhibit LYP in the initial screening at 10 μM. However, it did not make a cut in the top hits upon rescreening against LYP and counter-screening against PTP-PEST.

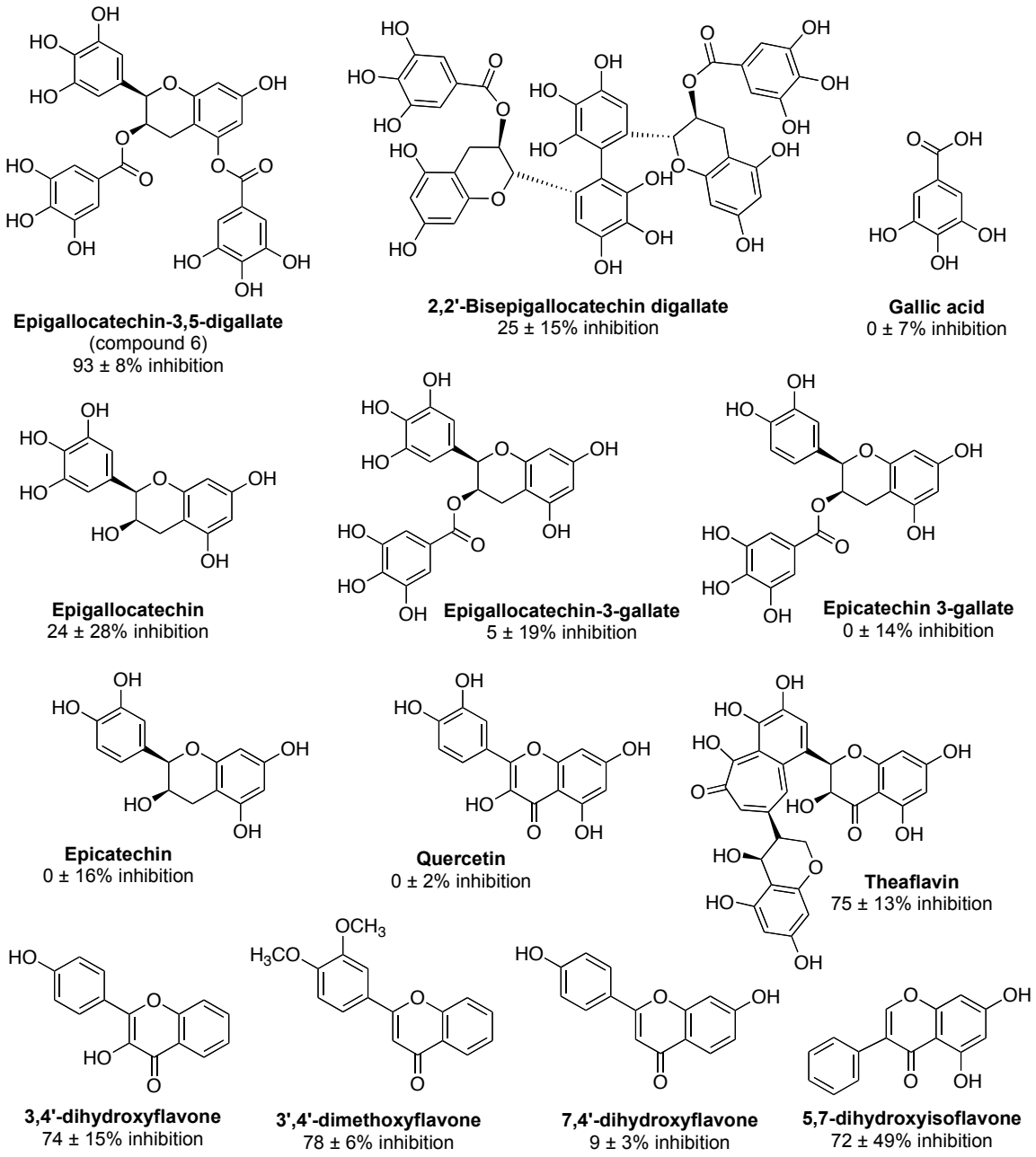

Figure 2.12. Structures and inhibition of LYP activity on **peptide 1** at 10 μM of selected compounds that are closely related to EGCDG structurally.

Table 2.5. Inhibition of LYP activity on **peptide 1** at 10 μM of selected compounds that are closely related to EGCDG structurally, other flavonoids and polyphenols from tea.

COMPOUND NAME	% ACTIVITY REMAINING	ERROR
EPIGALLOCATECHIN 3,5-DIGALLATE	7	8
2',2'-BISEPIGALLOCATECHIN DIGALLATE	73	15
EPIGALLOCATECHIN	77	28
EPIGALLOCATECHIN-3-MONOGALLATE	96	19
EPICATECHIN MONOGALLATE	104	14
EPICATECHIN	114	17
EPICATECHIN PENTAACETATE	101	5
CATECHIN PENTAACETATE	110	1
CATECHIN PENTABENZOATE	114	6
CATECHIN TETRAMETHYLETHER	92	19
GALLIC ACID	118	7
4'-METHOXYFLAVONE	82	18
5,7-DIMETHOXYISOFLAVONE	114	10
3',6-DIHYDROXYFLAVONE	119	8
3,4',5,6,7-PENTAMETHOXYFLAVONE	119	7
6,4'-DIMETHOXYFLAVONE	75	18
5-HYDROXY-2',4',7,8-TETRAMETHOXYFLAVONE	102	14
7,8-DIHYDROXYFLAVONE	104	12
3,5-DIHYDROXYFLAVONE	97	3
6,4'-DIHYDROXYFLAVONE	92	6
7,4'-DIHYDROXYFLAVONE	91	3
3',4'-DIMETHOXYFLAVONE	22	6
3,4'-DIHYDROXYFLAVONE	26	15
7,2'-DIHYDROXYFLAVONE	116	20
5,7-DIHYDROXYISOFLAVONE	28	49
2-METHYL-5,7,8-TRIMETHOXYISOFLAVONE	86	60
6,7-DIHYDROXYFLAVONE	115	9
APIGENIN	97	5
TANGERITIN	106	13
CHRYSIN	105	15
DIOSMIN	119	1
QUERCETIN	103	2
FISETINIDOL	98	11
FISETIN	96	9
HESPERETIN	103	7
NARINGENIN	106	4
THEAFLAVIN	25	13
THEAFLAVIN MONOGALLATES	89	7
THEAFLAVIN DIGALLATE	92	3
EPITHEAFLAVIN MONOGALLATE	74	15
TANNIC ACID	120	4

Gallate esters of theaflavin did not inhibit LYP. Another class of polyphenols from tea includes tannins and the representative compound of this group, tannic acid did not inhibit LYP in our initial screening.

2.3 Conclusions

Here, we tested the hypothesis that the use of a more biologically relevant, peptide-based substrate in PTP inhibitor screens would result in hits with greater potential for biological activity. Our experimental screens for LYP inhibitors using both DiFMUP and **peptide 1** as substrates demonstrated that, in some cases, different hits are identified with the two different substrates and, most importantly, that potency against the peptide substrate correlated more strongly with biological activity. Epigallocatechin-3,5-digallate (EGCDG) was identified as the most potent inhibitor of LYP to date, with an IC_{50} value of 50 nM and cellular activity at 500 nM. A first molecular model for the interaction of EGCDG with LYP was proposed based on molecular docking modeling, providing the basis for future lead optimization efforts. A first molecular model for the interaction of EGCDG with LYP was proposed based on molecular docking modeling, providing the basis for future lead optimization efforts. Interestingly, all the interactions observed in the binding of EGCDG were sampled by the peptide substrate in MD simulation, further endorsing the use of this peptidic substrate in inhibitor screens.

2.4 Experimental section

2.4.1 General considerations

All of the reagents were purchased from commercial sources and used without further purification. The library of compounds, the Spectrum collection, was purchased from Microsource Discovery Systems, Inc. The pCAP residue and **peptide 1** were synthesized as described previously by Mitra *et al.* (*32*). Stock solutions and serial dilutions of the substrates and inhibitors were made in DMSO. The catalytic domain of human recombinant CD45 was obtained from Biomol. The modified pBAD plasmid encoding the catalytic domain of HePTP (aa 44-339) in frame with a noncleavable 6xHis tag was obtained as a generous gift from Lutz Tautz. cDNA fragments encoding the catalytic domains of LYP (aa 2-309) and PTP-PEST (aa 2-323) were cloned between the BamH1 and the Xho1 sites of pET28a plasmid (Novagen) in frame with a cleavable N-terminal 6xHis-tag. Recombinant proteins were purified from lysates of IPTG-induced *Escherichia coli* BL21 cells by affinity chromatography on Ni-nitrilotriacetic acid columns. 6xHisHePTP was eluted using 250 mM imidazole. Untagged LYP and PTP-PEST were eluted by incubating columns with thrombin, followed by removal of thrombin from the protein preparation by a second chromatography step on benzamidine columns. All of the enzyme activity assays were performed at ambient temperature using a buffer containing 50 mM Tris, pH 6.5, 100 mM NaCl, 1 mM dithiothreitol (DTT), 2 mM EDTA, and 0.01% Brij 35. Fluorescence data were collected on a Molecular Devices Spectramax M5 multimode plate reader with excitation and emission at 360 and 455 nm, respectively. The increase in the fluorescence due to the hydrolysis of the substrates was

measured every 60 s for 30 min and the fluorescence values in the linear range of the Michaelis-Menten kinetics curve were used for the data analysis.

2.4.2 Library screening

The Spectrum collection obtained consisted of 25 96-well plates, each of which contained 200 μM DMSO solutions of 80 compounds in columns 2-11. A 5 μL aliquot of each of these compounds was transferred to corresponding position in the assay plate. A 5 μL aliquot of DMSO was transferred to each well of column 12 of the assay plate to serve as a control. A 1 μL aliquot of a DMSO solution of DiFMUP (150 μM stock) or **peptide 1** (1 mM stock) was also transferred to the wells of the assay plates. The total amount of DMSO in each reaction well was held constant at 6% of the total reaction volume (100 μL). A 50 nM solution of enzyme in activity buffer was preincubated with 1 mM DTT for 30 min to ensure complete activation. The preactivated enzyme was further diluted with the activity buffer just prior to addition to the assay plate, so that addition of a 94 μL of the diluted enzyme to each well would result in a final enzyme concentration of 5 nM. The final DTT concentration in each reaction well was 100 μM. The final concentrations of the substrates used were 1.5 μM and 10 μM for DiFMUP and **peptide 1**, respectively. The final concentration for each compound screened in the library was 10 μM. Upon addition of the preactivated enzyme, the enzyme activity was monitored at room temperature (21-24˚C) in black 96-well plates. The activity of the enzyme was measured by monitoring the increase in fluorescence (l_{ex} = 360 nm, l_{em} = 455 nm) every 60 s for 30 min as the enzyme dephosphorylated the substrate (either DiFMUP or **peptide 1**). Each source plate in the library was screened in triplicate with each of the substrates

and results were averaged. The percent relative activity for each compound was determined by factoring the measured fluorescence values for the compound treated wells over the control wells treated with DMSO only.

2.4.3 Inhibition assays

Stock solutions and serial dilutions of the compounds for determination of IC_{50} were made in DMSO. All the hits were screened at inhibitor concentrations ranging between 100 nM to 500 μM. The total DMSO concentration in each reaction was held constant at 6% of the total reaction volume (100 μL). The concentrations of enzymes, DTT and substrates were the same as those used in the library screening assays. The percent relative activity at different concentrations was determined by factoring the measured fluorescence values for the compound treated wells over the control wells treated with DMSO only. The resulting plot of inhibitor concentration versus percent enzyme activity provided the IC_{50} values.

2.4.4 Cell culture

Jurkat T cells expressing the SV-40 large T Antigen (JTAg) (*48*) were kept at logarithmic growth in RPMI 1640 medium (Mediatech, Manassas, VA) supplemented with 10% fetal bovine serum (Omega Scientific, Tarzana, CA), 2 mM glutamine, 1 mM sodium pyruvate, 10 mM HEPES pH 7.3, 2.5 mg/ml D-glucose, 100 units/ml of penicillin and 100 μg/ml streptomycin (Life Technologies, Carlsbad, CA).

2.4.5 Phospho-flow cytometry

JTAg cells were pretreated with the indicated concentrations of LYP inhibitors or DMSO for 30 min in RPMI 1640 at 37°C. Cells were then stimulated with supernatants of C305 hybridoma (*49*) for 2 min at 37°C. Cells were fixed immediately with BD Cytofix buffer, permeabilized using BD Phosflow Perm Buffer III and stained with AlexaFluor-488-conjugated anti-pZAP-70(Y319) antibody or anti-pSrc(Y418) antibody (which is cross-reactive with pLck(Y394), and labeled as such in Figure 2.9) according to the manufacturer's protocols (BD Biosciences, San Jose, CA). Cell fluorescence was analyzed by FACS using a BD LSR II (BD Biosciences). Data was analyzed using FlowJo software (TreeStar, Ashland, OR).

2.4.6 Docking Simulations

The Schrödinger suite of programs (*50*) was used for the docking studies. The crystal structure (PDB entry 2P6X) prepared for the simulation was utilized for docking the library of compounds. A scoring grid was precomputed by placing an outer cubical box of length 36 Å and an inner box of length 14 Å centered at the P-loop residues (227-231). The hydroxyl groups of all Ser, Thr, and Tyr residues in the binding site were allowed to be flexible during the grid generation process. Docking calculations were performed using Glide (version 5.7) (*51*). The ligand library comprised of hit compounds from the experimental screening and were prepared using LigPrep (*50*). Low energy conformations were generated for all possible protonation and ionization states (pH range 7.0 ± 2.0). All the ligands were docked using Glide extra precision (XP).

2.5 References

1. Hunter, T. (1995) Protein kinases and phosphatases: The yin and yang of protein phosphorylation and signaling, *Cell 80*, 225-236.

2. Stoker, A. W. (2005) Protein tyrosine phosphatases and signalling, *J. Endocrinol. 185*, 19-33.

3. Bialy, L., and Waldmann, H. (2005) Inhibitors of protein tyrosine phosphatases: Next-generation drugs?, *Angew. Chem. Int. Ed. 44*, 2-27.

4. Zhang, Z.-Y. (2002) Protein tyrosine phosphatases: Structure and function, substrate specificity, and inhibitor development, *Annu. Rev. Pharmacol. Toxicol. 42*, 209-234.

5. Barr, A. J. (2010) Protein tyrosine phosphatases as drug targets: Strategies and challenges of inhibitor development, *Future Med. Chem. 2*, 1563-1576.

6. He, R., Zeng, L. F., He, Y., Zhang, S., and Zhang, Z. Y. (2013) Small molecule tools for functional interrogation of protein tyrosine phosphatases, *FEBS J. 280*, 731-750.

7. Heneberg, P. (2009) Use of protein tyrosine phosphatase inhibitors as promising targeted therapeutic drugs, *Curr. Med. Chem. 16*, 706-733.

8. Zhang, S., and Zhang, Z.-Y. (2007) PTP1B as a drug target: Recent developments in PTP1B inhibitor discovery, *Drug Discov. Today 12*, 373-381.

9. Zhang, Z.-Y. (2001) Protein tyrosine phosphatases: Prospects for therapeutics, *Curr. Opin. Chem. Biol. 5*, 416-423.

10. Zhang, Z.-Y., and Lee, S. Y. (2003) PTP1B inhibitors as potential therapeutics in the treatment of type 2 diabetes and obesity, *Exp. Opin. Investig. Drugs 12*, 223-233.

11. Alonso, A., Sasin, J., Bottini, N., Friedberg, I., Friedberg, I., Osterman, A., Godzik, A., Hunter, T., Dixon, J., and Mustelin, T. (2004) Protein tyrosine phosphatases in the human genome, *Cell 117*, 699-711.

12. Zhang, Z.-Y. (2003) Chemical and mechanistic approaches to the study of protein tyrosine phosphatases, *Acc. Chem. Res. 36*, 385-392.

13. Barr, A. J., Ugochukwu, E., Lee, W. H., King, O. N., Filippakopoulos, P., Alfano, I., Savitsky, P., Burgess-Brown, N. A., Muller, S., and Knapp, S. (2009) Large-scale structural analysis of the classical human protein tyrosine phosphatome, *Cell 136*, 352-363.

14. Asante-Appiah, E., Ball, K., Bateman, K., Skorey, K. I., Friesen, R., Desponts, C., Payette, P., Bayly, C., Zamboni, R., Scapin, G., Ramachandran, C., and Kennedy, B. P. (2001) The YRD motif is a major determinant of substrate and inhibitor specificity in T-cell protein tyrosine thosphatase, *J. Biol. Chem. 276*, 26036-26043.

15. Shen, K., Keng, Y. F., Wu, L., Guo, X. L., Lawrence, D. S., and Zhang, Z.-Y. (2001) Acquisition of a specific and potent PTP1B inhibitor from a novel combinatorial library and screening procedure, *J. Biol. Chem. 276*, 47311-47319.

16. Zhang, S., Chen, L., Luo, Y., Gunawan, A., Lawrence, D. S., and Zhang, Z.-Y. (2009) Acquisition of a potent and selective TC-PTP inhibitor via a stepwise fluorophore-tagged combinatorial synthesis and screening strategy, *J. Am. Chem. Soc. 131*, 13072-13079.

17. Cohen, S., Dadi, H., Shaoul, E., Sharfe, N., and Roifman, C. M. (1999) Cloning and characterization of a lymphoid-specific, inducible human protein tyrosine phosphatase, Lyp, *Blood 93*, 2013-2024.

18. Karver, M. R., Krishnamurthy, D., Kulkarni, R. A., Bottini, N., and Barrios, A. M. (2009) Identifying potent, selective protein tyrosine phosphatase inhibitors from a library of Au(I) complexes, *J. Med. Chem. 52*, 6912-6918.

19. Krishnamurthy, D., Karver, M. R., Fiorillo, E., Orru, V., Stanford, S. M., Bottini, N., and Barrios, A. M. (2008) Gold(I)-mediated inhibition of protein tyrosine phosphatases: A detailed in vitro and cellular study, *J. Med. Chem. 51*, 4790-4795.

20. Xie, Y., Liu, Y., Gong, G., Rinderspacher, A., Deng, S.-X., Smith, D. H., Toebben, U., Tzilianos, E., Branden, L., Vidovic, D., Chung, C., Schurer, S., Tautz, L., and Landry, D. W. (2008) Discovery of a novel submicromolar inhibitor of the lymphoid tyrosine phosphatase, *Bioorg. Med. Chem. Lett. 18*, 2840-2844.

21. Yu, X., Sun, J.-P., He, Y., Guo, X., Liu, S., Zhou, B., Hudmon, A., and Zhang, Z.-Y. (2007) Structure, inhibitor and regulatory mechanism of LYP, a lymphoid-specific tyrosine phosphatase implicated in autoimmune diseases, *Proc. Natl. Acad. Sci. U.S.A 104*, 19767-19772.

22. Veillette, A., Rhee, I., Souza, C. M., and Davidson, D. (2009) PEST family phosphatases in immunity, autoimmunity, and autoinflammatory disorders, *Immunol. Rev. 228*, 312-324.

23. Bottini, N., Musumeci, L., Alonso, A., Rahmouni, S., Nika, K., Rostamkhani, M., MacMurray, J., Pellecchia, M., Eisenbarth, G. S., Comings, D., and Mustelin, T. A. (2004) A functional polymorphism in lymphoid tyrosine phosphatase is associated with type I diabetes, *Nat. Genet. 36*, 337-338.

24. Vang, T., Congia, M., Macis, M. D., Musumeci, L., Orru, V., Zavattari, P., Nika, K., Tautz, L., Tasken, K., Cucca, F., Mustelin, T., and Bottini, N. (2005) Autoimmune-associated lymphoid tyrosine phosphatase is a gain-of-function variant, *Nat. Genet. 37*, 1317-1319.

25. Vang, T., Miletic, A. V., Arimura, Y., Tautz, L., Rickert, R. C., and Mustelin, T. (2008) Protein tyrosine phosphatases in autoimmunity, *Annu. Rev. Immunol. 26*, 29-55.

26. Orru, V., Tsai, S., Rueda, B., Fiorillo, E., Stanford, S. M., Dasgupta, J., Hartiala, J., Zhao, L., Ortego-Centeno, N., D'Alfonso, S., Group, I. C., Arnett, F., Wu, H., Gonzalez-Gay, M., Tsao, B., Pons-Estel, B., Alarcon-Riquelme, M., He, Y., Zhang, Z.-Y., Allayee, H., Chen, X., Martin, J., and Bottini, N. (2009) A loss-of-function variant of PTPN22 is associated with reduced risk of systemic lupus erythematosus, *Hum. Mol. Genet. 18*, 569-579.

27. Obiri, D. D., Flink, N., Maier, J. V., Neeb, A., Maddalo, D., Thiele, W., Menon, A., Stassen, M., Kulkarni, R. A., Garabedian, M. J., Barrios, A. M., and Cato, A. C. (2012) PEST-domain-enriched tyrosine phosphatase and glucocorticoids as regulators of anaphylaxis in mice, *Allergy 67*, 175-182.

28. Stanford, S. M., Krishnamurthy, D., MD, F., Messina, R., Debnath, B., Li, S., Liu, T., Kazemi, R., Dahl, R., He, Y., Yu, X., Chan, A. C., Zhang, Z.-Y., Barrios, A. M., Woods, V. L., Jr., Neamati, N., and Bottini, N. (2011) Discovery of a novel series of inhibitors of lymphoid tyrosine phosphatase with activity in human T cells, *J. Med. Chem. 54*, 1640-1654.

29. Holmes, C., Macher, N., Grove, J., Jang, L., and Irvine, J. (2008) Designing better coumarin-based fluorogenic substrates for PTP1B, *Bioorg. Med. Chem. Lett. 18*, 3382-3385.

30. Feng, J., Chen, Y., Pu, J., Yang, X., Zhang, C., Zhu, S., Zhao, Y., Yuan, Y., Yuan, H., and Liao, F. (2011) An improved malachite green assay of phosphate: Mechanism and application, *Anal. Biochem. 409*, 144-149.

31. Montalibet, J., Skorey, K. I., and Kennedy, B. P. (2005) Protein tyrosine phosphatases: Enzymatic Assays, *Methods 35*, 2-8.

32. Mitra, S., and Barrios, A. M. (2005) Highly sensitive peptide-based probes for protein tyrosine phosphatase activity utilizing a fluorogenic mimic of phosphotyrosine, *Bioorg. Med. Chem. Lett. 15*.

33. Wu, J., Katrekar, A., Honigberg, L. A., Smith, A. M., Conn, M. T., Tang, J., Jeffery, D., Mortara, K., Sampang, J., Williams, S. R., Buggy, J., and Clark, J. M. (2006) Identification of substrates of human protein-tyrosine phosphatase PTPN22, *J. Biol. Chem. 281*, 11002-11010.

34. Wu, S., Bottini, M., Rickert, R. C., Mustelin, T., and Tautz, L. (2009) In silico screening for PTPN22 inhibitors: Active hits from an inactive phosphatase conformation, *ChemMedChem 4*, 440-444.

35. Debnath, A., Parsonage, D., Andrade, R., He, C., Cobo, E., Hirata, K., Chen, S., Garcia-Rivera, G., Orozco, E., Martinez, M., Gunatilleke, S., Barrios, A. M., Arkin, M., Poole, L., McKerrow, J., and Reed, S. (2012) A high-throughput drug screen for *Entamoeba histolytica* identifies a new lead and target, *Nat. Med. 18*, 956-960.

36. Gunatilleke, S. S., and Barrios, A. M. (2006) Inhibition of lysosomal cysteine proteases by a series of Au(I) complexes: A detailed mechanistic investigation, *J. Med. Chem. 49*, 3933-3937.

37. Gunatilleke, S. S., and Barrios, A. M. (2008) Tuning the Au(I)-mediated inhibition of cathepsin B through ligand substitutions, *J. Inorg. Biochem. 102*, 555-563.

38. Gunatilleke, S. S., de Oliveira, C. A., McCammon, J. A., and Barrios, A. M. (2008) Inhibition of cathepsin B by Au(I) complexes: A kinetic and computational study, *J. Biol. Inorg. Chem. 13*, 555-561.

39. Kocisko, D. A., Baron, G. S., Rubenstein, R., Chen, J., Kuizon, S., and Caughey, B. (2003) New inhibitors of scrapie-associated prion protein formation in a library of 2000 drugs and natural products, *J. Virol. 77*, 10288-10294.

40. Stallings-Mann, M., Jamieson, L., Regala, R. P., Weems, C., Murray, N. R., and Fields, A. P. (2006) A novel small-molecule inhibitor of protein kinase Ciota blocks transformed growth of non-small-cell lung cancer cells, *Cancer Res. 66*, 1767-1774.

41. Weisman, J. L., Liou, A. P., Shelat, A. A., Cohen, F. E., Guy, R. K., and DeRisi, J. L. (2006) Searching for new antimalarial therapeutics amongst known drugs, *Chem. Biol. Drug Des. 67*, 409-416.

42. Wang, Q., Janzen, N., Ramachandran, C., and Jirik, F. (1997) Mechanism of inhibition of protein-tyrosine phosphatases by disodium aurothiomalate, *Biochem. Pharmacol. 54*, 703-711.

43. Zhang, Y. L., Keng, Y. F., Zhao, Y., Wu, L., and Zhang, Z. Y. (1998) Suramin is an active site-directed, reversible, and tight-binding inhibitor of protein-tyrosine phosphatases, *J. Biol. Chem. 273*, 12281-12287.

44. Stanford, S. M., Panchal, R., Walker, L., Wu, D., Falk, M., Mitra, S., Damle, S., Ruble, D., Kaltcheva, T., Zhang, S., Zhang, Z.-Y., Bavari, S., Barrios, A. M., and Bottini, N. (2012) High-throughput screen using a single-cell tyrosine phosphatase assay reveals biologically active inhibitors, *Proc. Natl. Acad. Sci. U.S.A. 109*, 13972-13977.

45. McGovern, S. L., Caselli, E., Grigorieff, N., and Shoichet, B. K. (2002) A common mechanism underlying promiscuous inhibitors from virtual and high-throughput screening, *J. Med. Chem. 45*, 1712-1722.

46. Feng, B. Y., Shelat, A., Doman, T. N., Guy, R. K., and Shoichet, B. K. (2005) High-throughput assays for promiscuous inhibitors, *Nat. Chem. Biol. 1*, 146-148.

47. Jadhav, A., Ferreira, R. S., Klumpp, C., Mott, B. T., Austin, C. P., Inglese, J., Thomas, C. J., Maloney, D. J., Shoichet, B. K., and Simeonov, A. (2010) Quantitative analyses of aggregation, autofluorescence, and reactivity artifacts in a screen for inhibitors of a thiol protease, *J. Med. Chem. 53*, 37-51.

48. Shaw, J. P., Utz, P. J., Durand, D. B., Toole, J. J., Emmel, E. A., and Crabtree, G. R. (1988) Identification of a putative regulator of early T cell activation genes, *Science 241*, 202-205.

49. Weiss, A., and Stobo, J. D. (1984) Requirement for the coexpression of T3 and the T cell antigen receptor on a malignant human T cell line, *J. Exp. Med. 160*, 1284-1299.

50. Suite 2011: LigPrep, version 2.5, Schrödinger, LLC, New York, NY, 2011.

51. Friesner, R. A., Murphy, R. B., Repasky, M. P., Frye, L. L., Greenwood, J. R., Halgren, T. A., Sanschagrin, P. C., and Mainz, D. T. (2006) Extra precision glide: Docking and scoring incorporating a model of hydrophobic enclosure for protein−ligand complexes, *J. Med. Chem. 49*, 6177-6196.

CHAPTER 3

THIURAM DISULFIDES AS PSEUDO-IRREVERSIBLE INHIBITORS OF THE LYMPHOID TYROSINE PHOSPHATASE

3.1 Introduction

The improper regulation of tyrosine phosphorylation levels is implicated in multiple human diseases including diabetes, cancer, hypertension and autoimmunity (*1*). As a consequence, there is significant interest in identifying chemical inhibitors of the enzymes responsible for regulating tyrosine phosphorylation, namely the tyrosine kinases and protein tyrosine phosphatases (PTPs). One enzyme of particular interest in autoimmunity is the lymphoid tyrosine phosphatase (LYP, PTPN22), a negative regulator of early T cell receptor (TCR) signaling (*2*). An allelic gain of function variant of LYP is associated with various autoimmune disorders (*3, 4*), whereas an allelic loss of function variant is protective against systemic lupus erythematosus (*5*). LYP is also found to be a positive regulator of anaphylaxis and inhibition of LYP helps to mitigate anaphylaxis in mice (*6*). Taken together, these findings reinforce the potential of LYP inhibition for the treatment of autoimmune disorders.

The catalytic domains of PTPs are homologous and all contain the PTP signature motif, (H/V)**C**$(X)_5$**R**(S/T), in the conserved PTP active site (*7*). The local environment in the PTP active site lowers the pK_a of the active site cysteine residue making it highly nucleophilic and susceptible to oxidation (*8*). Therefore, several PTPs including LYP are inactivated and regulated by reversible or irreversible oxidation of the activated catalytic cysteine residue upon exposure to oxidizing agents such as H_2O_2 and NO (*8-11*). The Barrios laboratory has previously shown that nitrosating agents such as sodium nitroprusside and the active site-directed nitric oxide (NO)-donating peptide, Ac-ARLIEDNE-(HCyNO)-TAREG-NH_2, also cause reversible, competitive and covalent oxidative inactivation of LYP (*12*). Thiophilic heavy metals including zinc(II), gold(I)

and mercury(II) readily inhibit activities of several PTPs including LYP (*13-16*). In addition, *S*-thiolation can inhibit PTP activity. For example, PTP1B is inhibited by hydrogen sulfide-mediated *S*-thiolation during ischemia and reperfusion (*17*). Furthermore, in the presence of excess of H_2O_2 *in vitro*, the catalytic cysteine residue of LYP forms a disulfide bond with the backdoor C129 to reversibly inactivate the enzyme (*18*). These examples illustrate the diverse mechanisms by which PTP activity can be regulated by virtue of the reactivity of the catalytic cysteine residue.

In Chapter 1 of this dissertation, I have discussed in detail how potent and selective inhibitors of LYP can be developed by mimicking the mechanisms of biological regulation of LYP. We have also discussed advantages of chemical probes that can form covalent bond with LYP for addressing biological problems pertaining to LYP. Towards this end, we decided to exploit oxidation of the catalytic cysteine residue for inhibition of LYP. With this in mind, we looked for classes of compounds that can covalently modify low pK_a thiols by oxidation.

Thiuram disulfides are a chemically distinct class of disulfides that can inhibit enzymes containing low pK_a thiols by forming mixed disulfides (*19*). A prototype of this class of compounds, disulfiram (Figure 3.1, trade name Antabuse), is used clinically for the treatment of alcohol dependence (*20*). Disulfiram inhibits aldehyde dehydrogenase, an enzyme involved in alcohol metabolism, leading to acetaldehyde build-up and unpleasant symptoms following the ingestion of alcohol (*21*). Inhibition of aldehyde dehydrogenase by disulfiram is irreversible and recovery of the activity of aldehyde dehydrogenase is dependent on synthesis of new enzyme *in vivo* (*22*). The mechanism of irreversible inhibition of aldehyde dehydrogenase by disulfiram involves formation of a

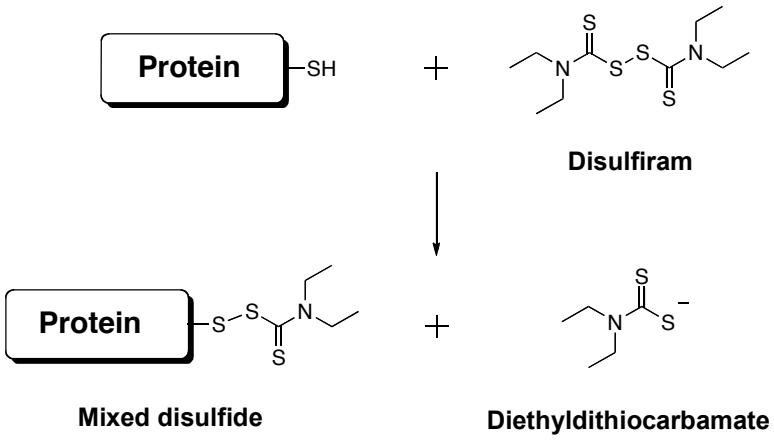

Figure 3.1. Mixed disulfide bond formation between disulfiram and proteins containing low pK_a thiols.

disulfide bond between disulfiram and a catalytically essential cysteine residue of the enzyme as shown in Figure 3.1 (*21, 23, 24*). The product of this reaction, diethyldithiocarbamate, is a metabolite of disulfiram and is capable of inhibiting aldehyde dehydrogenase *in vivo* but not *in vitro* (*22, 25, 26*). This observation has been attributed to oxidation of diethyldithiocarbamate to disulfiram *in vivo* (*27*). Disulfiram along with another thiuram disulfide, thiram and several dithiocarbamates have also been shown to possess anticancer activity (*28-31*). This potent anticancer activity of disulfiram has been attributed to *S*-thiolation of several biological targets including protein kinase C (PKC) (*19*), glutathione-*S*-transferase (GST) (*32*), nuclear factor-κB (*33*) and the caspases (*34*) along with other mechanisms. Based on the known biological activity of disulfiram and the knowledge that LYP is inactivated by oxidation and disulfide bond formation, we hypothesized that disulfiram and other thiuram disulfides can inhibit LYP by *S*-thiolation.

3.2 Results and discussion

To test this hypothesis, we first investigated the inhibition of LYP and other closely related PTPs by disulfiram. Disulfiram inhibited LYP activity with a moderate potency (IC_{50} = 47 ± 2 μM) but surprisingly did not inhibit the activity of PTP-PEST or CD45 at 500 μM. Disulfiram was then tested for in-cell LYP inhibition in the Jurkat T Antigen (JTAg) cells. LYP negatively regulates early stage T cell receptor (TCR) signaling by dephosphorylating Lck at position Y394 (*35*). Therefore, by following the phosphorylation at Lck Y394, activity of the cellular LYP can be monitored. Figure 3.2 shows that the treatment of JTAg cells with increasing concentrations of disulfiram resulted in dose-dependent increase in phosphorylation of LCK Y394 as observed with anti-pSrc(Y416) immunoblot that cross-reacts with pLCK(Y394) and phospho-flow cytometry. CD45 is another PTP found in T cells. It dephosphorylates pLCK(Y505) and this results in turning on of the TCR signaling (*4*). Therefore, inhibition of CD45 activity would counteract any benefit obtained from inhibition of LYP. To test whether disulfiram inhibited CD45 activity in JTAg cells we monitored levels of phosphorylation on Lck Y505. Diethyldithiocarbamate is the reduction product and metabolite of disulfiram and it inhibits aldehyde dehydrogenase *in vivo* but not *in vitro*. To test the effects of this compound, we decided to study its LYP and CD45 inhibition in JTAg cells. The results of this in-cell LYP and CD45 inhibition study for cells incubated in the presence and absence of either disulfiram or diethyldithiocarbamate, with and without TCR stimulation are shown in Figure 3.3. The TCR stimulated cells (lanes 2 and 4) show an increase in phosphorylation at Y394 in the presence of disulfiram as observed also in Figure 3.2 but not in the presence of diethyldithiocarbamate, indicating that diethyldithiocarbamate does

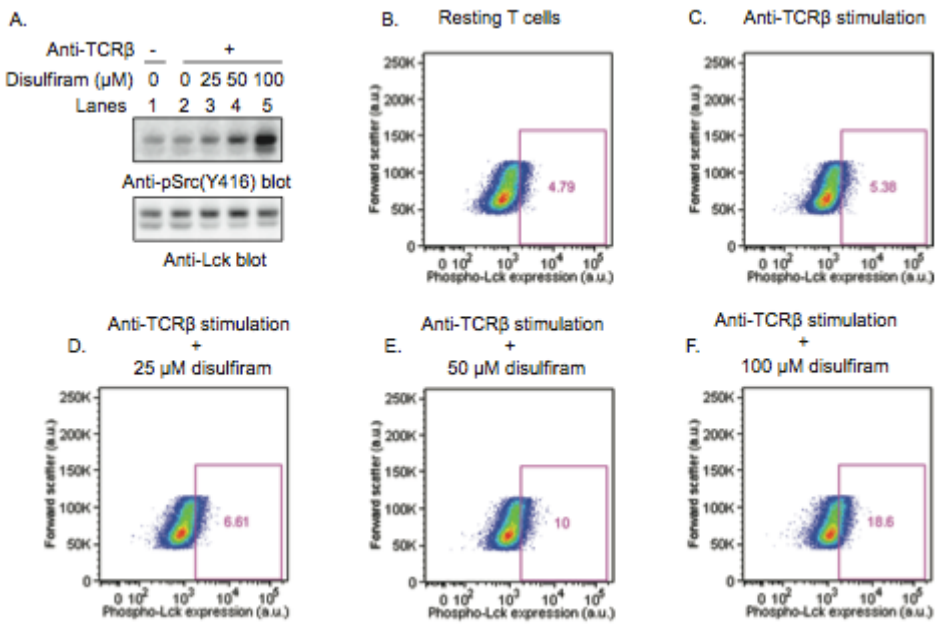

Figure 3.2. Intracellular dose-dependent inhibition of LYP by disulfiram. (A) JTAg cells were treated for 30 min with DMSO (lanes 1 and 2) or increasing concentrations of disulfiram (lanes 3-5), and stimulated for 2 min using C305 supernatant (lanes 2-5) or left unstimulated (lane 1). Upper panel shows anti-pSrc(Y416) immunoblot. Lower panel shows anti-Lck blot of the same samples. (B-F) Single-cell analysis of TCR-induced phosphorylation of Lck by phospho-flow cytometry. JTAg cells were treated for 30 min with DMSO (B and C) or increasing concentrations of disulfiram (D-F), and stimulated for 2 min using C305 supernatant (C-F) or left unstimulated (B). Cells were fixed and stained with an AlexaFluor-488-conjugated anti-pSrc(Y416) antibody. Graphs show relative pLck(Y394) levels of live cells gated by FSC versus SSC. Red gate within each panel includes cells with phospho-Lck expression equal to or higher than the top 5% of resting T cells. Percentage of cells within the gates are indicated.

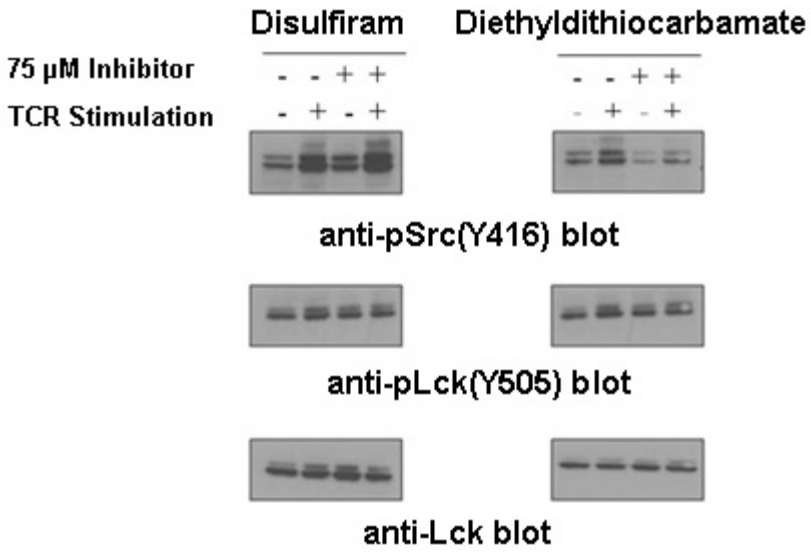

Figure 3.3. Intracellular inhibition of LYP by disulfiram and diethyldithiocarbamate. Top panels: anti-pSrc(Y416) immunoblots of lysates of Jurkat TAg cells treated with 75 µM of Disulfiram and Imuthiol (lanes 3 and 4 in each panel) or untreated (lanes 1 and 2 in each panel) and either left unstimulated (lanes 1 and 3 in each panel) or stimulated (lanes 2 and 4 in each panel) with C305 antibodies for 2 min. Middle panels: anti-pLck(Y505) blots of the same samples. Bottom panels: anti-Lck blot of the same samples.

not inhibit LYP activity in JTAg cells. Phosphorylation levels at position Y505 of Lck in the presence of either disulfiram or diethyldithiocarbamate are unaltered indicating that these compounds do not inhibit CD45 activity in cells. These results are consistent with the *in vitro* screening results, confirming that disulfiram inhibits LYP selectively over CD45 in cells.

Since disulfiram showed excellent dose-dependent inhibition of LYP in cells with a moderate potency, we decided to look for other thiuram disulfide inhibitors with greater potency. With this in mind, we screened a library of 16 commercially available thiuram disulfides (Figure 3.4) for inhibition of LYP. In our screen, we included the sodium salt of diethyldithiocarbamate (compound 17), which was expected to be a negative control based on our observation that it did not inhibit LYP in JTAg cells. We also included disulfiram (compound 1) and epigallocatechin-3,5-digallate (EGCDG) (compound 18), the most potent inhibitor of LYP and PTP-PEST reported so far as positive controls (*16*). Each compound in the library was screened in triplicate at 10 μM and 50 μM concentrations, except the positive control, EGCDG, which was screened at 100 nM and 500 nM concentrations. The results of this screening exercise are summarized in Figure 3.5. Compounds that showed more potent inhibition of LYP than disulfiram in the initial screening were carried forward for further validation and counter-screening against PTP-PEST. The IC_{50} values of these hits are summarized in Table 3.1.

Tetraethylthiuram disulfide (disulfiram, compound 1) was found to be a better inhibitor of LYP than tetramethyl (thiram, compound 2) and tetrabutyl (compound 4) analogs. However, increasing the steric bulk around the thiuram nitrogens with tetraisopropyl derivative (compound 3) lead to an increase in LYP inhibitory potency.

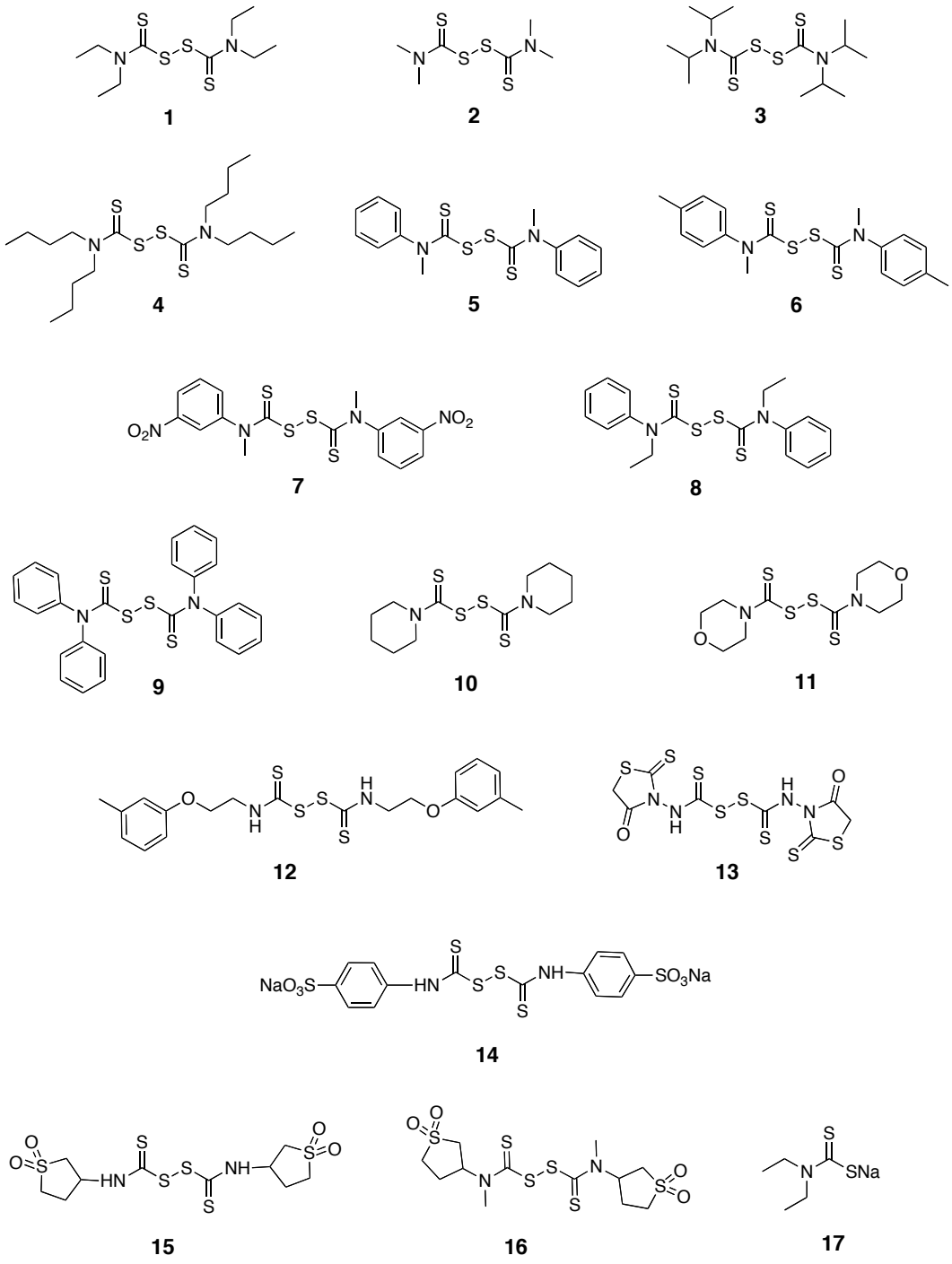

Figure 3.4. Structures of the compounds screened as LYP inhibitors.

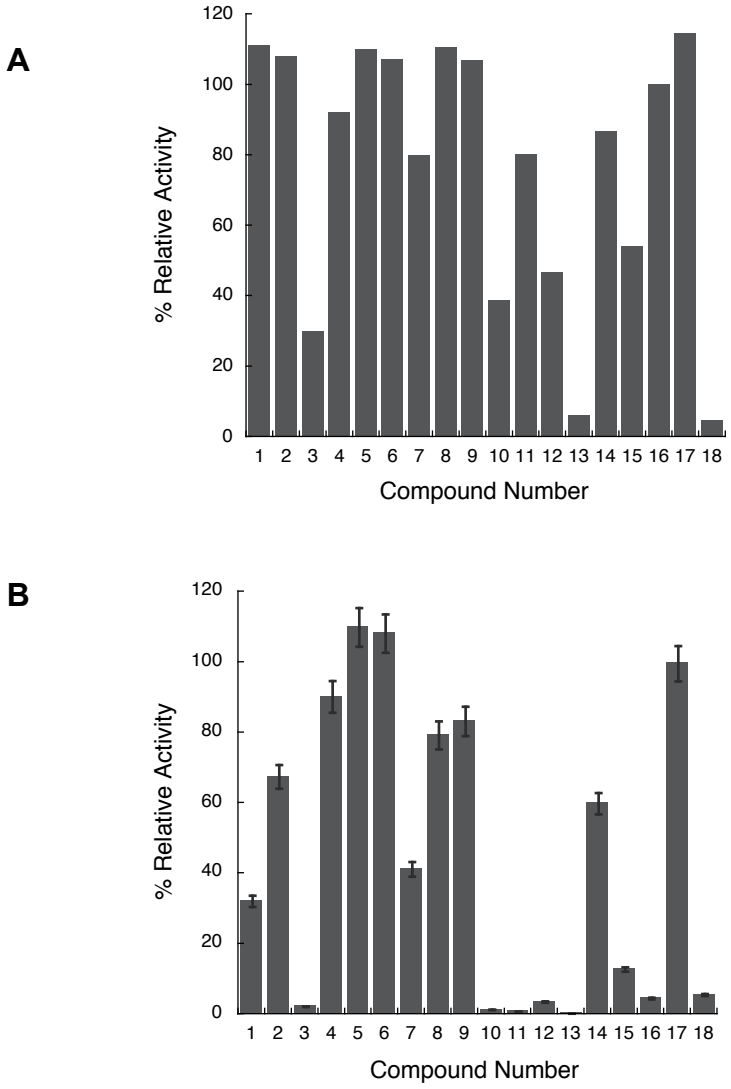

Figure 3.5. Results of initial screen to identify LYP inhibitors. (A) Compounds 1-17 were screened at 10 μM concentration, while epigallocatechin-3,5-digallate (compound 18) was screened at 100 nM, (B) compounds 1-17 were screened at 50 μM concentration, while epigallocatechin-3,5-digallate (compound 18) was screened at 500 nM.

Table 3.1. Hit validation and counter screening of selected hits against PTP-PEST. IC_{50} values are shown in μM.

Compound #	LYP	PTP-PEST
1	47 ± 2	> 500
3	7.0 ± 0.7	20 ± 1
10	15.0 ± 0.5	25 ± 2
11	23 ± 3	70 ± 5
12	10 ± 1	10 ± 2
13	3.0 ± 0.3	8.0 ± 0.5
15	13 ± 1	38 ± 5
16	34 ± 3	44 ± 6

Replacing one or both alkyl substituents of each thiuram nitrogen with an aryl substituent is generally not well tolerated, with compounds 5, 6, 8 and 9 showing no or very low inhibition of LYP. However, among the aromatic substituted compounds, compound 7, containing a strongly electron withdrawing aryl ring showed the best activity against LYP. Cyclizing the substituents on the thiuram nitrogens to form a piperidine (compound 10) or morpholine (compound 11) ring leads to more potent inhibition, providing additional evidence that increasing steric bulk around the thiuram nitrogens increases potency of LYP inhibition. Monosubstitution of the thiuram nitrogens is also well tolerated with compounds 12, 13 and 15 showing potent inhibition of LYP. However, monosubstitution with an electron withdrawing aryl ring is not nearly as well tolerated (with compound 14 showing only moderate inhibition of LYP). Monosubstitution with a

sulfolane moiety (compound 15) provided greater inhibition of LYP than disubstitution with one sulfolane moiety and a methyl group (compound 16). The most potent thiuram disulfide inhibitor was compound 13, in which both of the thiuram nitrogen atoms are monosubstituted with N-(2-thioxothiazolidin-4-one). In a counter-screen, all of the hits excluding compound 10 showed more potent inhibition of LYP than the highly similar PTP-PEST but none of these hits showed as much preference of LYP over PTP-PEST as the prototype, disulfiram (compound 1).

Disulfiram is known to inhibit several of its targets by forming mixed disulfides with low pK_a cysteine residues and this covalent inhibition can usually be reversed by adding thiol reducing agents such as DTT or 2-mercaptoethanol (*19, 24, 32*). To determine whether our top hit, compound 13, is a pseudo-irreversible inhibitor of LYP activity, we investigated characteristic features of covalent inhibition. With this in mind, we first tested whether washing away the inhibitor could reverse LYP inhibition of compound 13. For this, preactivated LYP was incubated with compound 13 to ensure inhibition and then subjected to prolonged dialysis with 3 exchanges of the dialysis buffer to give a total of 10^9-fold dilution (Figure 3.6). Only a little activity was lost even after prolonged dialysis, in the DMSO-treated control LYP while the activity of the compound 13-treated LYP could not be restored, indicating that the inhibitor cannot be washed away from the enzyme. When activity of LYP was monitored upon incubation with several concentrations of compound 13, compound 13 showed time-dependent and concentration-dependent inhibition (Figure 3.7*A*), indicating initial binding and formation of covalent bond. A plot of observed rate constants for the product formation versus the inhibitor concentration showed saturation kinetics (Figure 3.7*B*), a characteristic of

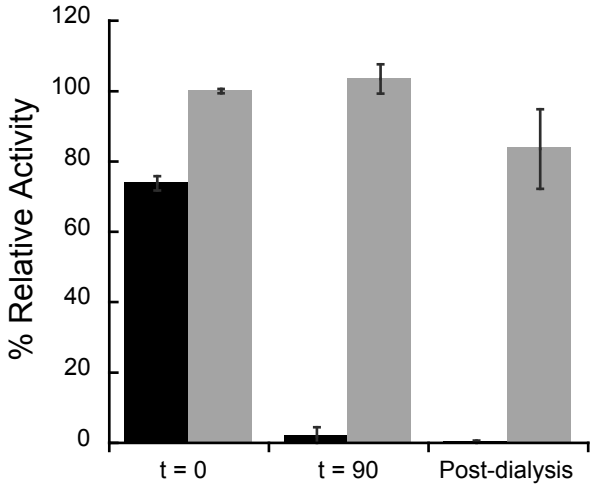

Figure 3.6. Inhibition of LYP by compound 13 cannot be reversed by dialysis**.** Twenty five μM LYP was incubated with 500 μM of compound 13 for 90 min and then dialyzed for 3 exchanges each of 1000-fold dialysis buffer to get a final 10^9-fold dilution. The activities of LYP are normalized to those obtained from DMSO-treated control sample at t=0. The black bar represents the activity of the compound 13 treated sample, while the activity of an untreated control is shown in grey.

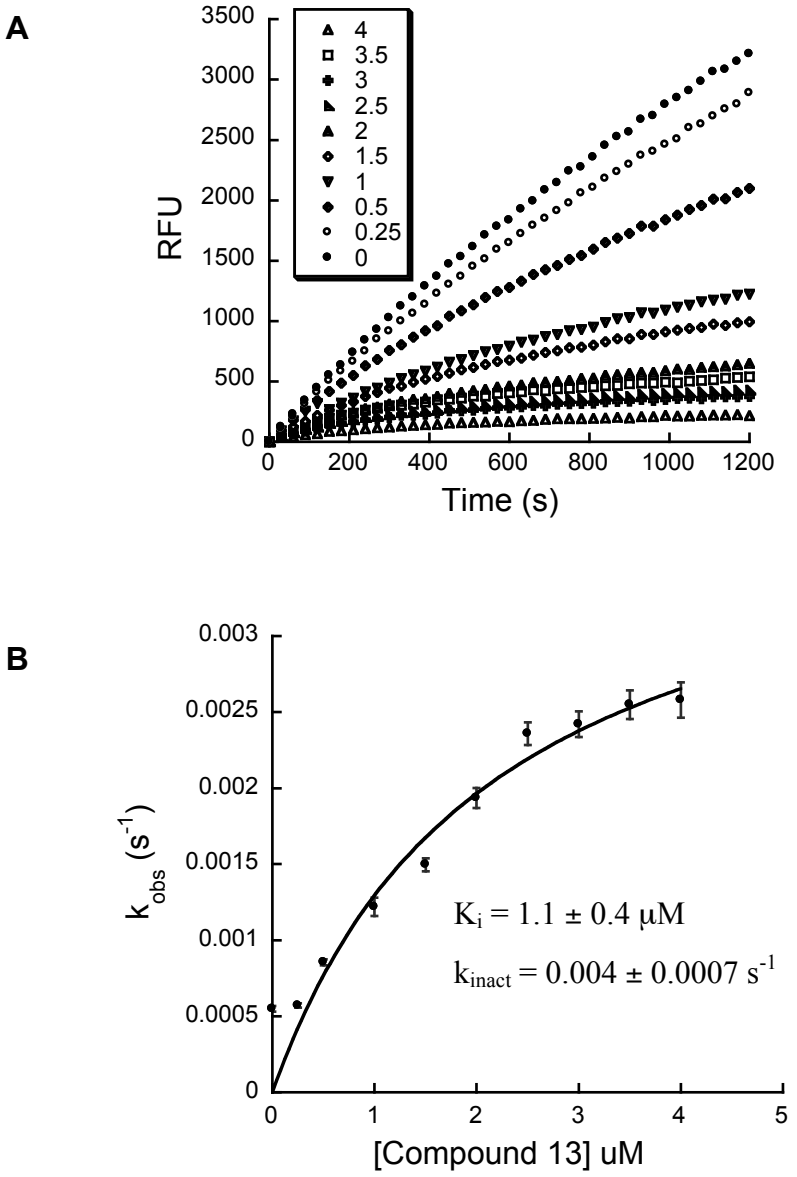

Figure 3.7. Compound 13 inhibits LYP in a time-dependent manner. (*A*) Activity of 2 nM LYP treated with various concentrations of compound 13 was measured at 30 s intervals and the observed rate constant (k_{obs}) for each reaction was calculated as described in the experimental section. (*B*) A plot of k_{obs} versus [compound 13] gave K_{app} and K_{inact} as described in the experimental section.

covalent inhibitors. Compound 13 was found to inhibit LYP with K_i of 1.1 ± 0.4 μM and k_{inact} of 0.0040 ± 0.0007 s^{-1}.

If the covalent bond between compound 13 and LYP is indeed a disulfide bond, this disulfide bond can at least be partially reversed by addition of thiol reducing agents. To test this, we incubated LYP with compound 13 to ensure inhibition and then incubated this inhibited LYP with several high concentrations of either DTT or glutathione. Inhibition of LYP by compound 13 was partially reversed in a dose-dependent manner by postincubation with DTT (Figure 3.8*A*) but could not be reversed significantly by glutathione, the physiological reducing agent (Figure 3.8*B*). Lack of 100% recovery of the LYP activity was not entirely surprising as reactivation kinetics for thiols is estimated to be 10-1000 times slower than inactivation by oxidation (*36, 37*). Together with the finding that inhibition of LYP by compound 13 is time-dependent and cannot be reversed by dialysis, we can conclude that compound 13 inhibits LYP covalently by *S*-thiolation, and although this inhibition can be partially reversed by DTT, it is likely to be irreversible under physiological conditions. When LYP was coincubated with compound 13 and reducing agent, either DTT (Figure 3.9*A*) or glutathione (Figure 3.9*B*), the ability of compound 13 to inhibit LYP was diminished significantly, indicating that the corresponding dithiocarbamate formed may have much lower LYP inhibitory potency *in vitro*.

To confirm this, we preincubated compound 13 with the reducing agents for 1 h to ensure reduction of compound 13 to the corresponding dithiocarbamate and we found significantly less inhibition of LYP upon preincubation (Figure 3.10). This is consistent

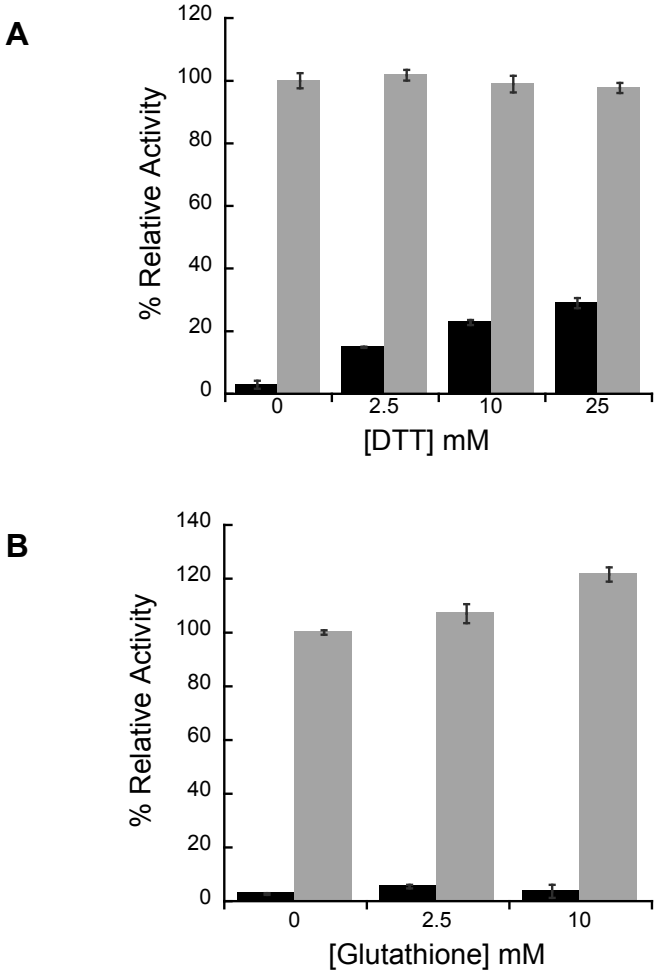

Figure 3.8. Inhibition of LYP by compound 13 can be partially reversed by posttreatment with DTT (*A*) but not by glutathione (*B*). Five nM LYP was incubated with 5 μM of compound 13 for 30 min followed by postincubation with various concentrations of (*A*) DTT or (*B*) glutathione for 1 h. The activities of LYP are normalized to those obtained from DMSO-treated control sample that are not treated with DTT. The black bar represents the activity of the compound 13 treated sample, while the activity of an untreated control is shown in grey.

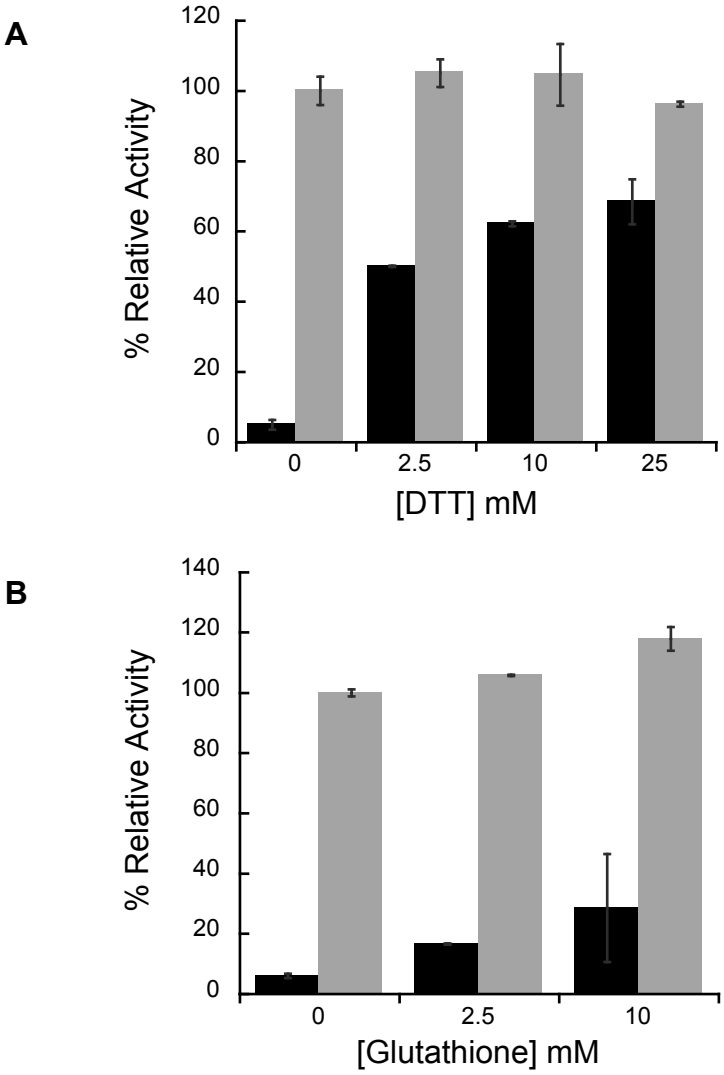

Figure 3.9. Ability of compound 13 to inhibit LYP diminishes significantly by co-incubation with DTT (*A*) and partially by coincubation with glutathione (*B*). Five nM LYP was coincubated simultaneously with 5 μM of compound 13 and various concentrations of DTT (*A*) or glutathione (*B*) for 1 h. The activities of LYP are normalized to those obtained from DMSO-treated control sample that are not treated with DTT. The black bar represents the activity of the compound 13 treated sample, while the activity of an untreated control is shown in grey.

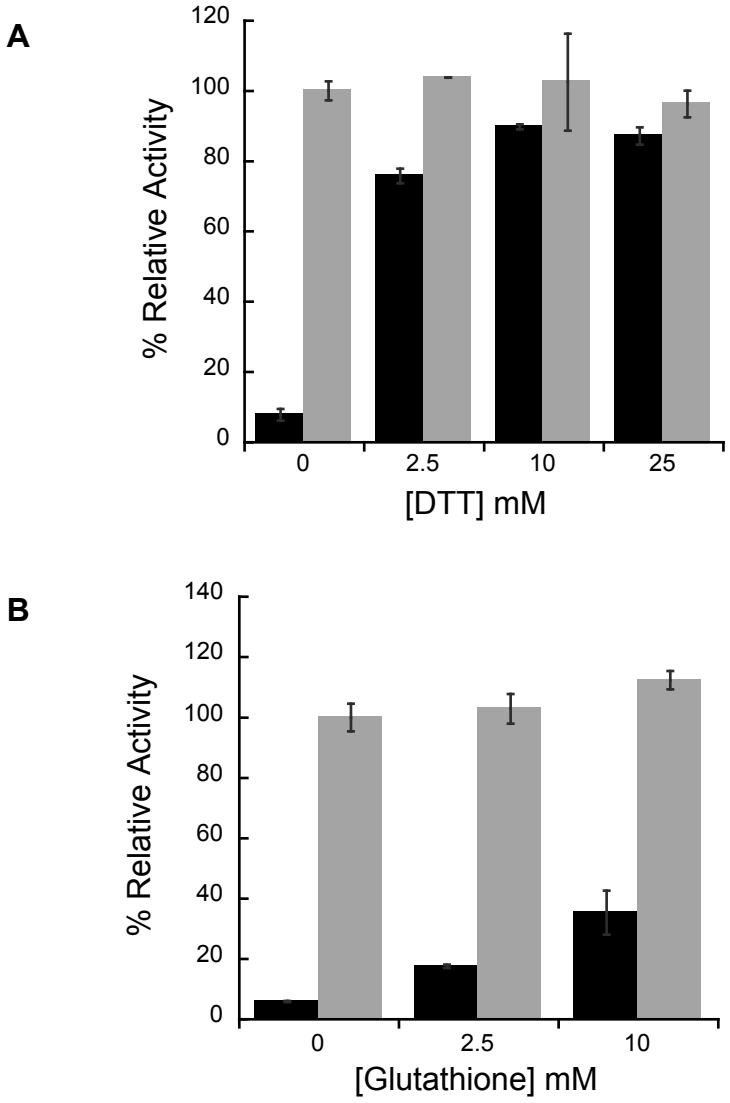

Figure 3.10. Ability of compound 13 to inhibit LYP diminishes significantly by pre-incubation with DTT (*A*) and partially by preincubation with glutathione (*B*). Five nM LYP was incubated for 30 min with 5 μM of compound 13 that was preincubated with various concentrations of DTT for 1 h. The activities of LYP are normalized to those obtained from DMSO-treated control sample that are not treated with DTT.

with our earlier finding that diethyldithiocarbamate (compound 17), a reduced form of disulfiram, did not inhibit LYP *in vitro* and in cells at the concentrations tested. Both these findings reinforce our hypothesis that the thiol-disulfide exchange is essential for potent LYP inhibition as the monosulfides showed weak inhibition.

With the aim of validating the biological relevance of our best hit, we then tested compound 13 for in-cell LYP inhibition in the JTAg cells. As mentioned earlier, LYP negatively regulates early stage T cell receptor (TCR) signaling by dephosphorylating Lck at position Y394 (*38*). Phosphorylation of Lck at Y394 activates the kinase which, in turn, phosphorylates ZAP-70 Y319. Therefore, by monitoring the phosphorylation levels of Y319 of ZAP-70, we obtain a sensitive read-out for LYP activity in JTAg cells (*16*). Upon treatment of JTAg cells with compound 13, phosphorylation levels of ZAP-70 Y319 increased in a dose-dependent manner in both unstimulated and stimulated cells, as measured by phospho-flow cytometry. These results indicate that compound 13 inhibits LYP activity in JTAg cells, promoting T cell activation (Figure 3.11).

In order to gain further insights into the structure activity relationship for LYP inhibition by the thiuram disulfides, Dr. Nadeem Vellore from Dr. Riccardo Baron's laboratory performed an atom-based 3D Quantitative-Structure-Activity-Relationship (QSAR) study (*39, 40*). By iteratively using 12 out of the 17 (70%) compounds as the training set, 3D QSAR model was generated to predict the remaining activity for the 30% of the compounds in the test set. Figure 3.12 displays the correlation between predicted versus experimental remaining activity (R^2 value of 0.8). The individual contribution of each parameter used to build the QSAR model is summarized in Table 3.2. These data

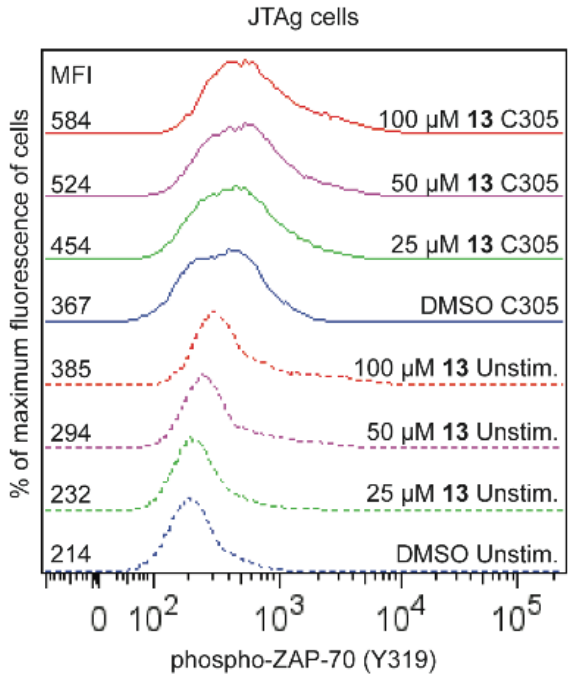

Figure 3.11. The LYP inhibitor compound 13 increases T cell activation. Compound 13 increases activation of ZAP-70 in human T cells. JTAg cells were preincubated with 25 µM (green graphs), 50 µM (purple graphs), or 100 µM (red graphs) compound 13 or with DMSO alone (blue graphs) for 30 min at 37°C, followed by stimulation with C305 supernatant (solid graphs) or left unstimulated (dashed graphs) for 2 min at 37°C. Graphs show cell fluorescence after staining with an AlexaFluor-488-conjugated antiphospho-ZAP-70 (Y319) antibody. Median fluorescence intensity (MFI) of each sample is shown. The % of positive cells was calculated for each sample by Overton subtraction (*41*). The % positive cells for the compound-treated TCR-stimulated samples compared to the DMSO-treated TCR-stimulated samples were 12.5%, 20.1%, and 26.0% for 25 µM, 50 µM, and 100 µM compound 13, respectively. The % positive cells for the compound-treated unstimulated samples compared to the DMSO-treated unstimulated samples were 8.0%, 28.6%, and 46.8% for 25 µM, 50 µM, and 100 µM compound 13, respectively.

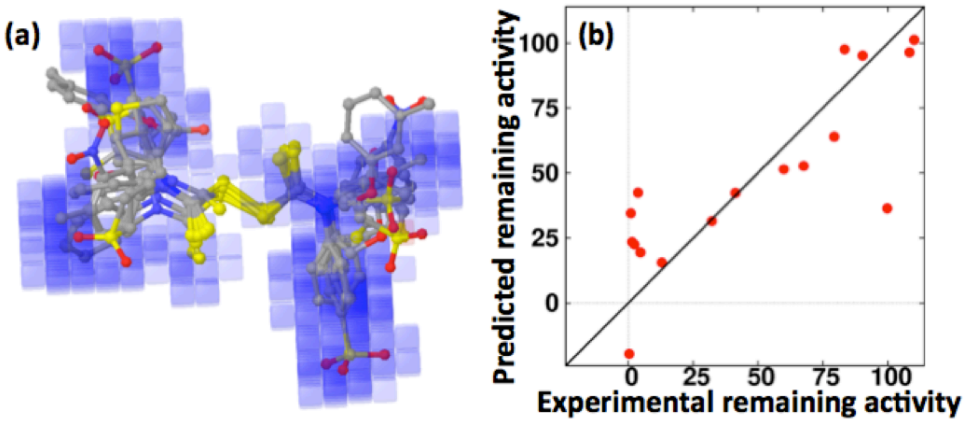

Figure 3.12. Atom-based QSAR study. (*A*) Aligned compounds with blue shading over the hydrophobic or nonpolar region of the compounds, highlighting the features that positively correlated with the experimental activity, (*B*) QSAR model scatter plot with experimental versus predicted activity remaining based atom-based 3D-QSAR approaches (values are in %).

Table 3.2. Percentage atomic property associated in predicting the activity based on atom-based QSAR model.

Atomic property	**Percentage contribution**
H-bond donor	0.16
Hydrophobic or nonpolar	63.61
Negative ionic	3.37
Positive ionic	0.61
Electron-withdrawing	12.99
Miscellaneous	19.22

indicate the physicochemical properties of the ligands contributing to the predicted QSAR. Overall, the presence of hydrophobic/nonpolar moieties and electron withdrawing groups on the thiuram nitrogen were the most important factors contributing to low micromolar LYP inhibition, accounting for a total of 77% of the overall contribution.

Disulfiram is known to inhibit several of its targets by forming mixed disulfides with low pK_a cysteine residues and its covalent inhibition can often be reversed by adding thiol reducing agents such as DTT or 2-mercaptoethanol (*19, 24, 32*). We suggest the following mechanistic interpretation based on the integration of our experimental and computational data. Substitution of thiuram nitrogen with electron withdrawing groups might aid in activating the nucleophilic attack by the catalytic cysteine residue of LYP onto the thiuram disulfide; whereas substitution with hydrophobic groups might provide favorable Van der Waals interactions with the active site of LYP.

3.3 Conclusions

In the present study, we have screened a library of thiuram disulfides against LYP to identify several low micromolar, covalent, pseudo-irreversible LYP inhibitors. Disulfiram inhibited LYP preferentially over CD45 both *in vitro* and in Jurkat T-cells. However, the reduced metabolite of disulfiram, diethyldithiocarbamate, did not inhibit LYP activity *in vitro* or in cells, indicating the importance of thiol-disulfide exchange reaction for the potency of thiuram disulfides. Computational modeling and Quantative-Structure-Activity-Relationship indicates that the presence of hydrophobic/nonpolar moiety and electron-withdrawing groups on the thiuram nitrogen were the most important

factors contributing to the LYP inhibition. Compound 13, an N-(2-thioxothiazolidin-4-one) analog, was the most potent LYP inhibitor in this library with IC_{50} of 3 μM and K_i of 1.1 μM. Compound 13 showed covalent inhibition of LYP that cannot be reversed by dialysis but can be partially reversed by treatment with DTT. The reduced product of compound 13, the corresponding dithiocarbamate, only weakly inhibited LYP. Compound 13 was further shown to inhibit LYP in Jurkat T-cells in a dose-dependent manner to activate T-cell signaling.

3.4 Experimental section

3.4.1 General considerations

All the reagents were purchased from commercial sources and used without further purification. The library of thiuram disulfides was purchased from Aldrich Market Select. Stock solutions and serial dilutions of the substrates were made in DMSO. cDNA fragments encoding the catalytic domains of LYP (aa 2-309) and PTP-PEST (aa 2-323) were cloned between the BamH1 and the Xho1 sites of pET28a plasmid (Novagen) in frame with a cleavable N-terminal 6xHis-tag. Recombinant proteins were purified from lysates of IPTG-induced *Escherichia coli* BL21 cells by affinity chromatography on Ni-nitrilotriacetic acid columns. 6xHisHePTP was eluted using 250 mM imidazole. Untagged LYP and PTP-PEST were eluted by incubating columns with thrombin, followed by removal of thrombin from the protein preparation by a second chromatography step on benzamidine columns. The catalytic domain of human recombinant CD45 was obtained from Enzo life sciences. All of the activity assays with all of the enzymes were performed at ambient temperature using a buffer containing 50

mM Bis-Tris, pH 6.5, 100 mM NaCl, 1 mM Tris (2-carboxyethyl)phosphine hydrochloride (TCEP), 2 mM EDTA, and 0.01% Brij 35. Fluorescence data were collected on a Molecular Devices Spectramax M5 multimode plate reader with excitation and emission at 360 and 455 nm, respectively. The increase in the fluorescence due to the hydrolysis of the substrates was measured every 60 s for 30 min and the fluorescence values in the linear range of the Michaelis-Menten kinetics curve were used for the data analysis.

3.4.2 In vitro assay for library screening

The library of thiuram disulfides was created in a source plate with 1 mM DMSO solution of compounds 1-17 and 10 μM DMSO solution of the compound 18 (epigallocatechin-3,5-digallate). A 5 μL aliquot or a 1 μL aliquot of each of these compounds was transferred to corresponding position in the assay plate for screening at inhibitor concentration of 50 μM or10 μM, respectively. A 4 μL aliquot of DMSO was transferred to each well containing inhibitor of the assay plate when screening at 10 μM inhibitor concentration but not when screening at 50 μM inhibitor concentration. A 5 μL aliquot of DMSO was transferred to each of the control wells. A 1 μL aliquot of a DMSO solution of DiFMUP (150 μM stock) was also transferred to the wells of the assay plates. The total amount of DMSO in each reaction well was held constant at 6% of the total reaction volume (100 μL). A 50 nM solution of enzyme in activity buffer was preincubated with 1 mM TCEP for 30 min to ensure complete activation. The preactivated enzyme was further diluted with the activity buffer just prior to addition to the assay plate, so that addition of a 94 μL of the diluted enzyme to each well would

result in a final enzyme concentration of 5 nM. The final TCEP concentration in each reaction well was 100 μM. The final concentration of DiFMUP was 1.5 μM. Each compound in the library was screened in triplicate and results were averaged. The percent relative activity for each compound was determined by factoring the measured fluorescence values for the compound treated wells over the control wells treated with DMSO only.

3.4.3 In vitro inhibition assays

Stock solutions and serial dilutions of the compounds for determination of IC_{50} were made in DMSO. All the hits were screened at inhibitor concentrations ranging between 500 nM to 500 μM. The total DMSO concentration in each reaction was held constant at 6% of the total reaction volume (100 μL). The concentrations of enzymes (both LYP and PTP-PEST), TCEP and substrates were the same as those used in the library screening assays. The percent relative activity at different concentrations was determined by factoring the measured fluorescence values for the compound treated wells over the control wells treated with DMSO only. The resulting plot of inhibitor concentration versus percent enzyme activity provided the IC_{50} values.

For determination of the dissociation constant, K_i, the final concentration of LYP used was 2 nM and the concentration of DiFMUP used was 5 μM. The remaining conditions were the same as those used in the library screening assay. The increase in the fluorescence due to the hydrolysis of the substrates was measured in 30 s intervals for 30 min and the fluorescence values in the linear range of the Michaelis-Menten kinetics curve were used for the data analysis. The dissociation constant (K_i) and the first order

rate constant for covalent bond formation (k_{inact}) were calculated as described by Gushwa *et al.* (*42*). In short, for each inhibitor concentration, an observed rate constant (k_{obs}) was calculated using the equation $P = (v_i/k_{obs})(1-e^{(-k_{obs}t)})$, where P = product formation, v_i = initial velocity, and t = time. The apparent dissociation constant (K_{app}) for the reversible enzyme inhibitor complex and the first order rate constant for covalent bond formation (k_{inact}) were obtained by a nonlinear regression analysis of the derived k_{obs} values at different inhibitor concentrations with equation $k_{obs} = k_{inact}[I]/(K_{app}+[I])$. The dissociation constant (K_i) was calculated using the formula $K_i = (K_{app}/(1+[DiFMUP]/K_{mDiFMUP})$ where $K_{mDiFMUP} = K_m$ of DiFMUP was determined experimentally.

3.4.4 Reversibility by dialysis

Twenty-five μM LYP was preincubated with 1 mM TCEP for 1 h to ensure complete activation. After this, 500 μM compound 13 or DMSO control was added to the enzyme and aliquots of these reactions were used to determine the activity of LYP at t=0 and after 90 min incubation using the conditions similar to those used in library screening assay. The reaction mixture was then dialyzed using Pierce Slide-a-Lyzer MINI 20k dialysis tubes against the activity buffer described in the general considerations for three exchanges of prolonged dialysis at 4°C to achieve 10^9-fold dilution. LYP activity was determined postdialysis and was normalized using the activity obtained with the DMSO control treated LYP at t=0.

3.4.5 Reversibility with reducing agents

Five nM LYP was preincubated with 1 mM TCEP for 1 h to ensure complete activation. For postincubation with reducing agent studies, we then incubated the activated LYP with either 5 μM compound 13 or DMSO for 30 min. After 30 min, different concentrations of DTT or glutathione were added to the reactions and incubated for 1 h and the LYP activity was measured as described in library screening assays, except that the concentration of DiFMUP used was 5 μM. For coincubation studies, activated LYP was incubated simultaneously with different concentrations of DTT or glutathione and 5 μM compound 13 for 1 h, following which the LYP activity was measured as described above. For preincubation studies, 5 μM compound 13 was preincubated with different concentrations of DTT or glutathione for 1 h and then this preincubated mixture was added to the preactivated LYP and incubated 30 min further, following which the LYP activity was measured as described above. For all these reactions, the LYP activity remaining was normalized using the activity obtained with the DMSO control treated LYP that was not treated with DTT or glutathione.

3.4.6 Antibodies

The polyclonal anti-pSrc(Tyr416) (cross-reactive with pLck(Tyr394)) and anti-pTyr505-Lck and antibodies were obtained from Cell Signaling Technology, Inc. The monoclonal anti-Lck antibody was obtained from Santa Cruz Biotechnology. The ECL-Plus chemiluminescence kit was obtained from GE-Amersham Biosciences.

3.4.7 Cell culture

Jurkat T cells expressing the SV-40 large T Antigen (JTAg) (*43*) were kept at logarithmic growth in RPMI 1640 medium (Mediatech, Manassas, VA) supplemented with 10% fetal bovine serum (Omega Scientific, Tarzana, CA), 2 mM glutamine, 1 mM sodium pyruvate, 10 mM HEPES pH 7.3, 2.5 mg/ml D-glucose, 100 units/ml of penicillin and 100 μg/ml streptomycin (Life Technologies, Carlsbad, CA).

3.4.8 Studies with JTAg Cells

Fixed concentrations of inhibitors or DMSO (control) were added to 20 X 10^6 cells suspended in 800 µL RPMI 1640, and incubated for 1 h at room temperature. The volume of DMSO added was held constant at less than 2% of the total volume. JTAg cells preincubated with DMSO or inhibitor were divided into 400 µL aliquots containing 10 X 10^6 cells and stimulated with supernatants of C305 hybridoma (*44*) for 2 min or left untreated. Cells were lysed in 20 mM Tris-HCl pH 7.5, 150 mM NaCl, 5 mM EDTA pH 8.0 containing 1% NP-40, 10 µg/mL aprotinin and leupeptin, 10 µg/mL soybean trypsin inhibitor, 1 mM Na_3VO_4, and 1 mM phenylmethylsulfonyl fluoride, after which lysates were clarified by centrifugation. The protein concentration in each cell lysate was determined by Bradford protein assay (Bio-Rad) in order to normalize the amount of protein used in SDS-PAGE.

3.4.9 SDS-PAGE and immunoblots

Aliquots of lysates were suspended in SDS sample buffer, heated at 95 °C for 5 min and the boiled samples run on 10% (single concentration) or 8% (dose-response)

SDS-polyacrylamide gels. Proteins resolved by gel electrophoresis were transferred onto nitrocellulose membranes (Hybond ECL, GE Healthcare), using appropriate dilutions per manufacturer's instructions of unconjugated primary antibodies followed by horseradish peroxidase-conjugated secondary antibodies (purchased from GE Healthcare). Blots were developed with the enhanced chemiluminescence detection system, ECL-Plus, following manufacturer's directions.

3.4.10 Phospho-flow cytometry

JTAg cells were pretreated with the indicated concentrations of LYP inhibitors or DMSO for 30 min in RPMI 1640 at 37°C. Cells were then stimulated with supernatants of C305 hybridoma (*44*) for 2 min at 37°C. Cells were fixed immediately with BD Cytofix buffer, permeabilized using BD Phosflow Perm Buffer III and stained with AlexaFluor-488-conjugated anti-pZAP-70(Y319) antibody or anti-pSrc(Y416) antibody (which is cross-reactive with pLck(Y394), according to the manufacturer's protocols (BD Biosciences, San Jose, CA). Cell fluorescence was analyzed by FACS using a BD LSR II (BD Biosciences). Data was analyzed using FlowJo software (TreeStar, Ashland, OR).

3.4.11 3D QSAR modeling

Quantitative structure activity relationship (QSAR) studies were performed on the selected 17 compounds (*39, 40*). Relative percentage activity remaining upon treatment with 50 μM inhibitor was used as the desired experimental activity, as IC_{50}s were not available for all the compounds and the activity remaining upon treatment with 50 μM inhibitor correlated well with the IC_{50}s of the most of the compounds. Three-dimensional

conformations of the all the compounds were generated using LigPrep module of Schrödinger program (*45*). Only the lowest energy conformations were retained for the analysis. These compounds were optimally aligned using atom-based flexible alignment method. To perform the atom-based 3D-QSAR, PHASE module of the Schrödinger program was used (*46*). This approach considers various properties of the molecule in space by constructing a potential grid around the aligned molecules. Each grid point in the 3D space is scored according to one or more of the following atomic properties: propensity for the site to be a H-bond donor, hydrophobic or nonpolar, negative or positive charge centers, electron withdrawing group (such as nonnitrogen and oxygen) and other atom-types. Using a grid spacing of 1 Å and partial least square (PLS) fitting model, QSAR model was generated. PLS factor of one was considered for the model generation and increasing the factor did not increase the predictive ability of the model. The model generated was visualized to understand the atomic properties and its role in predicting the binding activity.

3.5 References

1. Bialy, L., and Waldmann, H. (2005) Inhibitors of protein tyrosine phosphatases: Next-generation drugs?, *Angew. Chem. Int. Ed. 44*, 2-27.

2. Veillette, A., Rhee, I., Souza, C. M., and Davidson, D. (2009) PEST family phosphatases in immunity, autoimmunity, and autoinflammatory disorders, *Immunol. Rev. 228*, 312-324.

3. Alonso, A., Bottini, N., Bruckner, S., Rahmouni, S., Williams, S., Schoenberger, S. P., and Mustelin, T. (2004) Lck dephosphorylation at Tyr-394 and inhibition of T cell antigen receptor signaling by yersinia phosphatase YopH, *J. Biol. Chem. 279*, 4922-4928.

4. Mustelin, T., Vang, T., and Bottini, N. (2005) Protein tyrosine phosphatases and the immune response, *Nat. Rev. Immunol. 5*, 43-57.

5. Krishnamurthy, D., Karver, M. R., Fiorillo, E., Orru, V., Stanford, S. M., Bottini, N., and Barrios, A. M. (2008) Gold(I)-mediated inhibition of protein tyrosine phosphatases: A detailed in vitro and cellular study, *J. Med. Chem. 51*, 4790-4795.

6. Obiri, D., Flink, N., Maier, J., Neeb, A., Maddalo, D., Thiele, W., Menon, A., Stassen, M., Kulkarni, R. A., Garabedian, M., Barrios, A. M., and Cato, A. (2012) PEST-domain-enriched tyrosine phosphatase and glucocorticoids as regulators of anaphylaxis in mice, *Allergy 67*, 175-182.

7. Cole, P. A., Courtney, A. D., Shen, K., Zhang, Z., Qiao, Y., Lu, W., and Williams, D. M. (2003) Chemical approaches to reversible protein phosphorylation, *Acc. Chem. Res. 36*, 444-452.

8. den Hertog, J., Groen, A., and van der Wijk, T. (2005) Redox regulation of protein-tyrosine phosphatases, *Arch. Biochem. Biophys. 434*, 11-15.

9. Biswas, S., Chida, A. S., and Rahman, I. (2006) Redox modifications of protein-thiols: Emerging roles in cell signaling, *Biochem. Pharmacol. 71*, 551-564.

10. Verweij, C. L., and Gringhuis, S. I. (2002) Oxidants and tyrosine phosphorylation: Role of acute and chronic oxidative stress in T-and B-lymphocyte signaling, *Antioxid. Redox Signal. 4*, 543-551.

11. Mahadev, K., Zilbering, A., Zhu, L., and Goldstein, B. J. (2001) Insulin-stimulated hydrogen peroxide reversibly inhibits protein-tyrosine phosphatase 1b in vivo and enhances the early insulin action cascade, *J. Biol. Chem. 276*, 21938-21942.

12. Karver, C. E., Ahmed, V. F., and Barrios, A. M. (2011) Oxidative inactivation of the lymphoid tyrosine phosphatase mediated by both general and active site directed NO donors, *Bioorg. Med. Chem. Lett. 21*, 285-287.

13. Wilson, M., Hogstrand, C., and Maret, W. (2012) Picomolar concentration of free zinc (II) ions regulate receptor protein tyrosine phosphatase beta activity, *J. Biol. Chem. 287*, 9322-9326.

14. Karver, M. R., Krishnamurthy, D., Kulkarni, R. A., Bottini, N., and Barrios, A. M. (2009) Identifying potent, selective protein tyrosine phosphatase inhibitors from a library of Au(I) complexes, *J. Med. Chem. 52*, 6912-6918.

15. Karver, M. R., Krishnamurthy, D., Bottini, N., and Barrios, A. M. (2010) Gold(I) phosphine mediated selective inhibition of lymphoid tyrosine phosphatase, *J. Inorg. Biochem. 104*, 268-273.

16. Kulkarni, R. A., Vellore, N. A., Bliss, M. R., Stanford, S. M., Falk, M. D., Bottini, N., Baron, R., and Barrios, A. M. (2013) Substrate Selection Influences

Molecular Recognition in a screen for lymphoid tyrosine phosphatase inhibitors, *Submitted*.

17. Eaton, P., Byers, H. L., Leeds, N., Ward, M. A., and Shattock, M. J. (2002) Detection, quantitation, purification, and identification of cardiac proteins S-thiolated during ischemia and reperfusion, *J. Biol. Chem. 277*, 9806-9811.

18. Tsai, S. J., Sen, U., Zhao, L., Greenleaf, W. B., Dasgupta, J., Fiorillo, E., Orru, V., Bottini, N., and Chen, X. S. (2009) Crystal structure of the human lymphoid tyrosine phosphatase catalytic domain: Insights into redox regulation, *Biochemistry 48*, 4838-4845.

19. Chu, F., and O'Brian, C. A. (2005) PKC sulfhydryl targeting by disulfiram produces divergent isozymic regulatory responses that accord with the cancer preventive activity of the thiuram disulfide, *Antioxid. Redox Signal. 7*, 855-862.

20. Soyka, M., and Rosner, S. (2010) Emerging drugs to treat alcoholism, *Exp. Opin. Emerg. Drugs 15*, 695-711.

21. Koppaka, V., Thompson, D. C., Chen, Y., Ellermann, M., Nicolaou, K. C., Juvonen, R. O., Petersen, D., Deitrich, R. A., Hurley, T. D., and Vasiliou, V. (2012) Aldehyde dehydrogenase inhibitors: A comprehensive review of the pharmacology, mechanism of action, substrate specificity, and clinical application, *Pharmacol. Rev. 64*, 520-539.

22. Deitrich, R. A., and Erwin, V. G. (1971) Mechanism of the inhibition of aldehyde dehydrogenase in vivo by disulfiram and diethyldithiocarbamate, *Mol. Pharmacol. 7*, 301-307.

23. Lipsky, J. J., Shen, M. L., and Naylor, S. (2001) In vivo inhibition of aldehyde dehydrogenase by disulfiram, *Chem. Biol. Interact. 130-132*, 93-102.

24. Vallari, R. C., and Pietruszko, R. (1982) Human aldehyde dehydrogenase: Mechanism of inhibition by disulfiram, *Science 216*, 637-639.

25. Kitson, T. M. (1975) The effect of disulfiram on the aldehyde dehydrogenases of sheep liver, *Biochem. J. 151*, 407-412.

26. Kitson, T. M. (1982) Further studies of the action of disulfiram and 2,2'-dithiodipyridine on the dehydrogenase and esterase activities of sheep liver cytoplasmic aldehyde dehydrogenase, *Biochem. J. 203*, 743-754.

27. Kitson, T. M. (1983) Mechanism of inactivation of sheep liver cytoplasmic aldehyde dehydrogenase by disulfiram, *Biochem. J. 213*, 551-554.

28. Cvek, B. (2011) Targeting malignancies with disulfiram (Antabuse): Multidrug resistance, angiogenesis, and proteasome, *Curr. Cancer Drug Targets 11*, 332-337.

29. Iljin, K., Ketola, K., Vainio, P., Halonen, P., Kohonen, P., Fey, V., Grafstrom, R. C., Perala, M., and Kallioniemi, O. (2009) High-throughput cell-based screening of 4910 known drugs and drug-like small molecules identifies disulfiram as an inhibitor of prostate cancer cell growth, *Clin. Cancer Res. 15*, 6070-6078.

30. Kona, F. R., Buac, D., and A, M. B. (2011) Disulfiram, and disulfiram derivatives as novel potential anticancer drugs targeting the ubiquitin-proteasome system in both preclinical and clinical studies, *Curr. Cancer Drug Targets 11*, 338-346.

31. Wang, F., Zhai, S., Liu, X., Li, L., Wu, S., Dou, Q. P., and Yan, B. (2011) A novel dithiocarbamate analogue with potentially decreased ALDH inhibition has copper-dependent proteasome-inhibitory and apoptosis-inducing activity in human breast cancer cells, *Cancer Lett. 300*, 87-95.

32. Ploemen, J. H. T. M., van Iersel, M. L. P. S., Wormhoudt, L. W., Commandeur, J. N. M., Vermeulen, N. P. E., and van Bladeren, P. J. (1996) In vitro inhibition of rat and human glutathione-S-transferase isozymes by disulfiram and diethyldithiocarbamate, *Biochem. Pharmacol. 52*, 197-204.

33. Wang, W., McLeod, H. L., and Cassidy, J. (2003) Disulfiram-mediated inhibition of NF-kappaB activity enhances cytotoxicity of 5-fluorouracil in human colorectal cancer cell lines, *Int. J. Cancer 104*, 504-511.

34. Nobel, C. S. I., Kimland, M., Nicholson, D. W., Orrenius, S., and Slater, A. F. G. (1997) Disulfiram is a potent inhibitor of proteases of the caspase family, *Chem. Res. Toxicol. 10*, 1319-1324.

35. Vang, T., Yuli, X., Liu, W. H., Vidovic, D., Liu, Y., Wu, S., Smith, D. H., Rinderspacher, A., Chung, C., Gong, G., Mustelin, T., Landry, D. W., Rickert, R. C., Schurer, S. C., Deng, S. X., and Tautz, L. (2011) Inhibition of lymphoid tyrosine phosphatase by benzofuran salicylic acids, *J. Med. Chem. 54*, 562-571.

36. Denu, J. M., and Dixon, J. E. (1998) Protein tyrosine phosphatases: Mechanisms of catalysis and regulation, *Curr. Opin. Chem. Biol. 2*, 633-641.

37. Denu, J. M., and Tanner, K. G. (1998) Specific and reversible inactivation of protein tyrosine phosphatases by hydrogen peroxide: Evidence for a sulfenic acid intermediate and implications for redox regulation, *Biochemistry 37*, 5633-5642.

38. Vang, T., Miletic, A. V., Arimura, Y., Tautz, L., Rickert, R. C., and Mustelin, T. (2008) Protein tyrosine phosphatases in autoimmunity, *Annu. Rev. Immunol. 26*, 29-55.

39. Dixon, S. L., Smondyrev, A. M., Knoll, E. H., Rao, S. N., Shaw, D. E., and Friesner, R. A. (2006) PHASE: A new engine for pharmacophore perception, 3D QSAR model development, and 3D database screening: 1. Methodology and preliminary results, *J. Comput. Aided Mol. Des. 20*, 647-671.

40. Suite 2012: Phase, version 3.4, Schrödinger, LLC, New York, NY, 2012.

41. Overton, W. R. (1988) Modified histogram subtraction technique for analysis of flow cytometry data, *Cytometry 9*, 619-626.

42. Gushwa, N. N., Kang, S., Chen, J., and Taunton, J. (2012) Selective targeting of distinct active site nucleophiles by irreversible src-family kinase inhibitors, *J. Am. Chem. Soc. 134*, 20214-20217.

43. Shaw, J. P., Utz, P. J., Durand, D. B., Toole, J. J., Emmel, E. A., and Crabtree, G. R. (1988) Identification of a putative regulator of early T cell activation genes, *Science 241*, 202-205.

44. Weiss, A., and Stobo, J. D. (1984) Requirement for the coexpression of T3 and the T cell antigen receptor on a malignant human T cell line, *J. Exp. Med. 160*, 1284-1299.

45. Suite 2012: LigPrep, version 2.5, Schrödinger, LLC, New York, NY, 2012.

46. Liu, S., Zhou, B., Yang, H., He, Y., Jiang, Z. X., Kumar, S., Wu, L., and Zhang, Z. Y. (2008) Aryl vinyl sulfonates and sulfones as active site-directed and mechanism-based probes for protein tyrosine phosphatases, *J. Am. Chem. Soc. 130*, 8251-8260.

CHAPTER 4

COVALENT INHIBITION OF LYMPHOID TYROSINE PHOSPHATASE USING PEPTIDE-BASED PHOSPHOTYROSINE MIMICS

4.1 Introduction

The balancing actions of protein tyrosine kinases (PTKs) and protein tyrosine phosphatases (PTPs) regulate tyrosine phosphorylation levels of cellular proteins which in turn regulate a multitude of cellular pathways (*1*). Aberrations in this highly regulated dynamic interplay lead to human diseases ranging from cancer to autoimmunity (*2, 3*). Therefore, both PTPs and PTKs have been recognized as relevant therapeutic targets for the treatment of these human disorders, but only PTK inhibitors have made it to the clinic thus far (*4-6*). This can be attributed to the fact that our understanding about actions, targets, regulation and biological roles of PTKs has surpassed that of PTPs (*7*). This is in part due to earlier notion that PTPs were simply 'housekeeping' enzymes that would dephosphorylate any target regardless of the surrounding amino acid sequence (*3*). However, it is now clear that PTPs exert exquisite substrate specificities as well as distinct physiological functions *in vivo* and inhibition of PTPs can be beneficial for therapeutic purposes (*8, 9*).

The human genome contains 107 genes that are predicted to encode for PTPs or proteins with a domain homologous to the catalytic PTP domain and 81 of these genes encode for active PTPs (*10*). Although crucial roles played by several PTPs have been documented (*11*), there is still a dearth in knowledge about pathological and physiological roles of several other PTPs, their subcellular localization and mechanisms of regulations (*12*). While genomic techniques such as gene knockout, RNAi (RNA interference), real-time polymerase chain reaction (RT-PCR) and protein overexpression have contributed significantly to our understanding of PTPs to date, these approaches have limitations (*13*). These limitations are discussed in detail in Chapter 1. In short, gene

knockout is tedious and can lead to activation of compensatory mechanisms; RNAi suffers from insufficient delivery and nonspecific attenuation of translation; RT-PCR only determines the abundance of proteins and not the activities; and protein overexpression can lead to nonspecific activities of the protein (*14*). Chemical knockdown of proteins compliments genomic approaches by exerting their effects on the endogenous molecular targets under the physiological and pathological conditions to reveal key insights into the activities of the target proteins (*15*). In addition, the chemical probes used for the chemical knockdown can provide a direct validation of novel therapeutic targets and offer insights that can help in subsequent development of new therapeutic agents.

As discussed in earlier chapters, lymphoid tyrosine phosphatase (LYP or PTPN22) has been recognized as an intriguing therapeutic target due to its association with human autoimmunity (*16-19*). Recently, our collaborators have used a selective LYP inhibitor developed by the Barrios Laboratory, C28, to create chemical knockdown of LYP in mast cells (*20*). Complimentary use of C28-mediated chemical knockdown of LYP and gene knockout was instrumental in establishing the positive regulatory role of LYP in mast cell degranulation and anaphylaxis. Furthermore, chemical knockdown of PEST-domain enriched tyrosine phosphatase (PEP), the mouse ortholog of LYP, was shown to alleviate anaphylaxis in mice. It was also shown that inhibition of PEP is synergistic with dexamethasone in the treatment of anaphylaxis. More detailed information on this study can be found in Chapter 1, section 1.3.2. This study underlines the importance of chemical knockdowns in studying the physiological and pathological roles of PTPs.

Despite this significant finding, very little information is available about the substrates, abundance, localization and regulation of LYP in mast cells. As discussed in detail in Chapter 1, LYP is also a negative regulator of T-cell receptor signaling (*17*). However, details of regulation of LYP in TCR signaling are still missing especially those pertaining to the abundance and subcellular localization of active versus inactive LYP in the presence of, as well as in the absence of TCR stimulation. Selective chemical probes that can help in visualization of the target protein upon its chemical knockdown can help in addressing these questions.

Activity-based probes (ABPs) can effectively profile functional states of enzymes in complex environments which in turn can lead to target identification and discovery of previously uncharacterized enzyme activity by creating chemical knockdowns of the proteins of interest (*21-23*). ABPs used for protein profiling are comprised of three main structural features: a reactive unit (also known as a warhead), a linker and a tag (Figure 4.1) (*12*). The warhead inhibits target proteins by covalent bond formation with the active site. The reactivity of the warhead can be tailored to selectively target a subset of proteins (*24*). Several enzymes contain nucleophiles such as cysteine, serine or lysine in their active site and therefore, the warheads for these enzymes are electrophiles that can form covalent bonds with these nucleophiles. A visualization tag enables detection and characterization of proteins labeled by the warhead while a linker connects the warhead and the tag. Apart from imparting flexibility and accessibility, the linker region can also be designed to incorporate selectivity.

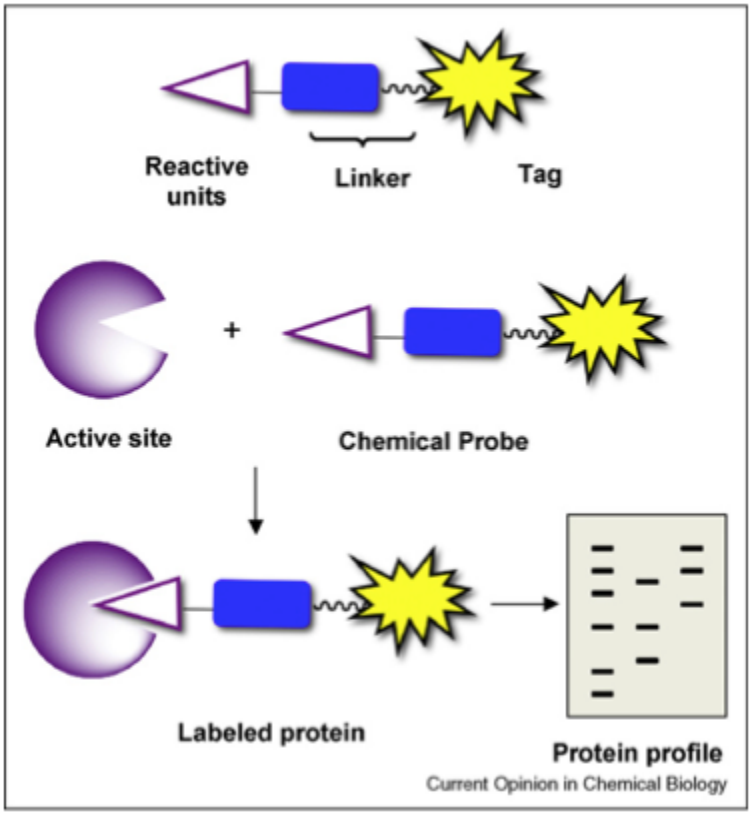

Figure 4.1. Structure and utility of ABPs. ABPs comprise of a reactive unit (warhead), a linker and a tag. Upon binding with the target proteins, ABPs label them covalently and the labeled proteins can then be visualized using the properties of the tag. This figure is reproduced with permission (*12*).

Although C28 has been instrumental in establishing role of LYP in anaphylaxis, unfortunately it cannot be used as a warhead in ABPs for LYP. This is because C28 is a gold(I) phosphine compound and the phosphine ligand falls off upon binding with LYP. Therefore, selective covalent inhibitors of LYP are necessary for developing ABPs for LYP as well as other PTPs.

All the PTPs have highly conserved active site and dephosphorylate their substrates through a common catalytic mechanism that uses a low pK_a, highly nucleophilic cysteine residue (*25, 26*). Therefore, it is quite intuitive that the ABPs for PTPs will contain phosphotyrosine (pY) mimicking, cysteine-reactive electrophilic moiety that form covalent bond with catalytic cysteine residue. Several such covalent inhibitors of PTPs have recently been described (Figure 4.2) (*27-30*). Some of the earliest molecules used for this purpose contained 4-fluoromethylphenyl phosphate moiety (for example, compound 1, Figure 4.2) that upon dephosphorylation by PTP generated a highly electrophilic quinone methide, which in turn can be attacked by a nucleophile to form a covalent bond (*29, 30*). Unfortunately, the quinone methide intermediate readily diffuses from the active site and has the undesired effect of covalently labeling other proteins nonspecifically. Other previously used warheads for PTPs contained α-bromobenzylphosphonates (compound 2), aryl vinyl sulfones (compound 3) and aryl vinyl sulfonates (compound 4) (*27, 28*). Although these probes showed good selectivity for PTPs over other cysteine dependent enzymes, they lacked selectivity among the PTPs. These probes therefore are useful for probing the global PTP proteome in a cell, but there is still a great need for probes that selectively target individual PTPs or the subfamilies of PTPs.

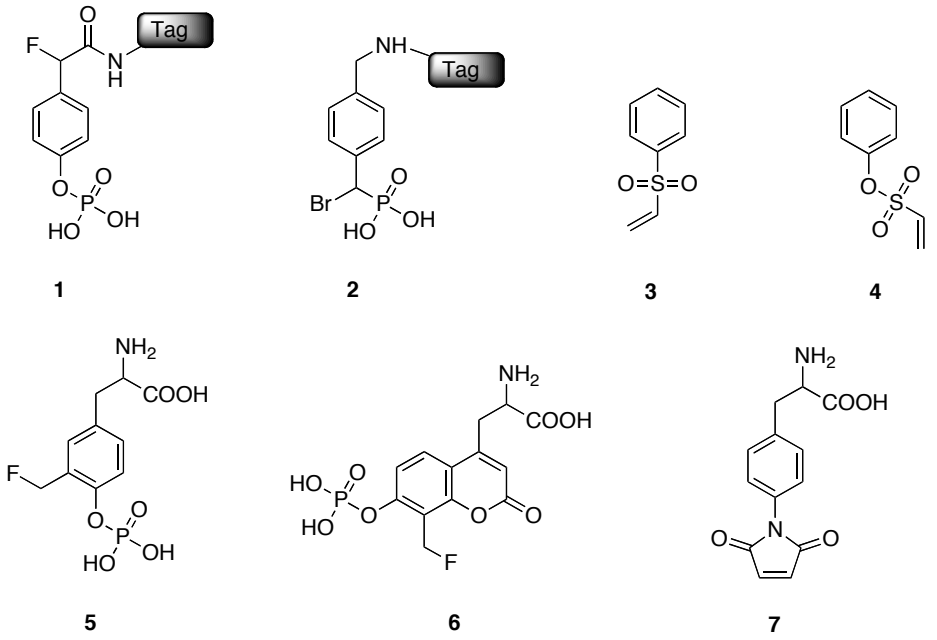

Figure 4.2. Covalent PTP inhibitors reported in literature. 1. Quinone-methide generating inhibitors 2. α-bromobenzylphosphonates 3. phenyl vinyl sulfone 4. phenyl vinyl sulfonate 5. 2-FMPT 6. 2-FMPCAP 7. Mal AA

It is well known that although PTPs have highly conserved active site, PTPs exhibit high specificities towards their substrates through interactions of amino acid residues flanking pY of the substrate with the nonconserved features on the PTP surface (*8*). PTPs also show higher catalytic efficiency towards turning over peptide sequences containing pY than pY alone (*31*). Also various pY-containing peptides show a range of k_{cat}/K_m values and both N- and C-terminal residues contribute to the substrate recognition of PTPs. These results indicate that residues flanking pY in a PTP substrate contribute towards catalytic efficiency and substrate recognition. Therefore, it has been

hypothesized that an ABP approach that combines the selectivity of using peptide-based inhibitors with the utility of an electrophilic pY mimic would be a potentially effective tool for selectively exploring activities of individual PTPs and subfamilies of PTPs (*12, 32*).

Progress has been made in this direction, with the development of several amino acid derived covalent inhibitors that can, in principle, be incorporated into optimized peptide sequences and used to specifically target one member of the family (*32-36*). The amino acids incorporating quinone-methide generating moieties such as 2-fluoromethylphosphotyrosine (2-FMPT, compound 5) (*34, 35*) and 2-fluoromethyl-phosphocoumaryl aminopropionic acid (2-FMPCAP, compound 6) (*33*), show improved selectivity when incorporated into peptide chain but still suffer from the inherent diffusibility of the quinone methides. L-bromophosphonomethylphenylalanine (BrPmp) (*36*) is quite challenging to synthesize in high purity and large quantities needed for peptide synthesis, compromising its feasibility as a widespread chemical probe. We have previously synthesized 4-maleimidophenyalanine (Mal AA, compound **7**) in high quantities for incorporation into peptides but owing to the inherent high reactivity of the maleimido group, the peptide incorporating Mal AA do not achieve desired selectivity (*32*). Therefore, significant work still needs to be done in this area to develop selective, easy to synthesize, peptide-based covalent inhibitors of PTPs.

4.2 Results and discussion

With the aim of developing a general approach that can be 'fine tuned' to target individual PTPs selectively, we designed peptide-based cysteine-reactive covalent

inhibitors. These inhibitor probes take advantage of the selectivity offered by the peptide sequence and the utility offered by the electrophilic warhead. By changing the peptide sequence that offers selectivity, these inhibitors can be tailored to target different PTPs. In order to narrow down the best peptide-based covalent inhibitor for LYP, we decided to optimize peptide sequence and the electrophilic warhead separately and then combine the best peptide sequence and the best warhead to obtain our desired probe. For optimizing the electrophilic warhead, we initially decided to synthesize several modified amino acids appended with cysteine reactive electrophilic groups that can be incorporated in peptide chains. However, syntheses of these modified amino acids in high purity and yields was quite challenging, with major difficulties arising from purification. Therefore, in order to simplify the syntheses and purification of the peptide-based covalent inhibitors, we decided to use click chemistry (Figure 4.3).

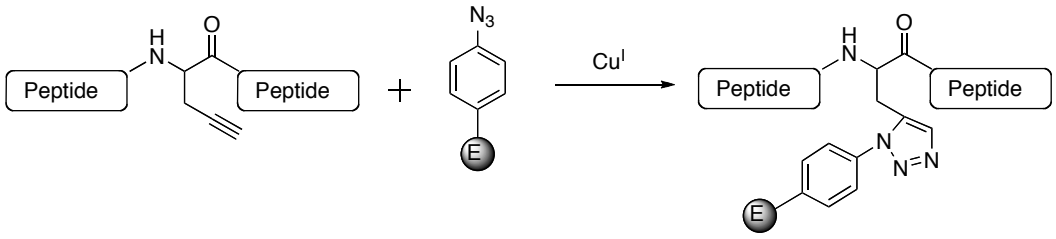

Figure 4.3. Simplified strategy for synthesis of peptide-based covalent inhibitors.

As per this strategy, for optimization of the warhead, we decided to first synthesize a generic peptide sequence that is appended with a handle for performing click chemistry. In Chapters 1 and 2, I have discussed in detail that ARLIEDNE-pY-TAREG-NH_2 is an accurate mimic of Lck pY394, a biological substrate of LYP (*37*). Therefore by replacing pY of the biological substrate with the propargylglycine (Pra) residue, we obtained Ac-ARLIEDNE-(Pra)-TAREG-NH_2. We also synthesized several aryl azides appended with electrophilic warheads (Figure 4.4) separately and clicked them onto Ac-ARLIEDNE-(Pra)-TAREG-NH_2 using copper catalyzed azide alkyne Huisgen cycloaddition to get the peptide-based covalent inhibitors of LYP.

First, commercially available 4-azidophenacyl bromide (compound **8**), an α-halomethyl ketone, was clicked on Ac-ARLIEDNE-(Pra)-TAREG-NH_2 to get Ac-ARLIEDNE-(PhAcBr)-TAREG-NH_2 (PhAcBr14mer) in a 45% yield. Other proposed aryl azides (Figure 4.4) are not commercially available and therefore we had to synthesize them.

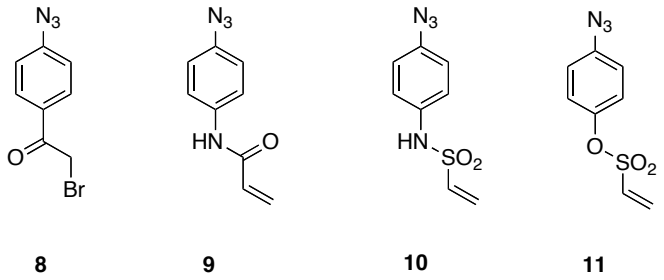

Figure 4.4. Aryl azide bearing pendant electrophiles for warhead optimization. 8. α-halomethyl ketones (phenacyl bromide) 9. acrylamide 10. vinylsulfonamide 11. vinylsulfonate.

For the synthesis of aryl azides bearing acrylamide electrophile (compound **9**), we first installed the electrophilic warhead onto 4-nitroaniline (Scheme 4.1). 4-Nitrophenylacrylamide (**12**) was generated by coupling acryloyl chloride with 4-nitroaniline using DIPEA as a base and DCM as solvent. The nitro group of the 4-nitrophenylacrylamide was then reduced chemoselectively to corresponding amine (**13**) using stannous chloride. 4-Aminophenylacrylamide (**13**) was then converted to 4-azidophenylacrylamide (**9**) by diazotization followed by substitution reaction using sodium azide. Compound **9** was then clicked onto Ac-ARLIEDNE-(Pra)-TAREG-NH_2 to get Ac-ARLIEDNE-(Acr)-TAREG-NH_2 (Acr14mer).

4-Azidophenyl vinylsulfonamide (**10**) was synthesized by reacting 4-azidoaniline hydrochloride with 2-chloroethanesulfonyl chloride in DCM using triethylamine (TEA) as a base (Scheme 4.2). Apart from coupling, triethylamine also helps in dehydrohalogenation of 2-chloroethanesulfonyl moiety to give the vinylsulfonyl moiety in one step. The resulting vinylsulfonamide was obtained in quantitative yield and was used for coupling with Ac-ARLIEDNE-(Pra)-TAREG-NH_2 to get Ac-ARLIEDNE-(VsN)-TAREG-NH_2 (VsN14mer).

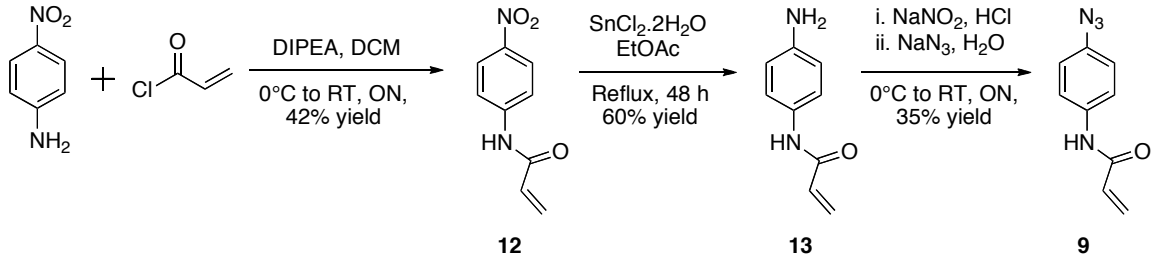

Scheme 4.1. Synthesis of 4-azidophenylacrylamide.

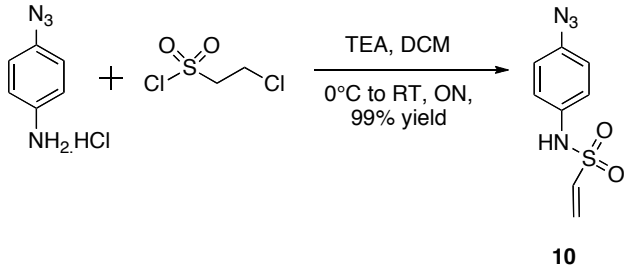

10

Scheme 4.2. Synthesis of 4-azidophenylvinylsulfonamide.

Synthesis of 4-azidophenylvinylsulfonate (**11)** was carried out in 3 steps (Scheme 4.3) starting with coupling of 4-*N*-Boc-aminophenol with 2-chloroethanesulfonyl chloride using sodium hydride as a strong base to obtain the vinylsulfonate (**14)**. *N*-Boc group was then cleaved off and the resultant free amine (**15)** was replaced with azide by diazotization followed by substitution using sodium azide. The resulting compound **11** was clicked onto Ac-ARLIEDNE-(Pra)-TAREG-NH_2 to get Ac-ARLIEDNE-(VsO)-TAREG-NH_2 (VsO14mer).

In order to establish that the clicked peptide-based covalent inhibitors have advantage over the small molecule warheads appended onto the peptides and just these flanking peptide sequence lacking the pY-binding pocket reactive moiety, we decided to study their LYP inhibition. VsO14mer (IC_{50} = 90 ± 8 μM) inhibited LYP much more potently than the corresponding small molecule, phenyl vinyl sulfonate (PhVsO, compound **4**, IC_{50} = 350 ± 10 μM) that has previously been used as ABP for PTPs (Figure 4.5*A*) (*28*). This result is consistent with previous observation that peptide sequences help in potent binding of the substrates to PTPs (*31*). For studying whether just the flanking peptide sequence are enough for LYP inhibition, we first synthesized a

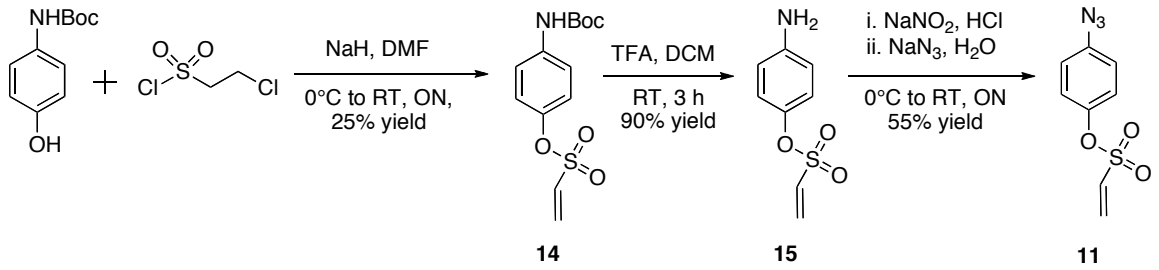

Scheme 4.3. Synthesis of 4-azidophenylvinylsulfonate

peptide based on the biological substrate of LYP but lacking a pY-binding pocket- (active site-) directed motif: Ac-ARLIEDNE-A-TAREG-NH_2 (Ala14mer) and a peptide-possessing the aryl ring to fit in active site but lack phosphate: Ac-ARLIEDNE-Y-TAREG-NH_2 (Tyr14mer). Tyr14mer is also the product of biological reaction of PTP. We found that while Tyr14mer (IC_{50} = 500 ± 25 μM) showed some inhibition of LYP at high concentrations, Ala14mer did not show much inhibition of LYP even at 1 mM concentration (Figure 4.5*B*). This indicates that the peptide sequence with some interactions with active site can help in potent inhibition of Lyp. However, higher inhibition potency can be derived through peptide sequenced that also contained a pY mimic (for example VsO14mer).

Next, LYP inhibitory potencies of the clicked peptide appended with different electrophilic warheads were compared to determine the optimum warhead for potent LYP targeting (Figure 4.6). Clicked peptide with a pendant vinyl sulfonamide warhead (VsN14mer, IC_{50} = 60 ± 3 μM) was found to be the most potent LYP inhibitor closely followed by VsO14mer (IC_{50} = 90 ± 8 μM). PhAcBr14mer (IC_{50} = 200 ± 15 μM) and Acr14mer (IC_{50} = 200 ± 10 μM) were found to be less potent inhibitors of LYP than

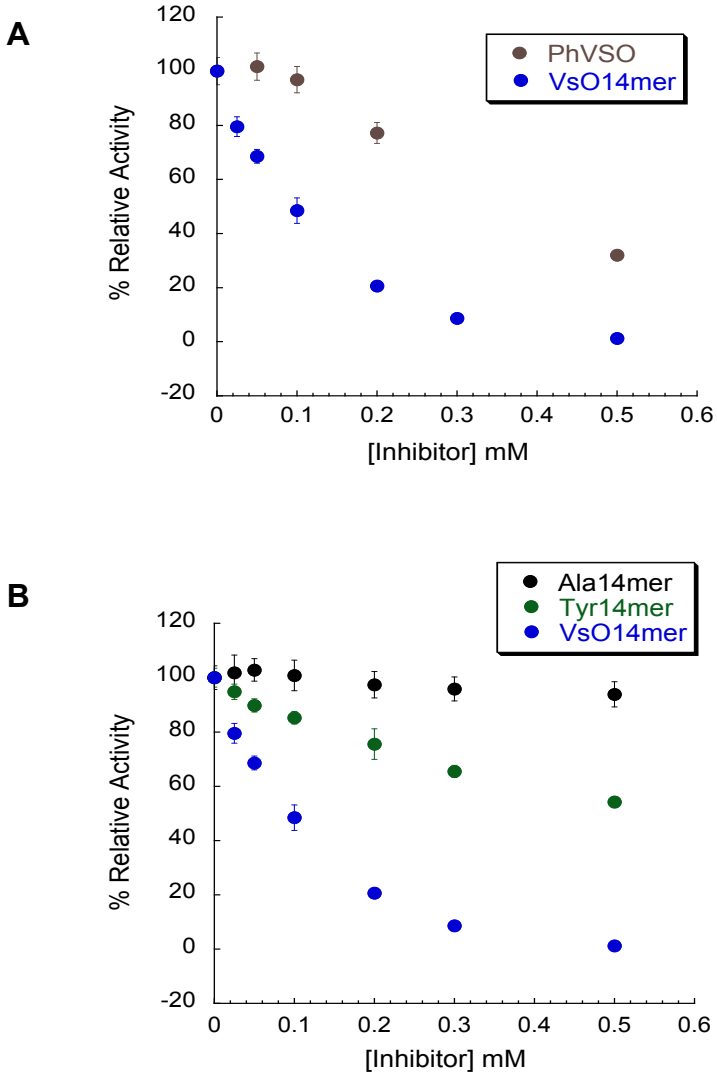

Fig. 4.5. Clicked peptides inhibit LYP more potently than the corresponding small molecule or the peptide sequence. (A) Comparison of LYP inhibition of phenyl vinyl sulfonate (PhVSO, compound **4**) and the clicked peptide containing vinyl sulfonate warhead. (B) Comparison of LYP inhibition of clicked peptide containing vinyl sulfonate warhead and control peptide sequences without any warhead.

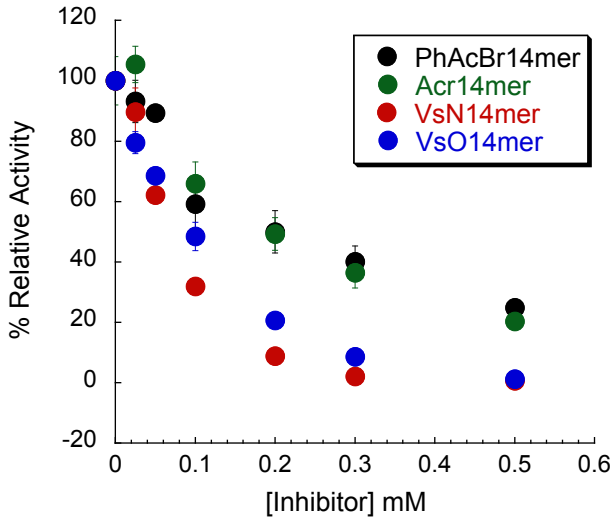

Fig. 4.6. Comparison of LYP inhibition of clicked peptides appended with different electrophilic warheads.

VsN14mer and VsO14mer but these peptides inhibited LYP with more potency than the small molecule compound 4, Ala14mer and Tyr14mer. This confirmed that our clicked peptides are superior inhibitors than the small molecule warheads and the peptide sequence itself and also the potency of LYP inhibition varies with the electrophilic warhead. Vinylsulfonamide warhead, owing to the most potent inhibition of LYP by VsN14mer, was confirmed as the optimum warhead for LYP.

For optimizing the peptide sequence for potent and selective targeting of LYP, Dr. Ryan Mathews in the Barrios Laboratory used one-bead-one-compound (OBOC) library approach to screen combinatorial peptide libraries to identify the best LYP substrate. Although this substrate activity screening exercise helped in identifying several excellent substrates of LYP, only a handful of these substrates showed good selectivity for LYP over PTP-PEST (*38*). Ac-LDLL-(pCAP)-SDDD-NH_2 was identified as an excellent LYP

substrate that showed the most selectivity over the other highly homologous PTPs including PTP-PEST with $k_{cat}/K_{m,}$ about 5-times higher for LYP than PTP-PEST. Combining the peptide sequence that showed the most selectivity for LYP over other homologous PTPs with the electrophilic warhead that showed most potent LYP inhibition, we obtained Ac-LDLL-(VsN)-SDDD-NH_2 (LDVsN). LDVsN (IC_{50} = 20 ± 1 µM) was found to inhibit LYP 3-fold more potently than VsN14mer (IC_{50} = 60 ± 3 µM), indicating that optimizing the peptide sequence can help in achieving desired inhibitory potency (Figure 4.7). Finally, the selectivity of LDVsN for targeting LYP was investigated by comparing LDVsN mediated inhibition of the homologous PTPs (Figure 4.8). LDVsN was found to inhibit LYP with high selectivity over PTP1B (IC_{50} > 50 µM) and TCPTP (IC_{50} > 50 µM), and with moderate selectivity over CD45 (IC_{50} = 48 ± 3 µM). However, LDVsN showed only low preference for inhibition of LYP over highly homologous PTP-PEST (IC_{50} = 33 ± 1 µM). These selectivity results were comparable to those obtained from substrate activity screening approach. In the future, our best covalent inhibitor, LDVsN will be tested in cells with the aim of using it in addressing biological problems relevant to LYP.

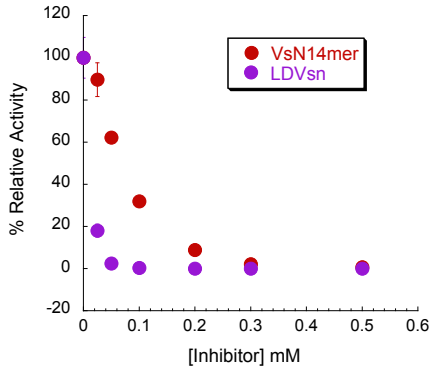

Fig. 4.7. Comparison of LYP inhibition of VsN14mer and LDVsN.

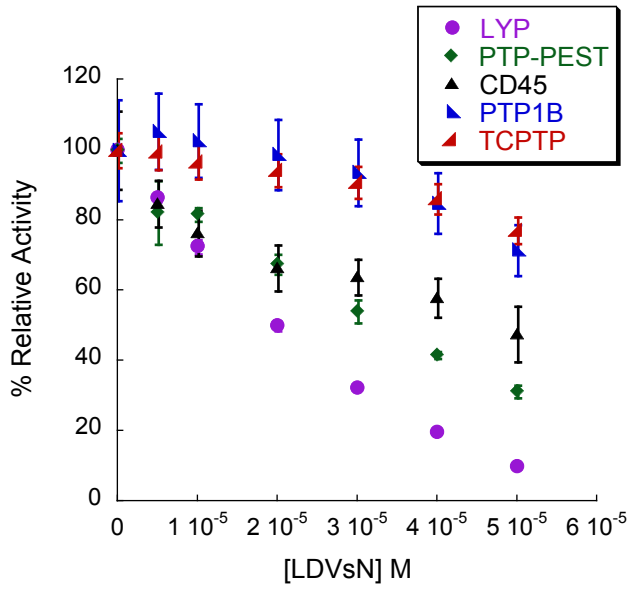

Fig. 4.8. Comparison of LDVsN mediated inhibition of LYP and other homologous PTPs.

4.3 Conclusions

Although several ABPs for PTPs are available, none of them target one PTP selectively over others. Peptide-based covalent inhibitors take advantage of the selectivity offered by the peptide sequence and the utility offered by the electrophilic warhead. Clicking aryl azides on Pra-peptides can help in synthesizing a combinatorial peptide-based covalent inhibitor library that can be fine-tuned to target different PTPs. Clicked peptides inhibit LYP more potently than the small molecule electrophile or the peptide sequence itself. Inhibition potencies of the clicked peptides vary with the electrophile and the peptide sequence used. Among the electrophilic warheads studied, vinylsulfonamide warhead was found to be the most potent LYP inhibitor. Combining this warhead with

separately optimized LYP selective sequence helped in designing LDVsN probe. LDVsN was found to inhibit LYP potently over VsN14mer and LDVsN inhibited LYP selectively over other homologous PTPs. LDLL-(VsN)-SDDD will be studied in cells in the future with the aim of using it in activity-based protein profiling.

4.4 Experimental section

All reagents were obtained from commercial sources and used without further purification. All NMR spectra were recorded on a Mercury 400 MHz spectrometer and were referenced to residual solvent peaks or TMS (δ 0.00 ppm). Column chromatography was performed on EMD silica gel (60-200 mesh) or EMD alumina (80-200 mesh). Thin layer chromatography was performed on EMD silica gel 60 F_{254} or aluminum oxide 60 F_{254} precoated aluminum plates (0.2mm thickness). cDNA fragments encoding the catalytic domains of LYP (aa 2-309) and PTP-PEST (aa 2-323) were cloned between the BamH1 and the Xho1 sites of pET28a plasmid (Novagen) in frame with a cleavable N-terminal 6xHis-tag. Recombinant proteins were purified from lysates of IPTG-induced *Escherichia coli* BL21 cells by affinity chromatography on Ni-nitrilotriacetic acid columns. 6xHisHePTP was eluted using 250 mM imidazole. Untagged LYP and PTP-PEST were eluted by incubating columns with thrombin, followed by removal of thrombin from the protein preparation by a second chromatography step on benzamidine columns. The catalytic domains of human recombinant CD45, PTP1B and TCPTP were obtained from Enzo life sciences. All of the activity assays involving LYP, PTP-PEST and CD45 were performed at ambient temperature using a buffer containing 50 mM Bis-Tris, pH 6.5, 100 mM NaCl, 2 mM EDTA, and 0.01% Brij 35. Activity assays involving

PTP1B and TCPTP were performed at ambient temperature using a buffer containing 50 mM Tris, pH 7.2, 100 mM NaCl, 2 mM EDTA, and 0.01% Brij 35. Enzymes were pre-incubated with 0.5 mM TCEP for 30 min before adding inhibitor. Enzyme activity was measured at room temperature (21-24˚C) in black 96-well plates. Fluorescence data were collected on a Molecular Devices Spectramax M5 multimode plate reader with excitation and emission at 360 and 455 nm, respectively. The increase in the fluorescence due to the hydrolysis of the substrates was measured every 60 s for 30 min. Fluorescence values in the linear range of the Michaelis-Menten kinetics curve were used for the data analysis.

4.4.1 Synthesis of 4-nitrophenyl acrylamide (12)

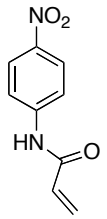

4-Nitroaniline (5 mmol) was taken in a RBF and dry DCM (25 mL) was added to it under N_2 atmosphere. The resulting solution was cooled to 0°C and then DIPEA (7.5 mmol) and acryloyl chloride (10 mmol) were added to it. The reaction was allowed to warm up to room temperature and stirred overnight at room temperature and monitored by TLC using EtOAc:hexanes (30:70) as mobile phase. Once the reaction was complete, it was quenched with methanol and water. Reaction mixture was extracted with DCM and washed with brine, dried over Na_2SO_4 and concentrated under reduced pressure. Crude product was then purified by column chromatography on silica gel using gradient of EtOAc in hexanes as mobile phase to get the pure product. (Yield 42%)

^{1}H NMR (400 MHz, DMSO-d_6) δ (ppm) 10.75 (s, 1H), 8.22 (d, J = 8.8 Hz, 2H), 7.90 (d, J = 9.2 Hz, 2H), 6.46 (dd, J = 10.4, 16.8 Hz, 1H), 6.32 (dd, J = 1.6, 17.2 Hz, 1H),

5.84 (d, J = 1.6, 10.0 Hz, 1H); ^{13}C NMR (100 MHz, DMSO-d_6) δ (ppm) 164.5, 145.9, 143.1, 131.9, 129.3, 125.7, 119.8.

4.4.2 Synthesis of 4-aminophenyl acrylamide (13)

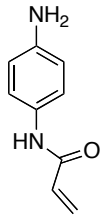

4-Nitrophenyl acrylamide (2 mmol) was taken in a RBF and EtOAc (50 mL) was added to it. To the resulting solution was added $SnCl_2.2H_2O$ (8 mmol). The reaction was stirred at room temperature overnight and was monitored by TLC using EtOAc:hexanes (50:50) as mobile phase. Since the reaction did not proceed significantly at room temperature, it was then refluxed at 78°C for 48 h. Once the reaction was complete, it was cooled down to room temperature and quenched by stirring with 2N NaOH (50 mL) for 30 min. Reaction mixture was then extracted with EtOAc and washed with brine, dried over Na_2SO_4 and concentrated under reduced pressure. Crude product was then purified by crystallization using EtOAc and hexanes. (Yield 60%)

^{1}H NMR (400 MHz, $CDCl_3$) δ (ppm) 7.35 (d, J = 8.4 Hz, 2H), 6.64 (d, J = 8.4 Hz, 2H), 6.38 (d, J = 16.8 Hz, 1H), 6.23 (dd, J = 10.0, 16.8 Hz, 1H), 5.69 (d, J = 9.6 Hz, 1H).

4.4.3 Synthesis of 4-azidophenyl acrylamide (9)

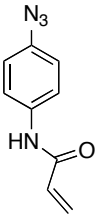

4-aminophenyl acrylamide (0.5 mmol) was taken in a RBF and dissolved in 2M HCl (5 mL) and 500 µL of methanol was added to it and the reaction was cooled to 0°C. Conc. HCl (5 drops) was added to the reaction and the solution was stirred at 0°C for 30 min away from light. To this reaction, was added, dropwise, prechilled solution of sodium nitrite (2 mmol) in water (2 mL)

taking care not to let the reaction warm up. The reaction mixture was further stirred at 0°C for 30 min. Then a pre-chilled solution of sodium azide (2.5 mmol) in water (2 mL) was added, dropwise, to the reaction slowly enough not to let the reaction warm up. The reaction was further stirred at 0°C for 2 h and then overnight away from the light, allowing it to gradually warm up to room temperature. The reaction was monitored by TLC using EtOAc:hexanes (30:70) as mobile phase. Once the reaction was complete, the reaction mixture was diluted with DCM and washed with chilled brine, dried over Na_2SO_4 and concentrated under reduced pressure. Crude product was then dissolved in DCM and purified by filtering over alumina bed and washing the alumina bed well with DCM. Combined DCM washings were evaporated under reduced pressure to get the pure product. (Yield 35%)

^{1}H NMR (400 MHz, $CDCl_3$) δ (ppm) 7.60 (d, J = 8.8 Hz, 2H), 7.00 (d, J = 8.8 Hz, 2H), 6.42-6.46 (m, 1H), 6.22-6.28 (dd, J = 10.0, 16.8 Hz, 1H), 5.78 (d, J = 10.0 Hz, 1H).

4.4.4 Synthesis of 4-azidophenyl vinylsulfonamide (10)

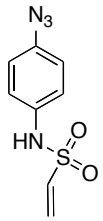

4-Azidoaniline hydrochloride (0.5 mmol) was taken in a RBF and dry DCM (10 mL) was added to it under N_2 atmosphere. The reaction mixture was cooled in the ice bath. Triethylamine (2 mmol) was then added to the RBF while stirring followed by 2-chloroethane sulfonyl chloride (1 mmol). The reaction was kept away from light and stirred overnight allowing it to warm up to room temperature and monitored by TLC using EtOAc:hexanes (30:70) as mobile phase. Once the reaction was complete, the reaction mixture was diluted with DCM and washed with chilled brine, dried over Na_2SO_4 and concentrated under reduced pressure. Crude product

was then dissolved in DCM and purified by filtering over alumina bed and washing the alumina bed well with DCM. Combined DCM washings were evaporated under reduced pressure to get the pure product. (Yield 99%)

^{1}H NMR (400 MHz, $CDCl_3$) δ (ppm) 7.77 (dd, *J* = 2.0, 8.8 Hz, 2H), 7.04 (dd, *J* = 10.4, 16.8 Hz, 1H), 6.99 (d, *J* = 8.4 Hz, 2H), 6.29 (d, *J* = 16.4 Hz, 2H), 6.16 (d, *J* = 9.6 Hz, 2H).

4.4.5 Synthesis of 4-*N*-Boc-aminophenyl vinylsulfonate (14)

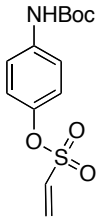

4-*N*-Boc-aminophenol (5 mmol) was taken in a RBF and dry DMF (50 mL) was added to it under N_2 atmosphere. The resulting solution was cooled to 0°C and sodium hydride (60% suspension in mineral oil) (16 mmol) was then added slowly to the RBF and stirred for 15 min. Next, 2-chloroethane sulfonyl chloride (10 mmol) was added, dropwise, to the reaction mixture while stirring. The reaction was allowed to warm up to room temperature and stirred overnight at room temperature and monitored by TLC using EtOAc:hexanes (30:70) as mobile phase. Once the reaction was complete, the reaction was quenched with methanol and water. Reaction mixture was extracted with DCM and washed with brine, dried over Na_2SO_4 and concentrated under reduced pressure. Crude product was then purified by column chromatography on silica gel using gradient of EtOAc in hexanes as mobile phase to get the pure product. (Yield 25%)

^{1}H NMR (400 MHz, $CDCl_3$) δ (ppm) 8.02 (s, 1H), 7.38 (d, *J* = 8.8 Hz, 2H), 7.15 (d, *J* = 8.8 Hz, 2H), 6.64 (d, *J* = 10.0, 16.8 Hz, 1H), 6.34 (d, *J* = 17.2 Hz, 1H), 6.15 (d, *J*

= 10.0 Hz, 1H), 1.51 (s, 9H); ^{13}C NMR (100 MHz, $CDCl_3$) δ (ppm) 152.8, 144.7, 137.8, 132.1, 123.1, 119.6, 81.2, 77.6, 77.5, 77.3.

4.4.6 Synthesis of 4-aminophenyl vinylsulfonate (15)

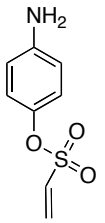

4-*N*-Boc-aminophenyl vinylsulfonate (1 mmol) was dissolved in DCM (10 mL) and trifluoroacetic acid (TFA) (1 mL) was added to it while stirring. The reaction was stirred at room temperature for 3 h and monitored by TLC using EtOAc:hexanes (50:50) as mobile phase. Once the reaction was complete, the reaction was basified with aq. $NaHCO_3$ to quench the acid. Reaction mixture was extracted with DCM and washed with aq. $NaHCO_3$, brine, dried over Na_2SO_4 and concentrated under reduced pressure. Crude product was then purified by column chromatography on neutral alumina using gradient of methanol in DCM as mobile phase to get the pure product. (Yield 90%)

^{1}H NMR (400 MHz, $CDCl_3$) δ (ppm) 7.00 (d, J = 8.4 Hz, 2H), 6.60-6.66 (m, 3H), 6.33 (d, J = 16.4 Hz, 1H), 6.13 (dd, J = 10.0 Hz, 1H).

4.4.7 Synthesis of 4-azidophenyl vinylsulfonate (11)

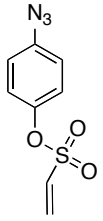

Diazotization followed by substitution by sodium azide was carried out using 4-aminophenyl vinylsulfonate (0.5 mmol) as described earlier in the synthesis of 4-azidophenyl acrylamide (**9**). (Yield 55%)

^{1}H NMR (400 MHz, $CDCl_3$) δ (ppm) 7.20 (d, J = 8.8 Hz, 2H), 7.03 (d, J = 8.8 Hz, 2H), 6.66 (dd, J = 9.6, 16.4 Hz, 1H), 6.37 (dd, J = 4.4, 16.8 Hz, 1H), 6.19 (d, J = 6.0, 10.0 Hz, 1H).

4.4.8 General procedure for peptide synthesis

Solid phase peptide synthesis was carried out using Aaptech Focus XC automated peptide synthesizer. Rink Amide AM resin (0.1 mmol) was added to the reaction vessel (RV) of the peptide synthesizer and each amino acid in the sequence (3 equiv each) along with HOBT (5 equiv) were dissolved in 3 mL DMF and were added to the respective assigned amino acid vessel on the peptide synthesizer. Rink Amide AM resin was allowed to swell in 5 mL DMF while mechanically mixing for 30 min. DMF was then drained and N-terminal 9-fluorenylmethoxycarbonyl (Fmoc) group of the resin was then cleaved off using 3 mL 2% w/v Diazabicyclo[5.4.0]undec7-ene (DBU) in DMF for 15 min. Deprotection step was repeated by draining this solution and then adding another 3 mL of 2% DBU and mixing for an additional 15 min. The fully deprotected resin was then washed with DMF (3x3 mL). The desired amino acid along with HOBT was then preactivated with DICI (5 equiv) for 10 min. The mixture was then added to the rinsed resin in RV and mixed for 90 min. After coupling, the solution was drained and rinsed with DMF (3x3 mL) and deprotected with 3 mL 2% DBU as before and the cycle was repeated until each amino acid from C-terminus to N-terminus was added. After the coupling of the final amino acid (G), the resin was transferred to a manual peptide synthesis vessel. The resin was then deprotected and N-terminus was acetylated using acetic acid (3 equiv), (2-(6-chloro-1H-benzotriazole-1-yl)-1,1,3,3-tetramethylaminium hexafluorophosphate) (HCTU) (5 equiv) and diisopropylethylamine (DIPEA) (10 equiv) in 1 mL of DMF. The resin was then washed with DMF (3x1 mL) and DCM (3x1 mL) and dried under vacuum. The peptide was cleaved from the resin using a cleavage cocktail containing 95% TFA (v/v), 2.5% water (v/v), and 2.5% TIS (v/v) overnight. The

peptide was then collected under vacuum and the resin was rinsed with 1 mL TFA and 10 mL water. The collected solution was diluted with approx 35 mL water and lyophilized. The peptide was then purified by HPLC and characterized by MALDI-TOF.

4.4.9 Synthesis of Ac-ARLIEDNE-(Pra)-TAREG-NH_2

Yield 20%. MS (MALDI-TOF) Calculated exact mass: 1608.8, Observed: 1609.8 (100%), 1591.8 (80%) (Corresponds to m-H_2O+1).

4.4.10 Synthesis of Ac-ARLIEDNE-A-TAREG-NH_2

Yield 10%. MS (MALDI-TOF) Calculated exact mass: 1584.8, Observed: 1585.8 (100%)

4.4.11 Synthesis of Ac-ARLIEDNE-Y-TAREG-NH_2

Yield 8%. MS (MALDI-TOF) Calculated exact mass: 1676.8, Observed: 1677.9 (60%), 1659.9 (100%)

4.4.12 Synthesis of Ac-LDLL-(Pra)-SDDD-NH_2

Yield 7%. MS (MALDI-TOF) Calculated exact mass: 1040.5, Observed: 1063.5 (100%)(Corresponds to m+Na).

4.4.13 General procedure for click chemistry

Peptide containing propargylglycine (3.5 μmol) was taken in a RBF and dissolved in a mixture of acetonitrile:DMSO:water (8:2:1) and stirred. To this, 2,6-lutidine (7

μmol), sodium ascorbate (3.5 μmol) and aryl azide (7 μmol) were added while stirring. After this, CuI (1.75 μmol) was added to the reaction mixture and the air in the reaction vessel was displaced by N_2. The reaction was stirred overnight under N_2, away from light. Upon completion, the solvents were lyophilized and the residue was dissolved in a mixture of acetonitrile and water and purified by HPLC and characterized by MALDI-TOF.

4.4.14 Synthesis of Ac-ARLIEDNE-(PhAcBr)-TAREG-NH_2

Yield 45%. MS (MALDI-TOF) Calculated exact mass: 1847.8, Observed: 1768.9 (100%, m+1-80), 1770.8 (60%, m+1-78) These peaks correspond to the cations formed after the loss of Br. In this case Br seems to be falling off during Maldi-TOF.

4.4.15 Synthesis of Ac-ARLIEDNE-(Acr)-TAREG-NH_2

Yield 30%. MS (MALDI-TOF) Calculated exact mass: 1797.9, Observed: 1798.8 (100%)

4.4.16 Synthesis of Ac-ARLIEDNE-(VsN)-TAREG-NH_2

Yield 40%. MS (MALDI-TOF) Calculated exact mass: 1832.8, Observed: 1833.6 (100%)

4.4.17 Synthesis of Ac-ARLIEDNE-(VsO)-TAREG-NH_2

Yield 40%. MS (MALDI-TOF) Calculated exact mass: 1833.8, Observed: 1834.9 (100%)

4.4.18 Synthesis of Ac-LDLL-(VsN)-SDDD-NH_2

Yield 30%. MS (MALDI-TOF) Calculated exact mass: 1264.5, Observed: 1287.8 (100%)

4.4.19 *In vitro* inhibition assay

The final concentration of Lyp used for *in vitro* assays was 5 nm. The final concentration of the DiFMUP used was 1.5 μM. The total DMSO concentration in each reaction was held constant at 6% of the total reaction volume (100 μL). Stock solutions and serial dilutions of the compounds for determination of IC_{50} were made in DMSO. Inhibitor was incubated with the enzyme for 15 min before initiating the activity assay by adding the substrate. The percent relative activity for each compound was determined by factoring the measured fluorescence values for the compound treated wells over the control wells treated with DMSO only. The resulting plot of inhibitor concentration versus percent enzyme activity provided the IC_{50} values.

4.5 References

1. Hunter, T. (1995) Protein kinases and phosphatases: The yin and yang of protein phosphorylation and signaling, *Cell 80*, 225-236.

2. Julien, S. G., Dube, N., Hardy, S., and Tremblay, M. L. (2011) Inside the human cancer tyrosine phosphatome, *Nat. Rev. Cancer 11*, 35-49.

3. Vang, T., Miletic, A. V., Arimura, Y., Tautz, L., Rickert, R. C., and Mustelin, T. (2008) Protein tyrosine phosphatases in autoimmunity, *Annu. Rev. Immunol. 26*, 29-55.

4. Bialy, L., and Waldmann, H. (2005) Inhibitors of protein tyrosine phosphatases: Next-generation drugs?, *Angew. Chem. Int. Ed. 44*, 2-27.

5. Vintonyak, V. V., Antonchick, A. P., Rauh, D., and Waldmann, H. (2009) The therapeutic potential of phosphatase inhibitors, *Curr. Opin. Chem. Biol. 13*, 272-283.

6. Zhang, Z.-Y. (2001) Protein tyrosine phosphatases: Prospects for therapeutics, *Curr. Opin. Chem. Biol. 5*, 416-423.

7. Neel, B. G., and Tonks, N. K. (1997) Protein tyrosine phosphatases in signal transduction, *Curr. Opin. Cell Biol. 9*, 193-204.

8. Barr, A. J., Ugochukwu, E., Lee, W. H., King, O. N., Filippakopoulos, P., Alfano, I., Savitsky, P., Burgess-Brown, N. A., Muller, S., and Knapp, S. (2009) Large-scale structural analysis of the classical human protein tyrosine phosphatome, *Cell 136*, 352-363.

9. Tiganis, T., and Bennett, A. M. (2007) Protein tyrosine phosphatase function: The substrate perspective, *Biochem. J. 402*, 1-15.

10. Alonso, A., Sasin, J., Bottini, N., Friedberg, I., Friedberg, I., Osterman, A., Godzik, A., Hunter, T., Dixon, J., and Mustelin, T. (2004) Protein tyrosine phosphatases in the human genome, *Cell 117*, 699-711.

11. Tonks, N. K. (2006) Protein tyrosine phosphatases: From genes, to function, to disease, *Nat. Rev. Mol. Cell Biol. 7*, 833-846.

12. Krishnamurthy, D., and Barrios, A. M. (2009) Profiling protein tyrosine phosphatase activity with mechanistic probes, *Curr. Opin. Chem. Biol. 13*, 375-381.

13. He, R., Zeng, L. F., He, Y., Zhang, S., and Zhang, Z. Y. (2013) Small molecule tools for functional interrogation of protein tyrosine phosphatases, *FEBS J. 280*, 731-750.

14. Zhang, Z. Y. (2005) Functional studies of protein tyrosine phosphatases with chemical approaches, *Biochim. Biophys. Acta 1754*, 100-107.

15. Smukste, I., and Stockwell, B. R. (2005) Advances in chemical genetics, *Annu. Rev. Genomics Hum. Genet. 6*, 261-286.

16. Cohen, S., Dadi, H., Shaoul, E., Sharfe, N., and Roifman, C. M. (1999) Cloning and characterization of a lymphoid-specific, inducible human protein tyrosine phosphatase, Lyp, *Blood 93*, 2013-2024.

17. Veillette, A., Rhee, I., Souza, C. M., and Davidson, D. (2009) PEST family phosphatases in immunity, autoimmunity, and autoinflammatory disorders, *Immunol. Rev. 228*, 312-324.

18. Xie, Y., Liu, Y., Gong, G., Rinderspacher, A., Deng, S.-X., Smith, D. H., Toebben, U., Tzilianos, E., Branden, L., Vidovic, D., Chung, C., Schurer, S., Tautz, L., and Landry, D. W. (2008) Discovery of a novel submicromolar inhibitor of the lymphoid tyrosine phosphatase, *Bioorg. Med. Chem. Lett. 18*, 2840-2844.

19. Yu, X., Sun, J.-P., He, Y., Guo, X., Liu, S., Zhou, B., Hudmon, A., and Zhang, Z.-Y. (2007) Structure, inhibitor and regulatory mechanism of LYP, a lymphoid-specific tyrosine phosphatase implicated in autoimmune diseases, *Proc. Natl. Acad. Sci. U.S.A 104*, 19767-19772.

20. Obiri, D., Flink, N., Maier, J., Neeb, A., Maddalo, D., Thiele, W., Menon, A., Stassen, M., Kulkarni, R. A., Garabedian, M., Barrios, A. M., and Cato, A. (2012) PEST-domain-enriched tyrosine phosphatase and glucocorticoids as regulators of anaphylaxis in mice, *Allergy 67*, 175-182.

21. Cravatt, B. F., Wright, A. T., and Kozarich, J. W. (2008) Activity-based protein profiling: from enzyme chemistry to proteomic chemistry, *Annu. Rev. Biochem. 77*, 383-414.

22. Evans, M. J., and Cravatt, B. F. (2006) Mechanism-based profiling of enzyme families, *Chem. Rev. 106*, 3279-3301.

23. Fonovic, M., and Bogyo, M. (2007) Activity based probes for proteases: Applications to biomarker discovery, molecular imaging and drug screening, *Curr. Pharm. Des. 13*, 253-261.

24. Jeffery, D. A., and Bogyo, M. (2003) Chemical proteomics and its application to drug discovery, *Curr. Opin. Biotechnol. 14*, 87-95.

25. Zhang, Z.-Y. (2003) Chemical and mechanistic approaches to the study of protein tyrosine phosphatases, *Acc. Chem. Res. 36*, 385-392.

26. Zhang, Z.-Y., Wang, Y., and Dixon, J. E. (1994) Dissecting the catalytic mechanism of protein tyrosine phosphatases, *Proc. Natl. Acad. Sci. U.S.A. 91*, 1624-1627.

27. Kumar, S., Zhou, B., Liang, F., Wang, W. Q., Huang, Z., and Zhang, Z. Y. (2004) Activity-based probes for protein tyrosine phosphatases, *Proc. Natl. Acad. Sci. U.S.A. 101*, 7943-7948.

28. Liu, S., Zhou, B., Yang, H., He, Y., Jiang, Z. X., Kumar, S., Wu, L., and Zhang, Z. Y. (2008) Aryl vinyl sulfonates and sulfones as active site-directed and mechanism-based probes for protein tyrosine phosphatases, *J. Am. Chem. Soc. 130*, 8251-8260.

29. Lo, L. C., Pang, T. L., Kuo, C. H., Chiang, Y. L., Wang, H. Y., and Lin, J. J. (2002) Design and synthesis of class-selective activity probes for protein tyrosine phosphatases, *J. Proteome Res. 1*, 35-40.

30. Wang, Q., Dechert, U., Jirik, F., and Withers, S. G. (1994) Suicide inactivation of human prostatic acid phosphatase and a phosphotyrosine phosphatase, *Biochem. Biophys. Res. Commun. 200*, 577-583.

31. Yu, X., Chen, M., Zhang, S., Yu, Z. H., Sun, J. P., Wang, L., Liu, S., Imasaki, T., Takagi, Y., and Zhang, Z. Y. (2011) Substrate specificity of lymphoid-specific tyrosine phosphatase (Lyp) and identification of Src kinase-associated protein of 55 kDa homolog (SKAP-HOM) as a Lyp substrate, *J. Biol. Chem. 286*, 30526-30534.

32. Karver, M. R., Kulkarni, R. A., and Barrios, A. M. (2013) Unpublished data.

33. Ge, J., Li, L., and Yao, S. Q. (2011) A self-immobilizing and fluorogenic unnatural amino acid that mimics phosphotyrosine, *Chem. Commun. 47*, 10939-10941.

34. Kalesh, K. A., Tan, L. P., Lu, K., Gao, L., Wang, J., and Yao, S. Q. (2010) Peptide-based activity-based probes (ABPs) for target-specific profiling of protein tyrosine phosphatases (PTPs), *Chem. Commun. 46*, 589-591.

35. Shen, K., Qi, L., Ravula, M., and Klimaszewski, K. (2009) Synthesis and peptide incorporation of an unnatural amino acid containing activity-based probe for protein tyrosine phosphatases, *Bioorg. Med. Chem. Lett. 19*, 3264-3267.

36. Tulsi, N. S., Downey, A. M., and Cairo, C. W. (2010) A protected l-bromophosphonomethylphenylalanine amino acid derivative (BrPmp) for synthesis of irreversible protein tyrosine phosphatase inhibitors, *Bioorg. Med. Chem. 18*, 8679-8686.

37. Wu, J., Katrekar, A., Honigberg, L. A., Smith, A. M., Conn, M. T., Tang, J., Jeffery, D., Mortara, K., Sampang, J., Williams, S. R., Buggy, J., and Clark, J. M. (2006) Identification of substrates of human protein-tyrosine phosphatase PTPN22, *J. Biol. Chem. 281*, 11002-11010.

38. Mathews, R. A., and Barrios, A. M. (2013) Unpublished data.